

**Fabrication of a pH Sensor Based on Metal Oxide Nanoparticle and Ion
Exchanging Surfaces**

by

Sanzida Mohosina Toma


A thesis submitted in partial fulfillment of the requirements for the degree of
Master of Science in Chemistry

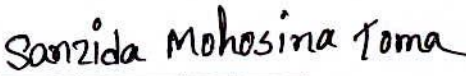


Khulna University of Engineering & Technology
Khulna 9203, Bangladesh
February 2018

Declaration

This is to certify that the thesis work entitled “*Fabrication of a pH Sensor Based on Metal Oxide Nanoparticle and Ion Exchanging Surfaces*” has been carried out by *Sanzida Mohosina Toma* in the Department of Chemistry, Khulna University of Engineering & Technology, Khulna, Bangladesh. The above thesis work or any part of this work has not been submitted anywhere for the award of any degree or diploma.


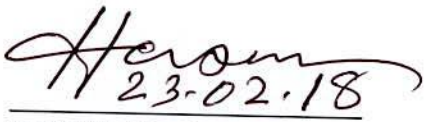
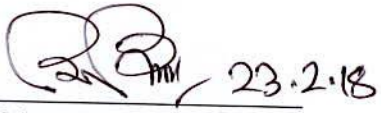
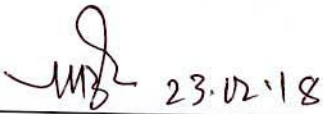


13.03.18
Signature of Supervisor


Signature of Candidate

Approval

This is to certify that the thesis work submitted by *Sanzida Mohosina Toma* entitled "*Fabrication of a pH Sensor Based on Metal Oxide Nanoparticle and Ion Exchanging Surfaces*" has been approved by the board of examiners for the partial fulfillment of the requirements for the degree of *M.Sc* in the Department of *Chemistry*, Khulna University of Engineering & Technology, Khulna, Bangladesh in February 2018.

BOARD OF EXAMINERS

- 
23.02.18
1. Dr. A. B. M. Mamun Jamal
Assistant Professor,
Department of Chemistry
Khulna University of Engineering & Technology
Chairman
(Supervisor)
 2. 
23.02.18
Head of the Department
Department of Chemistry
Khulna University of Engineering & Technology
Member
 3. 
23.2.18
Dr. Mohammad Abu Yousuf
Professor, Department of Chemistry
Khulna University of Engineering & Technology
Member
 4. 
23.02.18
Dr. Md. Mizanur Rahman Badal
Professor, Department of Chemistry
Khulna University of Engineering & Technology
Member
 5. 
Dr. Md. Qamrul Ehsan
Professor, Department of Chemistry
University of Dhaka
Member
(external)

Acknowledgements

All the praises are for almighty Allah, who helped me in difficulties and gave me enough strength and ability to successfully complete this research work.

I would like to express my deepest gratitude, sincere appreciation and respect to my honorable thesis advisor **Dr. A. B. M. Mamun Jamal**, Assistant Professor, Department of Chemistry, Khulna University of Engineering & Technology. He is an excellent supervisor and was very affectionate, for his scholastic guidance, support, valuable advice and inspiration throughout my thesis work, which make a lot of confidence in me to complete the thesis successfully.

I would like to thank Prof. Dr. Mohammad Hasan Morshed, Head, Department of Chemistry, KUET for providing me necessary laboratory facilities and continuous support. I would like to give my special thanks to Prof. Dr. Mohammad Abu Yousuf, Department of Chemistry, KUET for his excellent support, laboratory facilities, advice and enthusiasm throughout my M.Sc degree. I would like to express my true appreciation to all my teachers at the department, who always helped me whenever I needed. I gratefully remember all the staff of the department for their continuous support and assistance during my thesis work.

I would like to thanks University Grant Commission and Khulna University of Engineering & Technology for funding my research. I sincerely thank to all my lab mates and friends for their sincere co-operation and encouragement.

Finally, I would like to thank the two most special persons of my life my father and my husband for their constant encouragement and sacrifices and also all of my family members who have always been encouraging and supporting me throughout the period of my education.

Sanzida Mohosina Toma

Abstract

The nanostructures of metal oxides are attractive and important for nanosensor research in the broad range of applications in various fields of biological, environmental and analytical chemistry. Due to their potential applications and special properties metal oxides nanoparticle have concerned considerable attention which are strongly related with their size, structure and morphology. Among the metal oxide, cupric oxide (CuO) is found to be one of the most popular oxide. Owing to its exceptional electrochemical activity and the possibility of promoting electron transfer at a low potential, availability, stability, good morphological and structural control of the synthesized nanostructures, CuO is a good candidate for pH sensing application.

In this paper, an electrochemical pH sensor that has been fabricated using copper oxide modified glassy carbon electrode (CuO/GCE). The difference in peak potential shift while using CuO/GCE as pH sensor was measured using square wave voltammetry (SWV); and was found to be linear over the range of pH 3-9, with a sensitivity of 60 mVpH^{-1} . The sensor shows a potential drift of 1.97 –3.33 % after three hours of continuous use; and could retain 95% of its initial sensitivity after 1 week of use. The electrode was found to respond both in the presence and absence of oxygen, further expanding the potential applications to include it into de-oxygenated environments. This prototype has been tested in real samples and verified by using commercial pH meter. The CuO based sensor showed good sensitivity and long term stability that may show the way to develop a low cost solid state pH sensor for a wider range of applications.

Contents

	PAGE
Title page	i
Declaration	ii
Certificate of Research	iii
Acknowledgement	iv
Abstract	v
Contents	vi
List of Tables	ix
List of Figures	x
CHAPTER I	
Introduction	1-38
1.1 General	1
1.2 What is pH?	2
1.3 Necessity of pH measurement?	3
1.4 What is pH sensor?	3
1.5 Different types of pH sensor	4
1.5.1 ISFET based pH sensor	4
1.5.2 Image Sensor based on pH	5
1.5.3 Optical fiber pH sensor	5
1.5.4 Magnetoelastic pH sensor	6
1.5.5 Conductimetric pH sensor	6
1.5.6 Glass electrode pH sensor	6
1.5.7 Potentiometric pH sensor	7
1.6 Electrochemical sensors	7
1.6.1 Chemically modified electrodes	9
1.6.2 General methods of modification of electrodes	10
1.7 pH sensor components	14
1.8 Working of pH sensor	16
1.9 pH sensor applications	17
1.9.1 pH sensor for environment	18
1.9.2 pH sensor for living systems	18
1.9.3 pH sensor for food processing	19
1.9.4 pH sensor for bio-medical applications	20
1.10 Theoretical background	21
1.10.1 Fundamentals of electrochemistry	21

	1.11 Various electrochemical techniques	30
	1.11.1 Cyclic voltammetry (CV)	30
	1.11.2 Square-wave voltammetry (SWV)	34
	1.12 Sensor characterization	36
	1.12.1 Scanning Electron Microscopy (SEM)	36
	1.13 Objectives of the present work	38
CHAPTER II	Literature review	39-58
	2.1 Introduction	39
	2.2 Nanoparticle based pH sensor	40
	2.3 Metal / metal oxide based pH sensor	42
	2.4 polymers and poly nanocomposite based pH sensor	44
	2.5 Solid state pH sensor	47
	2.6 Potentiometric pH sensor	50
	2.7 Calibration curve	54
	2.8 Analytical performance of the pH sensor	55
CHAPTER III	Experimental	59-64
	3.1 Reagent and materials	59
	3.2 Equipments	59
	3.3 Preparation of iridium oxide nanoparticles	60
	3.4 Preparation of PANI electro-deposition solution	60
	3.5 Preparation of CuO nanoparticale	60
	3.6 Modification of working electrode	61
	3.7 Preparation of pH solutions	62
	3.8 Standardization of the system	62
	3.9 Electrochemical measurements	62
	3.10 Reproducibility and repeatability of the pH sensor	63
	3.11 Drift and stability of the pH sensor	64
	3.12 Effect of oxygen on the pH sensor	64
	3.13 Real sample test	64
CHAPTER IV	Results and Discussion	65-95
	4.1 Electrochemical setup standardization	65
	4.2 Synthesis of nanoparticle and its physical characterization	68
	4.3 Sensor fabrication	70
	4.4 Electrochemical characterization of CuO nanoparticle modified GCE	70
	4.5 Electrochemical characterization of bare GCE	71

4.6 Electrochemical characterization of polyaniline modified PGE	73
4.7 Electrochemical characterization of polyaniline modified GCE	75
4.8 Electrochemical characterization of iridium oxide nanoparticle modified GCE	78
4.9 Electrochemical characterization of WO ₃ /PGE using SWV	80
4.10 Electrochemical characterization of CuO /PGE using SWV	82
4.11 Electrochemical characterization of CuO/GCE using SWV	84
4.11.1 Zero current potentiometric (OCP) sensing and analytical performance of pH sensor	87
4.12 Electrochemical characterization of CuO /GCE in the presence and absence of oxygen	89
4.13 Real sample test	90
4.14 Repeatability and reproducibility measurement	92
4.15 Drift and stability measurement	93
CHAPTER V Conclusions and Recommendation	96
References	97

LIST OF TABLES

Table No	Description	Page
2.1	List of pH sensing materials that has been used as pH sensors	57
4.1	Electrochemical parameters obtained from voltammograms	66
4.2	Comparison of different pH sensors	95

LIST OF FIGURES

Figure No	Description	Page
1.1	Commercial pH sensor	4
1.2	Schematic diagram of ISFET structure	5
1.3	Mechanism of electrochemical sensor	8
1.4	Structure of Chitosan	13
1.5	Chemical structure of Nafion	14
1.6	A pH Measuring Electrode	14
1.7	A pH Reference Electrode	15
1.8	Preamplifier	15
1.9	Transmitter or Analyzer	16
1.10	Working of pH Sensor	17
1.11	Schematic representation of the electrical double layer	23
1.12	Mass transfer to and from the electrode surface	24
1.13	Schematic diagram of a three-electrode cell and set-up for electrochemical measurements	26
1.14	Glassy carbon working electrode	27
1.15	Ag/AgCl reference electrode	28
1.16	Platinum (Pt) electrode	29
1.17	A potentiostat with circuit diagram of a three-electrode system	30
1.18	A CV potential waveform with switching potentials	31
1.19	Typical CV response for a reversible redox couple.	32
1.20	Potential waveform (A); one potential cycle (B); and typical voltammogram in SWV (C); The response consists of a forward (anodic, Y _f), backward (cathodic, Y _b) and net (Y _{net}) component	36
1.21	Different types of signals produced when high-energy electron impinges on a material	37
1.22	Schematic diagram of a SEM	38
3.1	Schematic diagram of modification of working electrode	61
3.2	Electrochemical experimental setup	63
4.1	CV of Ferricyanide based on GCE at concentration of 2mM of Ferricyanide in 0.1 M KNO ₃ as supporting electrolyte, scan rate of 20, 40, 60, 80, 100, 120, 140, 160 mV/s	65
4.2	The anodic and the cathodic peak heights as function of the square root of the scanning rate based on glassy carbon electrode	67
4.3	(a-d) Scanning electron microscopy (SEM) images of CuO nanoparticles at different magnifications (5000 to 50000X)	69
4.4	Energy Dispersive X-ray spectroscopy (EDX) images of CuO nanoparticles	69

4.5	Schematic diagram of stepwise fabrication of the pH sensor	70
4.6	CVs detailing the effect of scan rate (60 - 160) mV / s using CuO/GCE at 0.1M PBS	71
4.7	CVs of 0.1 M buffer at different pH values (3-9) on bare GCE (scan rate 0.05 mV / s)	72
4.8	SWV of bare GCE at different pH values (3-9) on bare GCE in 0.1M PBS buffer	72
4.9	pH sensitivity measured from pH 3 to 9 at bare GCE	73
4.10	CVs of electrochemical polymerization of aniline on bare PGE(scan rate 0.05 mV / s)	74
4.11	SWV of 0.1M PBS buffer at different pH values (3-9) on PANI/PGE	74
4.12	pH sensitivity measured from pH 3 to 9 using PANI/PGE	75
4.13	CVs of electrochemical polymerization of aniline on bare GCE(scan rate 0.05 mV / s)	76
4.14	SWV of 0.1 M PBS buffer at different pH values (3-9) on PANI/GCE	77
4.15	pH sensitivity measured from pH 3 to 9 using PANI/GCE	77
4.16	CVs of electrodeposition of Iridium Oxide nanoparticle on bare GCE (scan rate 0.05 mV / s)	79
4.17	SWV of Iridium Oxide nanoparticle/GCE in 0.1 M buffer at different pH values 3 to 9	79
4.18	pH sensitivity measured from pH 3 to 9 using Iridium Oxide nanoparticle on GCE	80
4.19	CVs of 0.1 M buffer at different pH values based on WO ₃ /PGE (scan rate 0 .05 mV / s)	81
4.20	SWV of WO ₃ /PGE at different pH values (3 to 9) in 0.1 M PBS buffer	81
4.21	pH sensitivity measured from pH 3 to 9 using WO ₃ /PGE	82
4.22	CVs of 0.1 M buffer at different pH values in the presence of CuO/PGE (scan rate 0.05 mV / s)	83
4.23	SWV of CuO/PGE at different pH values (3-9) in 0.1M PBS buffer	83
4.24	pH sensitivity measured from pH 3 to 9 using CuO/PGE.	84
4.25	CVs of 0.1 M buffer at different pH values (3-9) on CuO/GCE (scan rate 0.05 mV / s)	86
4.26	SWV of CuO/GCE at different pH values (3-9) in 0.1M buffer	86
4.27	pH sensitivity measured from pH 3 to 11 using CuO/GCE	87
4.28	Zero current potentiometry (OCP) of 0.1 M buffer at different pH values (3-9) in the presence of CuO/GCE	88
4.29	pH sensitivity measured from pH 3 to 9 using CuO/GCE	88

4.30	CVs showing the response of the CuO immobilized layer to the presence and absence of oxygen at pH 6	89
4.31	Electrochemical signal (SWV) obtained in “real” unbuffered samples for malt vinegar using CuO / GCE	90
4.32	Electrochemical signal (SWV) obtained in “real” unbuffered samples for antacid using CuO/GCE	91
4.33	Electrochemical signal (OCP) obtained in “real” unbuffered samples for malt vinegar using CuO/GCE.	91
4.34	Electrochemical signal (OCP) obtained in “real” unbuffered samples for antacid using CuO/GCE	92
4.35	Repeatability and reproducibility test of three CuO NPs pH sensor electrodes at various pH buffer solutions	93
4.36	Electrode drift of CuO nanoparticle immobilized on the GCE; potential readings of pH 5, 7 and 9, signals have been taken every 30 min over period over 3 hours	94

CHAPTER I**Introduction****1.1 General**

Analytical chemistry is a branch of chemistry that deals with the separation, identification and quantification of chemical compounds. Chemical analyses can be qualitative, as in the identification of the chemical components in a sample, or quantitative, as in the determination of the amount of a certain component in the sample. The area of chemistry that deals with the inter conversion of electrical energy and chemical energy is called electrochemistry. An electrochemical catalysis is a crucial phenomena in the field of electrochemistry, that can be used for various applications such as sensors, energy storage, diagnosis, coating industries, batteries.

Nanotechnology has recently become one of the most exciting forefront fields in electrochemistry. Nanosize enhance the surface area and improves the catalytic properties of targeted materials [1]. Owing to their small size (normally in the range of 1 – 100 nm), nanoparticles exhibit unique chemical, physical and electronic properties that are different from those of bulk materials, and can be used to construct novel and improved technological devices; in particular, electrochemical sensors, biosensors, energy storages [2,3].

In recent years, metal oxides nanoparticles have attracted considerable attention on account of their potential applications and unique physical and chemical properties, which are strongly influenced by their size, morphology, and structure .They exhibit size-dependent features i.e. at the nanometer scale, their properties significantly differ from its bulk material, conferring it new optical, magnetical and electronic characteristics [4].

Among the oxide materials being studied, copper oxide (CuO) is an important p-type semiconductor that exhibits a narrow band gap (1.2–2.6 eV) [5].Thanks to its unique properties such as high stability and excellent electrical conductivity, CuO finds applications in the fields of catalysis, fuel cells, electronics, batteries and sensors [6].

CuO is found to be a promising material for pH sensor, owing to its excellent electrochemical activity and the possibility of promoting electron transfer at a low potential, availability, stability, good morphological and structural control of the synthesized nanostructures CuO is a good candidate for pH sensing application.

In 2011, S. Zaman [7] reported CuO nanoflower as an electrochemical pH sensor, where authors have reported the effect of the pH on growth of morphology on by changing the pH solution. On Au coated glass electrode the sensor exhibited a linear electrochemical response within a pH range of (2-11) with a sensitivity 28 mV/pH. Also, in 2013, Jamal *et al.* [8] has reported gold nanowire array based pH sensor with better sensitivity compare to the GCE.

In this work, a facile, stable and sensitive pH sensor is fabricated by synthesizing CuO nanoparticle using hydrothermal method, and drop cast the nanoparticle along with chitosan and Nafion mixture that acts as a ion exchanging surface onto the GCE. The sensing abilities of the electrode were investigated in terms of static and dynamic properties such as calibration, sensitivity, time response, stability as well as oxygenated and deoxygenated environment. This method allowed the fabrication will open up the door to fabricate a miniaturized carbon based sensing platform which would be suitable both in clinical and environmental applications.

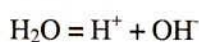
1.2 What is pH

The term pH is derived from “p,” the mathematical symbol for negative logarithm, and “H,” the chemical symbol for Hydrogen. This definition of pH was introduced in 1909 by the Danish biochemist, Soren Peter Lauritz Sorensen. The formal definition of pH is: the negative logarithm of Hydrogen ion activity. It is expressed mathematically as:

$$\text{pH} = -\log a_{\text{H}^+}$$

where: H^+ is hydrogen ion concentration in mol/L

In any collection of water molecules a very small number will have dissociated to form hydrogen (H^+) and hydroxide (OH^-) ions:



Every aqueous solution can be measured to determine its pH value. This value ranges from 0 to 14 pH. Values below 7 pH exhibit acidic properties. Values above 7 pH exhibit basic (also known as caustic or alkaline) properties. Since 7 pH is the center of the measurement scale, it is neither acidic nor basic, it is called "neutral."

1.3 Necessity of pH Measurement

Almost all processes containing water have a need for pH measurement.

- ❖ pH has great importance in laboratory measurements. So many chemical and biological processes in laboratory are dependent on pH. So controlling pH is very important in order to optimize the desired reaction or to prevent unwanted reactions
- ❖ pH measurement is used in a wide variety of applications: agriculture, soil analysis wastewater treatment, industrial processes, environmental monitoring, and in research and development.
- ❖ All things in life sciences related such as cell culture blood and other bodily fluid analysis bioreactor monitoring are depend on pH value.
- ❖ pH is very important in marine research and monitoring such as Seawater analysis Home and commercial aquariums.
- ❖ It is also essential to measure pH in food and beverage processing pharmaceutical processing general manufacturing of products.

1.4 What is pH sensor

The pH sensor usually combined into one device that's called a combination pH electrode. The measuring electrode is usually glass and quite fragile. pH sensors measure the level of pH in sample solutions by measuring the activity of the hydrogen ions in the solutions. This activity is compared to pure water (a neutral solution) using a pH scale of 0 to 14 to determine the acidity or alkalinity of the sample solutions.



Figure 1.1: Commercial pH sensor

1.5 Different types of pH sensor

There are different types of pH sensor. Brief of some pH sensor are given below:

1.5.1 ISFET based pH sensors

Ion-Sensitive Field-Effect Transistor (ISFET) has been used for detection of the ionic activity in an electrolyte solution attached to the gate oxide of a Metal-Oxide-Semiconductor (MOS) structure. One of the most useful parameters to be measured in biochemistry is the hydrogen concentration, or pH. ISFET is one of the leading pH sensors using semiconductor technologies [9- 11]. It has recently attracted more interest because of many advantages compared to other pH sensing methods such as litmus papers and glass pH electrodes. It has a relatively high sensitivity, smaller size, and it can be used at high temperature. Moreover, it suits continuous monitoring, has potential for large-scale integration, and may be fabricated using conventional CMOS process. ISFETs have been adopted in various lab-on-chip and health-care applications. It found use also in agriculture, environmental monitoring, and food industries [12]. As the sensitivity of an ISFET is an important parameter determining its performance, many attempts for modeling were reported. All these attempts use an approximate analytical expression to describe the electrostatics of the underlying MOSFET.

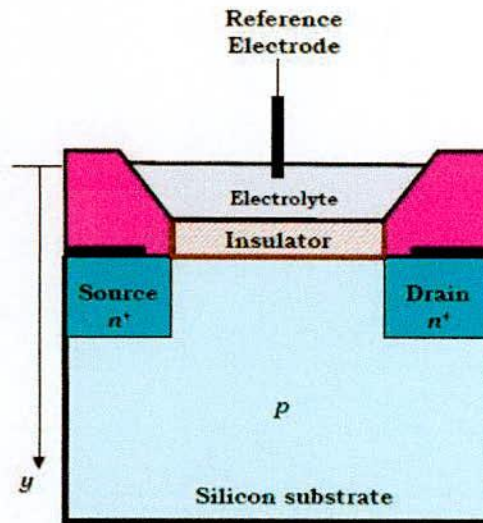


Figure 1.2: Schematic diagram of ISFET structure

1.5.2 Image Sensor based on pH

pH dependent image sensors have various applications related to industries both in real time and chemical. pH image sensor works on the principle of charge transfer. The chemical variations are monitored by the dynamic images and two dimensional distributions provided by the image sensors. pH image sensors are fabricated on the CMOS process technology. They are used to take two dimensional distributions and dynamic images of chemical variations [13].

1.5.3 Optical fiber pH sensors

Optical pH sensor offers an alternative approach. As compared to pH electrodes, optical pH sensors have several advantages. They can be miniaturized down to submicrometer or even nanometer dimensions. pH optical fiber sensors and pH nanosensors have been extensively studied and applied for monitoring intracellular pH. Optical pH sensors do not need a reference sensor and their performance is not affected by electrical or electromagnetic interferences. They can be used for remote and on-line sensing with minimal invasiveness. Optical pH sensors are capable of continuous measurements. However, they also have some disadvantages. One of the most severe issue is the limited

long-term stability due to dye leaching and/or photo-bleaching, which could be improved or avoided through the choice of right pH indicator dyes, the sensing mechanism, and referenced or ratio-metric sensing strategy. Temperature and ionic concentration also need to be taken into account for reliable measurements [14].

1.5.4 Magnetoelastic pH sensors

The working principle of magnetoelastic pH sensor is based on the inter conversion of magnetic and elastic energies. Electrical field is applied on drive coil which cause the induction of the magnetic field. Due to this magnetic field the substrate starts to vibrate with a certain frequency. Due to change in the pH, the mass of the pH sensitive material changes, due to swelling or shrinking of the material, which cause the change in the frequency of vibration and is detected by the pickup coil. So, in this way the pH of the material can be calculated. If the mass increases, the frequency of the vibration decreases and *vice versa*. In recent years there has been an increasing interest in magnetoelastic sensors, as they provide an opportunity to remotely monitor a variety of quantities [15].

1.5.5 Conductimetric pH sensors

A conductimetric pH sensor is based on the measurement of the conductivity of a pH-responsive hydrogel and other materials. It is constructed by coating planar interdigitated electrode arrays with a photolithographically patterned hydrogel membrane [16]. The hydrogel sensing layer swells or shrinks to a hydration determined by the pH of a solution in which it is immersed. Sensing layer must respond to analyte of interest and produce a measureable change in the electrical properties.

1.5.6 Glass electrode pH sensors

In 1909, based on observations of cremer (1906) at glass membranes, F. Haber and Z. Klemensiewicz developed the pH glass electrode [17]: a glass bubble filled with strong electrolyte and a silver|silver chloride electrode inside. Improved pH selective glasses were found by Mcinnes in 1930. Present glasses contain, e.g., 63% SiO₂, 28% Li₂O, 5% BaO, 2% La₂O₃ [18]. UO₂ and TiO₂ improve the performance in alkaline solutions. pH of

the solution is very difficult to measure directly. So the measurement of pH is done by comparing the potential of the solutions of known H ions with the solution of unknown H ions. The solution with known H⁺ ions is called reference solution. The potential between these two solutions is measured by using two cells. One is called reference half cell and the other is called sensing half cell.

1.5.7 Potentiometric pH sensors

The most widely used potentiometric device is the pH electrode, which has been used for several decades. Its success is attributed to a series of undisputed advantages, such as simplicity, rapidity, non destructiveness, low cost, applicability to a wide concentration range and, particularly, to its extremely high selectivity for hydrogen ions [19-20]. In potentiometric sensors the signal is measured as potential difference (voltage) between the working electrode and the reference electrode. The working electrode's potential depends on the concentration of the analyte in the gas or solution phase. The reference electrode is needed to provide a defined reference potential. Potentiometric pH sensors consist of for example Pt/PtO₂, W/W₂O₃, Pb/PbO₂, Ir/IrO₂ etc [21]. pH sensitive material is applied on the working electrode and when the voltage is changed between the working electrode and reference electrode, that potential difference is measured. In this way the change in the pH can be measured. These sensors are very efficient over a wide pH range, at high temperature and pressure. The response time of these sensors are also fast as compared to other sensors.

1.6 Electrochemical Sensors

An electrochemical sensor can be defined as a device that provides continuous information about its environment. Electrochemical Sensors are the devices, which are composed of an active sensing material with a signal transducer. The role of these two important components in sensors is to transmit the signal without any amplification from a selective compound or from a change in a reaction. These devices produce any one of the signals as electrical, thermal or optical output signals which could be converted into digital signals for further processing. One of the ways of classifying sensors is done based on these output signals. Among these, electrochemical sensors have more advantage over

the others because; in these, the electrodes can sense the materials which are present within the host without doing any damage to the host system. On the other hand, sensors can be broadly classified in to two categories as chemical sensors and biosensors. The biosensors can be defined in terms of sensing aspects, where these sensors can sense biochemical compounds such as biological proteins, nucleotides and even tissues [22].

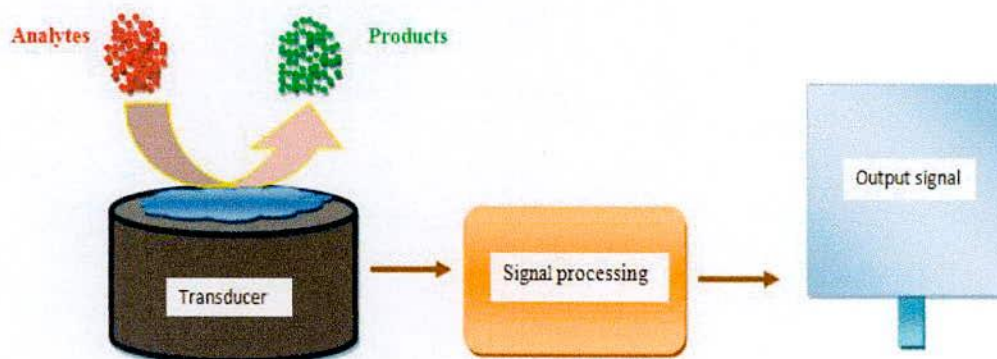


Figure 1.3: Mechanism of electrochemical sensor

There are three main types of electrochemical sensors: potentiometric, voltammetric and conductometric. For potentiometric sensors, a local equilibrium is established at the sensor interface, where either the electrode or membrane potential is measured, and information about the composition of a sample is obtained from the potential difference between two electrodes. Voltammetric sensors exploit the use of a potential applied between a reference and a working electrode, to cause the oxidation or reduction of an electroactive species; the resultant current is measured. On the other hand, conductometric sensors are involved with the measurement of conductivity at a series of frequencies. Examples of transduction techniques include:

- ❖ **Potentiometric** – The measurement of the potential at zero current. The potential is proportional to the logarithm of the concentration of the substance being determined.
- ❖ **Voltammetric** – Increasing or decrease the potential that is applied to a cell until the oxidation or reduction of the analyte occurs. This generates a rise in current that is proportional to the concentration of the electroactive potential. Once the

desired stable oxidation/reduction potential is known, stepping the potential directly to that value and observing the current is known as amperometry.

- ❖ **Conductimetric** – Observing changes in electrical conductivity of the solution. [23].

The selection and development of an active material is a challenge. The active sensing materials may be of any kind as whichever acts as a catalyst for sensing a particular analyte or a set of analyte. The recent development in the nanotechnology has paved the way for large number of new materials and devices of desirable properties which have useful functions for numerous electrochemical sensor and biosensor applications [24].

With remarkable achievements in nanotechnology and nanoscience, nanomaterial-based electrochemical signal amplifications have great potential of improving both sensitivity and selectivity for electrochemical sensors and biosensors. First of all, it is well-known that the electrode materials play a critical role in the construction of high-performance electrochemical sensing platforms for detecting target molecules through various analytical principles [25, 26].

Furthermore, in addition to electrode materials, functional nanomaterials can not only produce a synergic effect among catalytic activity, conductivity, and biocompatibility to accelerate the signal transduction but also amplify biorecognition events with specifically designed signal tags, leading to highly sensitive biosensing. Significantly, extensive research on the construction of functional electrode materials, coupled with numerous electrochemical methods, is advancing the wide application of electrochemical devices [27].

1.6.1 Chemically modified electrodes

Chemically modified electrodes (CMEs) comprise a relatively modern approach to electrode systems a wide spectrum of basic electrochemical investigations, including the relationship of heterogeneous electron transfer and chemical reactivity to electrode surface chemistry, electrostatic phenomena at electrode surfaces, and electron and ionic transport phenomena in polymers, and the design of electrochemical devices and systems for applications in chemical sensing, energy conversion and storage, molecular electronics, electrochromic displays, corrosion protection, and electro-organic syntheses.

Compared with other electrode concepts in electrochemistry, the distinguishing feature of a CME is that a generally quite thin film (from a molecular monolayer to perhaps a few micrometers-thick multilayer) of a selected chemical is bonded to or coated on the electrode surface to endow the electrode with the chemical, electrochemical, optical, electrical, transport, and other desirable properties of the film in a rational, chemically designed manner [28].

One of the common approaches for incorporating a modifier onto the surface has been coverage with an appropriate polymer film. Most polymers are applied to electrode surfaces by a combination of adsorptive attraction and low solubility in the electrolyte solution, using preformed polymers or electrochemical polymerisation. An early approach in the use of pre-formed polymers was their use as anchoring groups for coordinating metal complexes to pyrolytic graphite electrodes [29]. Examples include poly (4-vinylpyridine) (PVP), poly (vinylferrocene) (PVF), poly (p-nitro styrene), metal polymers and others, used as redox monomers in polymer modification schemes after synthetic procedures [30]. The advantages of preconcentrating CME were obtained by coating the electrode surface with a thin film of an ion exchange polymer [31]. The strategy of coating an anion exchange polymer onto an electrode surface is similar to the stripping voltammetric method principle. These techniques solid electrodes coated with a thin layer of an ion exchange polymer, which allows the quick pre-concentration and simultaneous amperometric detection of an ion redox analyte.

Different types of inorganic films, such as metal oxide, clay, zeolite, and metal ferrocyanide, can also be formed on electrode surfaces. These films are of interest because they frequently show well-defined structures, are thermally and chemically stable, and are usually inexpensive and readily available [32].

1.6.2 General methods of modification of electrodes

The concept of chemically modified electrodes (CMEs) is one of the exciting developments in the field of electroanalytical chemistry. Many different strategies have been employed for the modification of the electrode surface. The motivations behind the modifications of the electrode surface are: (i) improved electrocatalysis, (ii) freedom from

surface fouling and (iii) prevention of undesirable reactions competing kinetically with the desired electrode process [33]. The increasing demand for it has led to the development of a rapid, simple and non-separation method for the simultaneous determination of isomers where the CMEs have emerged as an efficient and versatile approach, and have attracted considerable attention over the past decades due to its advantages in terms of reduced costs, automatic and fast analysis, high sensitivity and selectivity [34-38]. There are numerous techniques that may be used to modify electrode surfaces. Among various CMEs, polymer-modified electrodes (PMEs) are promising approach to determination. Some modification processes are-

Covalent Bonding: This method employs a linking agent (e.g. an organosilane) to covalently attach one of several monomolecular layers of the chemical modifier to the electrode surface [36].

Drop-Dry Coating (or solvent evaporation): A few drops of the polymer, modifier or catalyst solution are dropped onto the electrode surface and left to stand to allow the solvent to dry out.

Dry-Dip Coating: The electrode is immersed in a solution of the polymer, modifier or catalyst for a period sufficient for spontaneous film formation to occur by adsorption. The electrode is then removed from solution and the solvent is allowed to dry out [34].

Composite: The chemical modifier is simply mixed with an electrode matrix material, as in the case of an electron-transfer mediator (electro catalyst) combined with the carbon particles (plus binder) of a carbon paste electrode. Alternatively, intercalation matrices such as certain Langmuir-Blodgett films, zeolites, clays and molecular sieves can be used to contain the modifier [38].

Spin-Coating (or Spin-Casting): also called spin casting, a droplet of a dilute solution of the polymer is applied to the surface of a rotating electrode. Excess solution is spun off the surface and the remaining thin polymer film is allowed to dry. Multiple layers are applied in the same way until the desired thickness is obtained. This procedure typically produces pinhole-free thin films for example; oxide xerogel film electrodes prepared by spin-coating a viscous gel on an indium oxide substrate [35].

Electrodeposition: In this technique the electrode is immersed in a concentrated solution ($\sim 10^{-3} \text{ molL}^{-1}$) of the polymer, modifier or catalyst followed by repetitive voltammetry scans. The first and second scans are similar, subsequent scans decrease with the peak current. For example, electrochemical deposition of poly (o-toluidine) on activated carbon fiber [38].

Electro-polymerisation: A solution of monomer is oxidized or reduced to an activated form that polymerizes to form a polymer film directly on the electrode surface. This procedure results in few pinholes since polymerization would be accentuated at exposed (pinhole) sites at the electrode surface. Unless the polymer film itself is redox active, electrode passivation occurs and further film growth is prevented.

In this technique the electrode is immersed in a polymer, modifier or catalyst solution and layers of the electropolymerized material builds on the electrode surface. Generally, the peak current increases with each voltammetry scan such that there is a noticeable difference between the first and final scans indicating the presence of the polymerized material. For example, electro polymerization of aniline on platinum electrode perturbations.

Chitosan: Chitosan, sometimes known as deacetylated chitin, is a natural polycationic linear polysaccharide derived from partial deacetylation of chitin. Chitin is the structural element in the exoskeleton of insects, crustaceans (mainly shrimps and crabs) and cell walls of fungi, and the second most abundant natural polysaccharide after cellulose. It is a linear polyaminosaccharaide composed of randomly distributed β -(1, 4)-linked D-glucosamine and N-acetyl-D-glucosamine groups. The interesting characteristics of chitosan such as biocompatibility, non-toxicity, low allergenicity and biodegradability allow it to be used in various applications [39, 40]. Due to its structure, chitosan possesses good adhesion and cheapness properties; therefore it has been used as an immobilization matrix. Although it has poor electrical conductivity, but it usually has been combined with carbon nanotubes, redox mediator and metal nanoparticles [41].

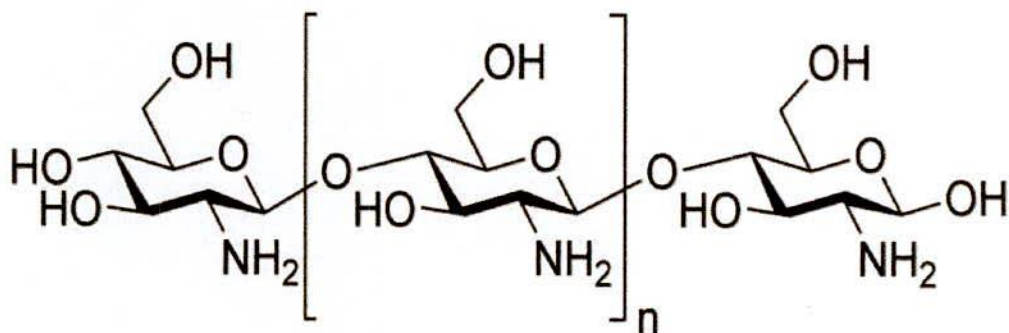


Figure 1.4: Structure of Chitosan

Chitosan is soluble in aqueous acidic media at $\text{pH} < 6.5$. When dissolved, it bears a high positive charge on its amino groups. Chitosan has gel-forming properties as a result of its ability to adhere to negatively charged surfaces and aggregate polyanionic compounds.

Nafion and its ions exchanging capability on electrode surfaces: Nafion is a sulfonated tetrafluoroethylene copolymer that was discovered in the late 1960s by Dr. Walther Gustav Grot of DuPont de Nemours. Its unique ionic properties are the result its hydrophobic polytetrafluoroethylene backbone chain and perfluorovinyl ether groups terminated with sulfonic cation exchange sites. Nafion possesses excellent thermal and mechanical stability. The combination with sulfonic acid group results in its highly cationconductive property. Nafion membrane coated on the electrodes can prevent interference mainly via two mechanisms: firstly its complex polymer structure (with small pores) only allows small molecules to pass through; and secondly its positive charge limits the diffusion of anionic components such as AA across the membrane. Nafion, due to its good biocompatibility, antifouling capacity, chemical inertness, and thermal stability, as well as high permeability to water molecules and small cations has been widely used in electrochemistry to modify electrodes. Moreover, mixing Nafion with other materials can improve the interface adhesion between films and electrodes. To obtain a Nafion coated surface, the electrodes are dipped in Nafion polymer solution and then dried.

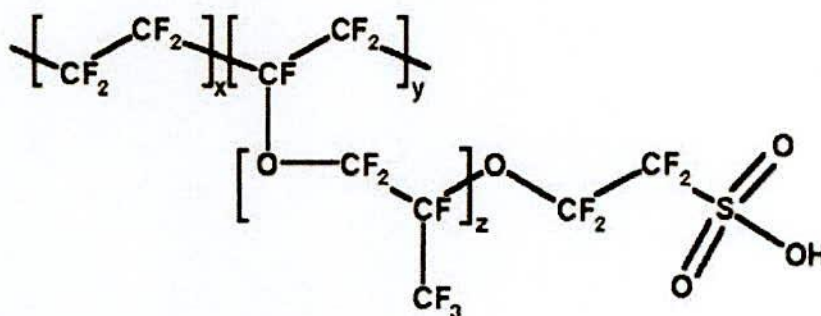


Figure 1.5: Chemical structure of Nafion

Nafion can also be used to generate composite films, coat electrodes, or repair damaged membranes [42].

1.7 pH sensor components

It is basically an electrode consisting of 4 components:

- **A measuring electrode:** It is a tube made up of glass and consists of a thin glass bulb welded to it, filled up with Potassium Chloride solution of known pH of 7. It also contains a block of silver chloride attached to a silver element. It generates the voltage used to measure pH of the unknown solution.

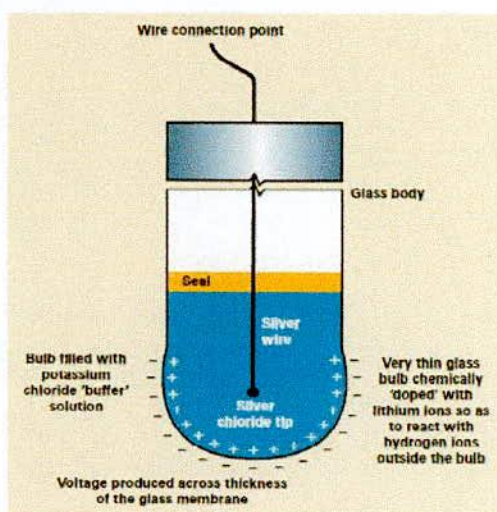


Figure 1.6: A pH Measuring Electrode

- **A Reference Electrode:** It is a glass tube consisting of potassium chloride solution in intimate contact with a mercury chloride block at the end of the potassium chloride. It is used to provide a stable zero voltage connection to the complete the whole circuit.

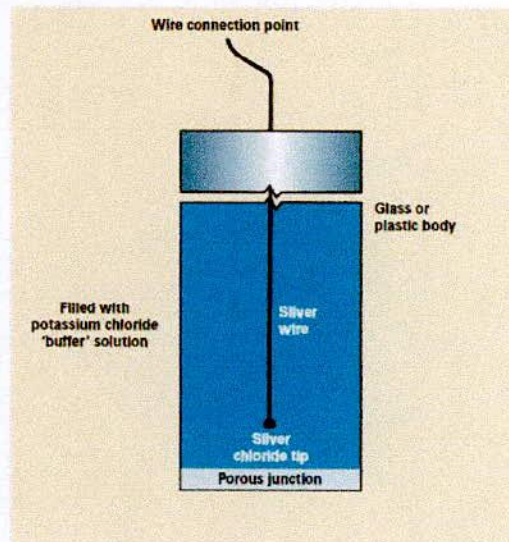
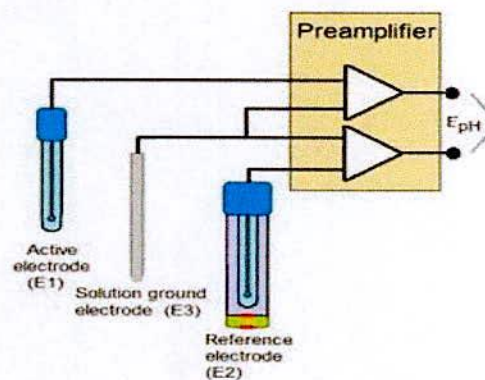


Figure 1.7: A pH Reference Electrode

- **Preamplifier:** It is a signal conditioning device and converts the high impedance pH electrode signal to a low impedance signal. It strengthens and stabilizes the signal, making it less susceptible to electrical noise.



$$E_{pH} = (E1 - E3) - (E2 - E3) = E1 - E2$$

E_{pH} is a function of the measured pH value

Figure 1.8: Preamplifier

- **Transmitter or Analyzer:** It is used to display the sensor's electrical signal and consists of a temperature sensor to compensate for the change in temperature.



Figure 1.9: Transmitter or Analyzer

1.8 Working of pH Sensor:

The electrode is placed inside the beaker filled with a solution whose pH is to be measured. The glass bulb welded at the end of the measurement electrode consists of lithium ions doped to it which makes it act as an ion selective barrier and allows the hydrogen ions from the unknown solution to migrate through the barrier and interact with the glass, developing an electrochemical potential related to the hydrogen ion concentration. The measurement electrode potential thus changes with the hydrogen ion concentration. On the other hand, the reference electrode potential doesn't change with the hydrogen ion concentration and provides a stable potential against which the measuring electrode is compared. It consists of a neutral solution which is allowed to exchange ions with the unknown solution through a porous separator, thus forming a low resistance connection to complete the whole circuit. The potential difference between the two electrodes gives a direct measurement of the hydrogen ion concentration or pH of the system and is first pre-amplified to strengthen it and then given to the voltmeter.

$$U = E_{\text{pH}} - E_{\text{ref}}$$

E_{pH} – Voltage potential of measurement electrode

E_{ref} – Voltage potential of reference electrode

The pH is calculated based on the Nernst equation which states that change in total potential for every change in pH is

$$U = -KTpH$$

K- boltzman's constant, T- temperature.

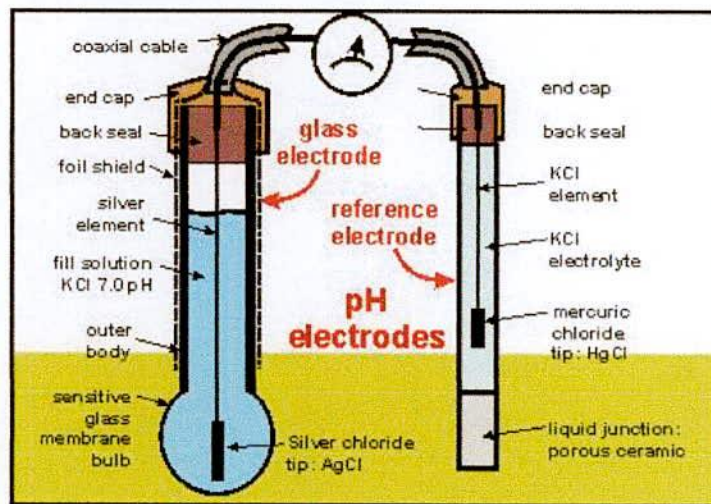


Figure 1.10: Working of pH Sensor

1.9 pH sensor applications

The most common method for pH measurement uses a pH electrode. These sensors act as a small battery, generating a voltage signal proportional to the solution pH. Manufacturers of pH measurement equipment offer hundreds of styles of pH electrodes to meet the demands of the thousands of unique application challenges. The measurement of pH is important for many applications in medicine, biology, chemistry, agriculture, forestry, environmental science, oceanography, civil engineering, chemical engineering, water treatment and water purification, food science, and nutrition.

1.9.1 pH sensor for environment:

The role of pH sensor in nature is closely related to that of water, and as such, it is extremely important for living organisms and the environment. The pH of natural water and soils controls the form of life sustained in these environments. The pH of the various parts of plants and living organisms defines their function, whereas that of foodstuffs their taste and function once in the food chain. Examples of the environmental importance of pH are acid rain (a result of industrial pollution, with detrimental effects on life and buildings) and ocean acidification as a result of increased carbon dioxide emissions (detrimental to living organisms in aquatic environments). Typical examples of biological processes involving pH changes include the production of carboxylic acids, such as lactic acid by muscle activity, the protonation of phosphate derivatives such as ATP, and the function of the oxygen-transport enzyme hemoglobin. Finally, an example of pH-related properties of foodstuff is the acidity of some juice fruits due to the presence of citric acid. Keeping the water in our lakes, rivers, and streams clean requires monitoring of water quality at many points as it gradually makes its way from its source to our oceans. Over the years ever increasing environmental concerns and regulations have heightened the need for increased diligence and tighter restrictions on wastewater quality. Control of water pollution was once concerned mainly with treating wastewater before it was discharged from a manufacturing facility into the nation's waterways. Today, in many cases, there are restrictions on wastewater that is discharged to city sewer systems or to other publicly owned treatment facilities. Many jurisdictions even restrict or regulate the runoff of storm water affecting not only industrial and commercial land, but also residential properties as well. Thereby, a reliable and stable pH sensor would help to overcome these problems.

1.9.2 pH sensor for Living Systems:

pH sensor is extremely important for living systems through its role in biochemical reactions. The pH of various parts and fluids of an organism is regulated by the acid–base homeostasis. For example, human blood should have a pH value in the 7.36–7.42 range, mainly controlled by the bicarbonate/carbonic acid buffer. A pH change as low as 0.2 pH units can result in death (via acute acidosis or alkalosis). Certain definite pH values are

needed for the activation of many enzymes in the body and the trigger of associated reactions. The parts and fluids of the human body have pH values that span the entire pH range, starting from gastric acid (pH 1.0), to human skin (pH 5.5), urine (pH 6.0), and blood (pH 7.4), to pancreatic fluid (pH 8.1). Thereby, a good pH sensor would help monitoring pH levels in biological system that would help both for diagnosis and for wound healing purposes.

1.9.3 pH sensor for Food processing:

Food processing covers a wide range of activities all of which require both food safety and quality standards to be met to ensure that consumers receive high quality products. One of the more vital parameters that plays a part in this is pH sensor since it governs both physical and chemical reactions during food production as well as inhibiting the growth of pathogens.

Ever since we discovered cheese and alcohol, man has been controlling the acidity of food in order to create different products. With an extraordinarily detailed understanding of how pH can affect the look, taste and quality of a food product, we have now introduced precise pH control as part of general food processing and safety programmes covered by national regulatory bodies.

Every micro-organism has a minimum, optimum and maximum pH for growth. Useful yeasts and moulds, for example can grow at low pH, but 4.6 and below is generally considered the level that will prevent the growth and toxin production of harmful pathogens. However, going too far can have detrimental effects of its own. It is therefore necessary to have suitable testing equipment that can measure pH with sufficient accuracy in order to ensure product quality and compliance with food safety regulations.

Monitoring of pH is also very important in the food production process especially in dairy products. Milk is tested for impurities and signs of infection both upon collection as well as at the point of delivery, while beer and wine producers rely on precise pH readings to determine the taste and quality of the final product. Finally, when a particular process is finished, an automated cleaning procedure can be used to prepare the production system

for the next batch; hence, ensuring correct pH levels are maintained is also crucial in the hygiene management system.

pH is also very important for foodstuff in many perspectives. It is a factor of major importance in water absorption, emulsification, and gelation of different protein sources. It affects significantly the physical and chemical properties of food ingredients such as proteins, sugars, and amino acids, to mention a few. The vast majority of foodstuffs, apart from egg whites and soda crackers, have a pH value 7 are limited, though the pH of some staple foods lies in the range of 4.5–7.0. Generally, foods that are products of plant origin have a pH that is lower than those of animal origin. On the basis of their pH, foods can be classified as high-acid (pH/43.7), acidic (pH/43.7–4.6), medium-acid (pH/44.6–5.3), or low-acid (pH/4over 5.30). pH sensor gives also information about food stability and preservation. It can be used to retard microbial spoilage that could happen in the presence of some pathogens such as bacteria, molds, and yeasts. Microorganisms usually show their best growth rate in the pH range of 6.5–7.5. Furthermore, the growing capability of molds and yeasts lies in a much broader pH range than that of microorganisms such as bacteria. In consideration of the fact that almost all of the pathogenic agents and most of deterioration bacteria cannot grow at pH 4.5 are less stable. Their stabilization by heat treatment demands a heat sterilization to remove all pathogens and corruption, including bacterial spores. Food acids, at pH Furthermore, the growing capability of molds and yeasts lies in a much broader pH range than that of microorganisms such as bacteria. In consideration of the fact that almost all of the pathogenic agents and most of deterioration bacteria cannot grow at pH 4.5 are less stable. Their stabilization by heat treatment demands a heat sterilization to remove all pathogens and corruption, including bacterial spores. Thereby, controlling and optimizing pH is crucial for the food processing industries, and requires a sensitive and stable pH sensor which does not require regular calibration.

1.9.4 pH sensor for bio-medical applications:

In biomedical field, main applications of pH sensor are as follows:

1. Detecting the information of clinical chemistry. In the field of medical clinic and basic research, the biology's information needs to be detected to ensure the present state of

given biology. For example, before operating on a patient, a doctor needs to know the pH in the body. Under this condition, clinic thermometer and pH sensor has to be employed to help doctor quickly detect pH in the body.

2. Continuously monitoring some parameters of biology outside and inside. In biomedical field, heart pH has to be monitored continuously by heart pH sensor for a few days after operation.

3. Control. In medicine, people usually utilize some parameter detected by biomedical sensor to control or adjust physiological course of body. In the food industry, biomedical sensor could be utilized to measure some enzyme and its concentration to control the process of fabricating food and to analyze the nutritional ingredient of food. Of course, biomedical sensor such as pH sensor could be also employed to detect our atmosphere and condition to improve our living situation.

1.10. Theoretical Background

Some fundamentals information of electrochemistry are given below:

1.10.1 Fundamentals of Electrochemistry

Faradic currents: The Faradaic current is the current that flows through an electrochemical cell that is generated by the change in oxidation state of the electroactive species occurring at the electrode surface, combined with the current contribution due to the charge transfer between the electrode and the background analyte present in solution. The faradic current obeys Faraday's law.

Examples of faradic currents include diffusion current which is the term of interest in polarographic analysis. Kinetic currents are part of the faradic current where it should be clear that reactions should be rapid but of lower rate than the diffusion of the analyte. Kinetic currents are sensitive to changes in temperature with just small contribution to the faradic current. Most of the faradic current thus originates from the diffusion current.

Non Faradic Currents: These do not obey faraday's laws of electrolysis and are thus of no analytical value. The most important contribution to non-faradic currents originates from what is called capacitive current. This capacitive current results from the double layer which is formed between the charged mercury drop and the counter ions at the solution interface. Another contribution comes from migration current which results from electrostatic attraction of analyte ions by the oppositely charged mercury drop. Addition of supporting electrolyte of enough concentration will make this term close to zero.

Charging currents and the Electrical Double Layer: The application of a potential to the electrode surface causes ions near the electrode surface to migrate towards or away from the electrode depending on the respective charge of the electrode and the ions. This forms an electrical double layer, comprised of the electrical charge at the surface of the electrode and the charge of the ions in the solution near the electrode. This double layer leads to the generation of a non-faradaic charging current. Whenever a charged solid surface is placed in any solution, the ions, carrying charge opposite to that carried by the surface, cluster around the solid surface. These sheet of ionic charge adjacent to the charged solid surface and the charged surface constitute a double layer. The electrical double layer is an array of charged particles and orientated dipoles. It is composed of two layers; the layer closest to the electrode is known as the inner Helmholtz plane (IHP) and the outer Helmholtz plane (OHP) Figure 1.11 [43]. The planes were discovered by Hermann von Helmholtz in 1853. The IHP is composed of solvent molecules and specifically adsorbed ions, whilst the OHP represents the imagined outer layer closest to the electrode that passes through the centre of solvated ions, but is separated by the molecules at the IHP. These layers are both held at the surface of the electrode. The behavior of the interface between the electrode and the solution is similar to that of a capacitor.

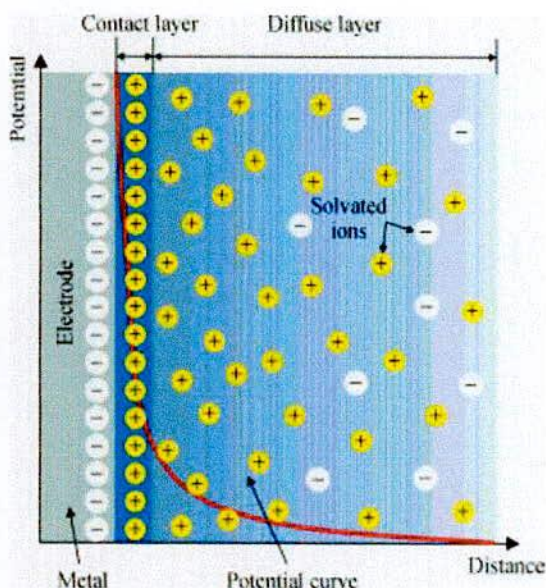


Figure 1.11: Schematic representation of the electrical double layer

Beyond the double layer, is a diffuse layer of scattered ions that extends into the bulk solution. These ions are ordered relative to the coulombic forces acting upon them and the random motion of the solution by thermal motion. The balance of the electrostatic forces on ions at the surface of the electrode, which are repelled or attracted dependent on their charge, is counterbalanced by the random motion of the diffuse layer. This causes a non-uniform distribution of ions near the electrode surface. As a result, the field strength of the potential applied to the electrode diminishes rapidly, thereby causing the double layer to be extremely thin at 10 – 20 nanometers in thickness [44]. It is also essential to use a high electrolyte concentration, typically a 100 fold greater than that of the analyte, as this concentrates the charge at the Helmholtz planes, therefore ensuring that diffusion is the dominant mechanism for mass transport [45].

Mass transfer process in voltammetry: Mass transfer is the movement of material from one location to another in solution. In electrochemical systems, three modes of mass transport are generally considered which a substance may be carried to the electrode surface from bulk solution including diffusion, convection and migration. Any of these or more than one might be operating in a given experiment which is depended on the experimental conditions [45].

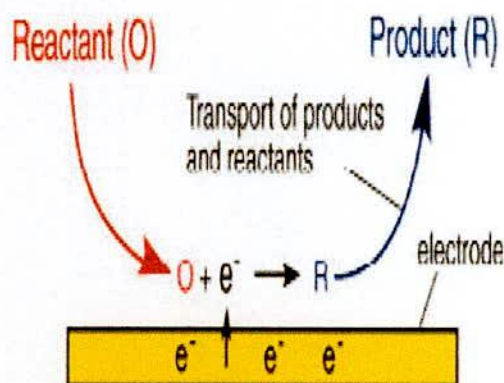


Figure 1.12: Mass transfer to and from the electrode surface

In general, there are three types of mass transfer processes:

- ✓ Migration
- ✓ Diffusion
- ✓ Convection

Migration

Migration involves the movement of charged ions under the influence of electric field. Since migration is nonspecific in nature, migration due to the electroactive ion cannot be distinguished from the migration of other charged species present in the solution. Therefore, it becomes necessary to add a large excess of inert electrolyte to the cell solution, in order to eliminate the migration of the electroactive ions of interest. The inert electrolyte, which is generally called the supporting electrolyte, neutralizes the electrostatic forces of attraction acting between the working electrode and electroactive ion by suppressing the transport number of the reactants. To achieve this inert electrolyte is added to the electrolytic solution (at least 50 to 100 times in excess of the electroactive ions). Inert or indifferent supporting electrolyte contains ions that do not take part in the electrolysis [46].

Diffusion

Diffusion refers to the process by which molecules intermingle as a result of their kinetic energy of random motion. Whereas a concentration difference between two regions of a solution, ions or molecules move from the more concentrated region to the dilute and leads to a disappearance of the concentration difference.

Diffusion is a natural mixing process facilitated by the natural vibration of atoms and molecules. It is driven by entropy which seeks to even out any in homogeneities in a system, thereby eliminating localised concentrations as disorder is spread through the system. The rate of diffusion, first described mathematically by Fick, is dependent upon the concentration gradient. In this model it is assumed that the electrode is perfectly flat and of infinite dimensions. The direction of mass transport to and from the electrode occurs in a direction normal to the electrode surface. Ignoring any electrostatic effects, the rate of diffusion at a given point in the solution is dependent on the concentration gradient at that point. Fick's first law of diffusion terms this flow of material flux.

$$\text{flux} = j = -D_B \frac{\delta[B]}{dx}$$

The one kind of mode of mass transfer is diffusion to an electrode surface in an electrochemical cell. The rate of diffusion is directly proportional to the concentration difference. When the potential is applied, the cations are reduced at the electrode surface and the concentration is decreased at the surface film. Hence a concentration gradient is produced. Finally, the result is that the rates of diffusion current become larger.

Convection

By mechanical way reactants can also be transferred to or from an electrode. Thus forced convection is the movement of a substance through solution by stirring or agitation. This will tend to decrease the thickness of the diffuse layer at an electrode surface and thus decrease concentration polarization. Natural convection resulting from temperature or density differences also contributes to the transport of species to and from the electrode. At the same time a type of current is produced. This current is called convection current. Removing the stirring and heating can eliminate this current. Convection is a far more efficient means of mass transport than diffusion.

Electrochemical setup

Electrochemical Cell: An electrochemical cell is where the electrochemical reactions are take place. An electrochemical cell consists two half-cells. Each half-cell consists of an electrode and an analyte. An electrode is an electrical conductor used to make contact with a non-metallic part of a circuit (eg. a semiconductor, an electrolyte or a vacuum).An electrolyte is a substance that ionizes when dissolved in suitable ionizing solvent.

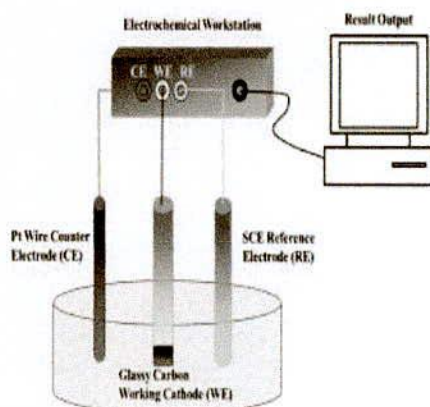


Figure 1.13: Schematic Diagram of a three-electrode cell and set-up for electrochemical measurements CE: counter electrode, WE: Working electrode, RE: Reference electrode

Electrodes:

An electrode is an electrical conductor used to make contact with a nonmetallic part of a circuit (e.g. a semiconductor, an electrolyte or a vacuum). Types of electrode

- ❖ Working electrode
- ❖ Reference electrode
- ❖ Counter electrode

Working electrode: The Working Electrode is the electrode where the potential is controlled and where the current is measured. The working electrode makes contact with the analyte and transfer charge to and from the analyte. The Working Electrode is an "inert" material such as gold, platinum, or glassy carbon.

Advantages of working electrode:

- ✓ Available wire, flat plate & tube, large range of sizes.

- ✓ Larger cathodic potential range.
- ✓ Wide potential range low background current inexpensive

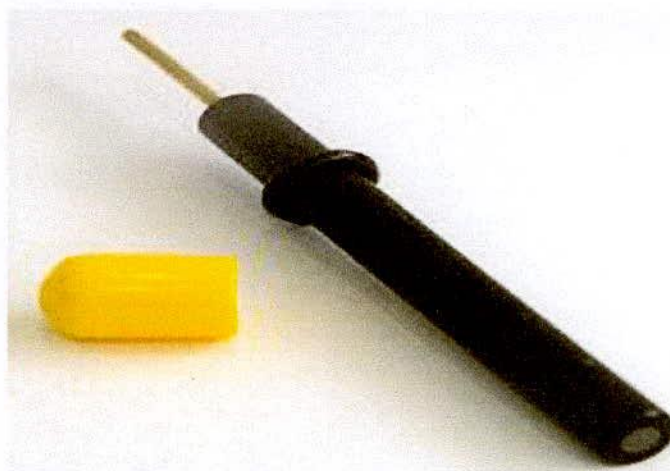


Figure 1.14: Glassy carbon working electrode

Function of Working Electrode: It serves as a surface on which the electrochemical reaction takes place.

Reference Electrode: A reference electrode is an electrode which has a stable and well-known electrode potential. The high stability of the electrode potential is usually reached by employing a redox system with constant (buffered or saturated) concentrations of each participants of the redox reaction.

A reference electrode is used in measuring the working electrode potential. A Reference Electrode should have a constant electrochemical potential as long as no current flows through it. The reference electrode acts as reference in measuring and controlling the working electrode's potential.

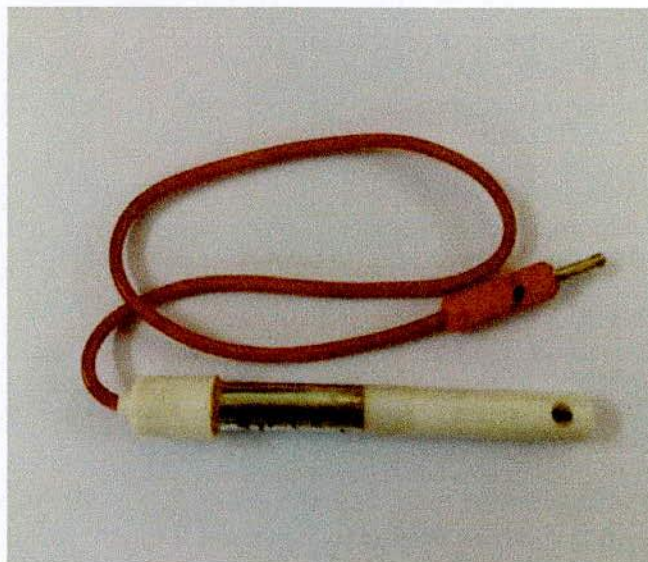


Figure 1.15: Ag/AgCl reference electrode

Function of R.F: The most common lab Reference Electrodes are the Saturated Calomel Electrode (SCE) and the Silver/Silver Chloride (Ag/AgCl) electrodes.

Counter electrode: The Counter, or Auxiliary, Electrode is a conductor that completes the cell circuit. The Counter Electrode in lab cells is generally an inert conductor like platinum or graphite. In field probes, it's generally another piece of the Working Electrode material. The current that flows into the solution via the Working Electrode leaves the solution via the Counter Electrode. The auxiliary electrode passes all the current needed to balance the current observed at the working electrode. Auxiliary electrodes are often fabricated from electrochemically inert materials such as gold, platinum, or carbon.



Figure 1.16: Platinum (Pt) electrode

Function of CE: Remove the solution resistance and measure only the electrode potential.

Potentiostats for electrochemistry: A potentiostat is a device that controls the potential between a pair of electrodes while measuring the resulting current flow. The resulting electrochemical plot is then used to determine various parameters relevant to the experiment [47]. A potentiostat adjusts the voltage difference between the anode and the cathode in order to maintain a constant working electrode potential. A potential is applied to the working electrode, resulting in a flow of charge towards the counter electrode. A potential drop (iR) is caused by the electrolyte conductivity, the distance between the electrodes, the magnitude of the current and resistance across the electrode material. If the iR drop is uncompensated, the reaction will no longer operate at the desired potential, and the reaction may cease. The reference electrode monitors the potential at the working electrode and feeds the value back to the opamp. If a difference in potential is observed between the RE and WE, the potential applied to the CE is altered to compensate. A second op-amp is used as a current-voltage converter to measure the flow of current, with a resistor used to output the voltage per unit current.

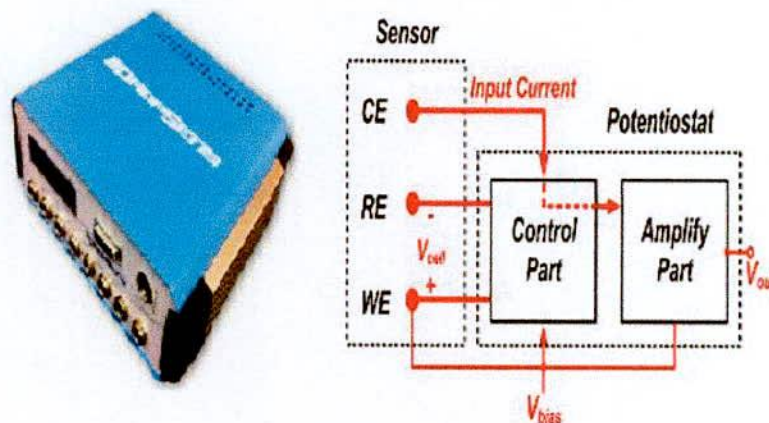


Figure 1.17: A potentiostat with circuit diagram of a three-electrode system

1.11 Various electrochemical techniques

A short brief of various electrochemical techniques are given below:

1.11.1 Cyclic voltammetry (CV)

CV is an electrochemical method which measures the current that develops in an electrochemical cell under conditions where voltage is in excess of that predicted by the Nernst equation. CV is performed by cycling the potential of a working electrode, and measuring the resulting current. CV can be used to study qualitative information about electrochemical processes under various conditions, such as the presence of intermediates in oxidation-reduction reactions, or the reversibility of a reaction. CV can also be used to determine:

- Electron stoichiometry of a system
- Diffusion coefficient of an analyte
- Formal reduction potential

A CV is obtained by applying a linear potential sweep (that is, a potential that increases or decreases linearly with time) to the working electrode. The potential of the working electrode is measured against a reference electrode which maintains a constant potential, and the resulting applied potential produces an excitation signal such as that of figure

1.18. In the forward scan of figure 1.18, the potential first scans negatively, starting from a greater potential (a) and ending at a lower potential (d). The potential extrema (d) is call the switching potential, and is the point where the voltage is sufficient enough to have caused an oxidation or reduction of an analyte. The reverse scan occurs from (d) to (g), and is where the potential scans positively. Figure 1.18 shows a typical reduction occurring from (a) to (d) and an oxidation occurring from (d) to (g). It is important to note that some analytes undergo oxidation first, in which case the potential would first scan positively. This cycle can be repeated, and the scan rate can be varied. The slope of the excitation signal gives the scan rate used.

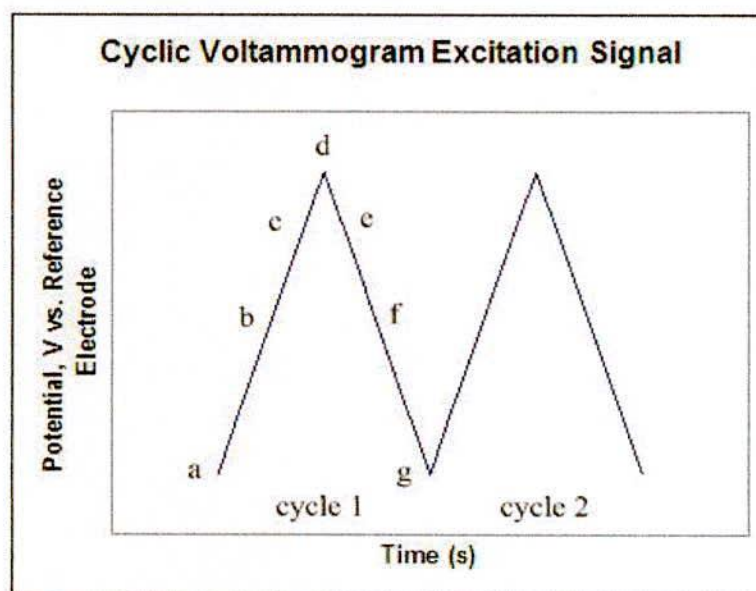


Figure 1.18: A CV potential waveform with switching potentials

The equipment required to perform cyclic voltammetry consists of a conventional three-electrode potentiostat connected to three electrodes (working, reference, and auxiliary) immersed in a test solution. The potentiostat applies and maintains the potential between the working and reference electrode while at the same time measuring the current at the working electrode. (During the experiment, charge flows between the working electrode and the auxiliary electrode.) A recording device (such as a computer or plotter) is used to record the resulting CV as a graph of current versus potential.

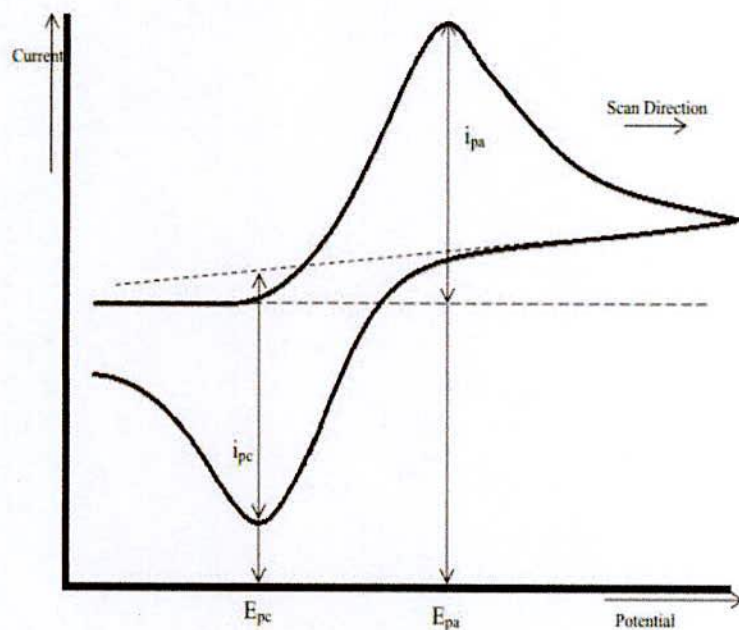


Fig 1.19: Typical CV response for a reversible redox couple

CV are characterized by six important parameters.

- The cathodic (E_{pc}) and anodic (E_{pa}) peak potentials
- The cathodic (i_{pc}) and anodic (i_{pa}) peak currents
- The cathodic half-peak potential ($E_{p/2}$)
- The half wave potential ($E_{1/2}$)

CV linearly applies a triangular potential ramp to the working electrode at a defined scan rate until it has reached a set switching potential as shown in Fig 1.19. Once the switching potential on the triangular excitation potential ramp is reached, it begins a scan in the reverse direction. During the potential sweep, the current is measured resulting from the potential applied. The resulting plot of current vs. potential is known as a cyclic voltammogram, as illustrated in Fig. 1.19.

The two peak currents (i_{pc}/i_{pa}) and two peak potentials (E_{pc}/E_{pa}) form the basis for the analysis of the cyclic voltammetric response to the analyte. The shape of the voltammogram is due to the concentration of the reactant (R) or product (P) at the

electrode surface during the scan. Ideally, the scan begins at a potential of negligible current flow whereby the analyte is neither oxidized nor reduced. As the potential is ramped linearly, electron transfer between the electrode and the analyte in the solution begins to occur; this leads to an accumulation of product and a depletion of the reactant. The ramp increases in accordance to the Nernst Equation.

$$E = E^0 + \frac{0.059}{n} \log \frac{[OX]}{[Red]}$$

Where E is the applied potential and E^0 the formal potential; [OX] and [Red] represent surface concentrations at the electrode solution interface, not bulk solution concentrations. Note that the Nernst equation may or may not be obeyed depending on the system or on the experimental conditions.

At the peak of the anodic wave the reaction becomes diffusion controlled, as the diffusion layer has grown sufficiently from the electrode that the flux of the product to the electrode is too slow to satisfy the Nernst equation. As a result, the concentration of the reactant at the surface reaches zero. Subsequently, the rate of diffusion then decreases, reducing the current flow, in accordance with the Cottrell equation. Once the potential ramp has reached the switching potential, the potential is ramped in the opposite direction resulting in a cathodic potential being applied.

The peak current for a reversible system is described by the Randles-Sevcik equation [48]. The current is directly proportional to the concentration and increases in respect to the square root of the scan rate. This dependence on scan rate implies the reaction at the electrode is controlled by mass transport. The equation applies at standard temperatures. (25°C, n = number of electrons involved, A = electrode area, D = diffusion coefficient, C_B = bulk electrode concentration and v = scan rate).

$$i_p = (2.69 \cdot 10^5) n^{\frac{3}{2}} A D^{\frac{3}{2}} C_B v^{\frac{1}{2}}$$

The reversibility of an electrochemically reversible couple can be identified by the measurement of the potential difference between the two peak potentials. An electrochemically reversible system based on a one electron transfer process is denoted in equation A. A fast one electron transfer exhibits a ΔE_p of 59 mV.

$$\Delta E_p = E_{pa} - E_{pc} = \frac{59}{n} \text{ mV}$$

1.11.2 Square-wave voltammetry (SWV)

SWV is a powerful electrochemical technique suitable for analytical application mechanistic study of electrode processes and electro kinetic measurements [49-51]. Nowadays it is considered as one of the most advanced voltammetric techniques, which unifies the advantages of pulse techniques (enhanced sensitivity), cyclic voltammetry (insight into the electrode mechanism) and impedance techniques (kinetic information of very fast electrode processes). Square-wave voltammetry, as one of the most advanced voltammetric techniques is frequently used in analytical applications and fundamental studies of various com-pounds recognized as medicaments, physiologically important systems, biologically active substances, pesticides and many more. When used for analytical applications, SWV shows a broad range of advantages over other voltammetric techniques. These are recognized in the greater sensitivity, short analysis time and the ability for significant reduction of capacitance currents. Advantages of SWV are also found in the sensitivities of different modes that can be applied for enrichment of the electroactive (or studied) material to be determined.

Typical potential modulation used in SWV consists of a staircase potential ramp modified with square-shaped potential pulses (Figure 1.20A). At each step of the staircase ramp, two equal in height and oppositely directed potential pulses are imposed. The latter two potential pulses complete a single potential cycle in SWV (Figure 1.20B). The potential cycle in SWV is repeated at each step of the staircase ramp in the course of the voltammetric experiment. For historical reasons, the height of a single potential pulse is termed as SW amplitude (E_{sw}). Relative to the direction of the staircase ramp, one recognizes forward and backward potential pulses. More specifically, the potential pulses with odd serial number are forward pulses, whereas those with even serial numbers are assigned as backward (or reverse) pulses. In the course of a single potential cycle, the electrode reaction is driven in both anodic and cathodic directions, thus providing an insight into the electrode mechanism. Consequently, the critical time of the voltammetric experiment is represented by the duration of a single potential cycle (t), or the duration of a single potential pulse, $t_p = t/2$. The voltammetric data can be interpreted in terms of t , t_p ,

or the frequency of the potential modulation f , defined as $f=1/t$. The physical meaning of the frequency can be understood as a number of potential cycles in a unit of time. Typical frequency range provided by commercially available instrumentation is from 5 to 2000 Hz, which corresponds to the duration of a single potential pulse from 0.25 to 100 ms.

In order to discriminate against the charging current, the current sampling is performed at the end of each potential pulse. The currents associated with forward and backward potential pulses compose the forward and backward (reverse) component of the SW voltammogram, respectively (Figure 1.20C). It is important to stress that both forward and backward components are plotted versus the potential of the staircase ramp, i.e. the mid potential of the two neighboring pulses composing one potential cycle. Thus, to each step potential, two current values are assigned. Obviously, there is a difference between the actual potential at which the current is measured and the one given in the SW voltammogram. Subtracting the forward and backward currents of a single potential pulse, a net current value is obtained. The net currents corresponding to each potential cycle compose the net component of the SW voltammogram (Figure 1.20C). For most electrode mechanisms, the net SW component is a bell shaped curve, enabling precise determination of its position and height. We note that the charging current depends on the potential of zero charge; hence, in most of the cases the charging current is almost identical at two neighboring pulses, provided the SW amplitude is low. Hence, the subtraction procedure of the forward and backward currents contributes further in canceling out the remaining charging current, which is one of the reasons for the high quality and enhanced sensitivity of experimentally collected net SWV.

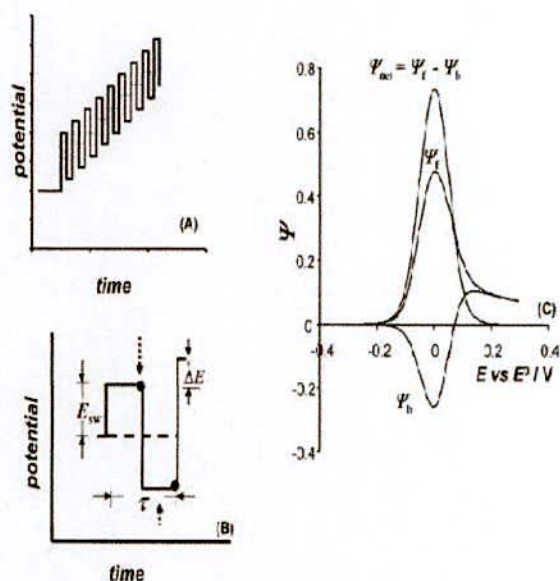


Figure 1.20: Potential waveform (A), one potential cycle (B), and typical voltammogram square-wave voltammetry (C). The response consists of a forward (anodic, Ψ_f), backward (cathodic, Ψ_b) and net (Ψ_{net}) component

1.12 Sensor characterization

1.12.1 Scanning Electron Microscopy (SEM)

A Scanning Electron Microscope (SEM) is a powerful magnification tool that utilizes focused beams of electrons to obtain information. It is a frequently used instrument, in both academia and industry, to study, for example, surface topography, composition, crystallography and properties on a local scale. The spatial resolution is better than that of the optical microscope although not quite as good as for the transmission electron microscope (TEM). The SEM has an extremely large depth of focus and is therefore well suited for topographic imaging.

Besides surface topographic studies the SEM can also be used for determining the chemical composition of a material, its fluorescent properties, the formation of magnetic domains and so on.

The specimen is bombarded by a convergent electron beam, which is scanned across the surface. This electron beam generates a number of different types of signals, which are emitted from the area of the specimen where the electron beam is impinging (Fig. 1.21).

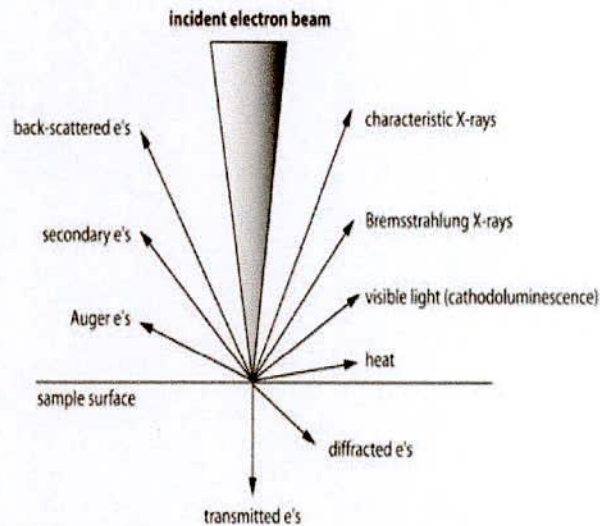


Figure 1.21: Different types of signals produced when high-energy electron impinges on a material

The induced signals are detected and the intensity of one of the signals (at a time) is amplified and used to as the intensity of a pixel on the image on the computer screen. The electron beam then moves to next position on the sample and the detected intensity gives the intensity in the second pixel and so on.

The working principle of the SEM is shown in Figure 1.22 [52]. For improved signal-to-noise ratio in the image, one can use a slower scan speed. This means that the electron beam stays a longer time at one position on the sample surface before moving to the next. This gives a higher detected signal and increased signal-to-noise ratio.

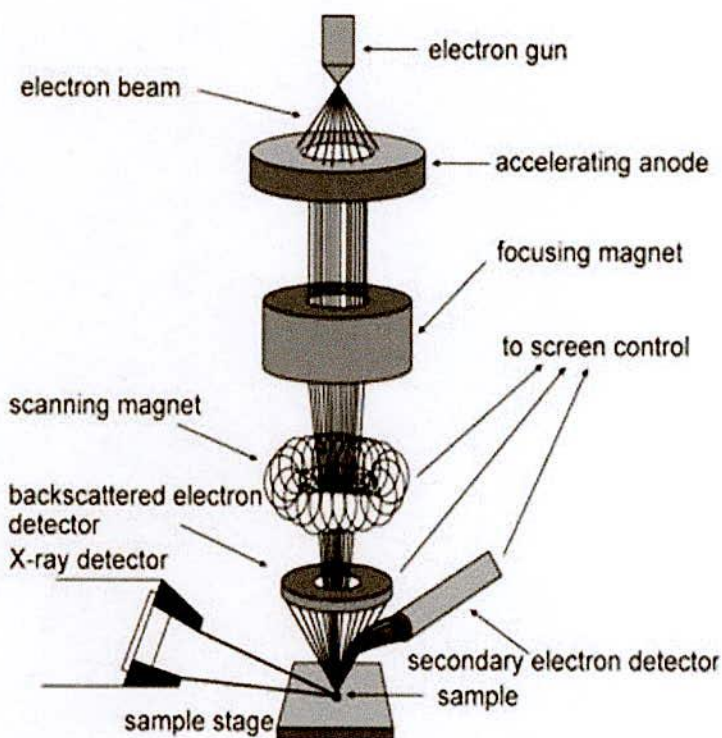


Figure 1.22: Schematic diagram of a SEM

1.13 Objectives of the present work

The objective of this research is

- i) to synthesis of CuO nanoparticles by hydrothermal method.
- ii) to modify glassy carbon electrode with CuO nanoparticle.
- iii) to characterize the sensor using electrochemical methods (CV, SWV), Scanning Electron Microscope, Raman & Energy Dispersive X-ray microanalysis (EDX).
- iv) to develop a pH sensor and also to study the sensitivity, selectivity, stability of this sensor using various electrochemical techniques.

In the next chapter, more details on literature review have been explained.

Chapter II**Literature Review****2.1 Introduction**

A sensor is a device that detects and responds to some type of input from the physical environment. The specific input could be light, heat, motion, moisture, pressure, or any one of a great number of other environmental phenomena. The output is generally a signal that is converted to human-readable display at the sensor location or transmitted electronically over a network for reading or further processing. We are surrounded by sensors and sensing networks that monitor a multitude of parameters in view of enhancing our safety and quality of life.

Nanotechnology-enabled sensors (nanosensors) are providing new solutions in physical, chemical, and biological sensing that enable increased detection sensitivity, specificity, and multiplexing capability in portable devices for a wide variety of health, safety, and environmental assessments. Nanoscale features have a great impact on many (though not all) sensing systems, in particular where the surface-to-volume ratio plays a fundamental role, such as in certain chemical and gas sensors. The high surface-to-volume ratios of nonporous and nanostructured materials have led to their implementation in sensing systems since sensing research first began to engage with the nanotechnology. Over the last decade significant progress has been made in the development of immobilized electrochemical sensors for monitoring pH. This review discusses application of nanostructure and metal oxide based pH sensor platform for the biomedical and environmental applications.

2.2 Nanoparticle and nanocomposite based pH sensor

Currently, much attention has been focused on developing nanomaterials, which are used for signal amplification in electrochemical sensors. Nanomaterials are usually used to take advantage of a larger surface area for biomolecules to be immobilized. This generally increases the number of binding sites available for the detection of a specific chemical analyte [53]. Various types of nanomaterials are used in electrochemical sensors.

Nanoparticles are nanometer size materials with unique physical and chemical properties and have been widely used for many years. Organic molecules, also in the nanometer size range, possess functionalities that enable recognition and self assembly. The combination of nanoparticles and chemical or biological molecules is very attractive and has gained tremendous attention from academic and industry, because such combination could create new materials for electronics and optics and lead to new applications in genomics, proteomics, bio-medical and bio-analytical areas. For environmental application, nanometer size particles and their self assemblies offer the potential of novel functional materials, processes and devices with unique recognition activities, enhanced mobility in environmental and desired application flexibility.

Recently, S. Zaman *et al.* [7] developed a nanoparticle based pH sensor. In this work, authors have reported a CuO nano-flower as an electrochemical pH sensor; and the effect of pH on the growth morphology of CuO nanostructures. The sensor exhibited a linear electrochemical response within a pH range of 2-11 with a sensitivity of 28 mV/decade on the gold coated glass as working electrode.

Lidia *et al.* [54] developed a nanoparticle based flexible pH sensor. These flexible pH sensors based on WO₃ nanoparticles with a high surface area were produced by electrodeposition on gold electrodes with a sensing area of 1 mm². At first time the wax printed layer, here used as an insulator, was proven to be cytocompatible and therefore, a good alternative for sensor assembly. In open circuit voltage measurements, the pH sensitivity of these electrodes shows a near-Nernstain response of -56.7 ± 1.3 mV/pH and reversibility was confirmed for three complete cycles in a pH range of 9-5.

Sh. Nadzirah *et al.* [55] developed TiO₂ nanoparticles-based interdigitated electrode as pH electrodes and measured quantitatively. TiO₂ was synthesized via sol-gel method while interdigitated electrodes were fabricated by conventional photolithography method. Deposition of TiO₂ solution on the fabricated electrodes forms a sensor that promising for development of TiO₂ nanoparticles based biosensors. The extremely small amount of current measurement of this device towards hydrogen and hydroxide ions was measured by Keithley 6487 picoammeter.

Yi. Chen *et al.* [56] reported the fabrication and characterization of a nanocomposite pH sensor made with titanium dioxide (TiO₂)/multiwall carbon nanotube (MWCNT)/cellulose hybrid. The TiO₂-coated MWCNTs are synthesized by hydrothermal process. The X-ray diffraction and Raman spectra observations show that high anatase crystalline TiO₂ nanoparticles are well formed on the surface of MWCNTs. After blending the TiO₂/MWCNTs with cellulose solution, the TiO₂/MWCNT/cellulose hybrid nanocomposite is made and used for the pH sensor. This nanocomposite pH sensor exhibits two linear regions in its conductance between pH 1 and 12. Large surface area of the hybrid nanocomposite increases adsorption sites of ions so as to increase the pH sensitivity as well as sensing range. The long-term stability test and reusable test demonstrate that this hybrid nanocomposite pH sensor is useful for many practical applications.

Xin Chen *et al.* [57] reported silver nanoparticles capped with mercaptoacetic acid and 2-aminoethanethiol short-chain alkanethiols; that were prepared by a one-step method in aqueous solution for monitoring pH and a range of heavy metal ions. The mode of transduction is optical, based on the change in aggregation of the nanoparticles in solution. Because of the different ionic interactions between the modified nanoparticles, these nanoparticle based sensors can rapidly detect Pb²⁺, Cu²⁺ and Fe²⁺ with detection limits as low as 1×10^{-5} M, 5×10^{-7} M and 5×10^{-5} M respectively. Furthermore, the same functionalized nanoparticles were also sensitive to pH; exhibiting a good linear dynamic response between pH 1 and 10.

Feng Gao *et al.* [58] developed on a novel Rhoda mine-*b*-Isothiocyanate doped silica fluorescent core-shell nanoparticle based pH sensor using reverse micro-emulsion technique. The fluorescent core-shell nanoparticles are pH-sensitive, and the pH dynamic

range of the sensing nanoparticles is between 5–10. The method offers the advantages of adequate sensitivity, accuracy and rapid detection of pH. The results are in good agreement with those using the standard glass electrode method. It showed an excellent stability and high reproducibility when used as pH sensors.

Milica Jovica *et al.* [59] developed a flexible potentiometric pH sensor based on iridium oxide nanoparticles. The sensor was fabricated using the simple layer-by-layer (LbL) deposition technique, where alternate layers of the oppositely charged iridium oxide nanoparticles and the poly(diallyl dimethyl ammonium chloride) (PDDA) polymer were deposited on the flexible indium tin oxide foil (ITO/PET). Sensitivity of 74 mV/pH (14-bilayer) was obtained using the ink-jet printing technology.

Zhenhua Bai *et al.* [60] recently developed a fluorescent pH sensor based Ag@SiO₂ Core-Shell Nanoparticle. The shell thickness of 8 nm, maximum fluorescence enhancements of 4 and 9 times were achieved when excited by 405 and 455 nm, respectively. The ratio of emission intensity at 513 nm excited at 455 nm to that excited at 405 nm is correlated well with the pH value of aqueous solution, over the pH range of 5–9. The pH sensitivity and linearity are demonstrated over the physiological region. The excellent structural and optical properties make these core-shell nanoparticles promising in application as intracellular pH sensor.

2.3 Metal/metal oxide-based pH sensor

Metal oxide-based pH sensors have many appealing features that include chemical resistance, insolubility, stability, outstanding mechanical strength, electrocatalyst and manufacturing technology. Metal oxides have been widely reported to have pH-sensitivity, and many of which have been exploited in pH sensing devices. The pH of a solution, biological or non-biological is vitally important in order to use the solutions effectively. For example, if the pH of the blood varies slightly, the shape of proteins become distorted due to the excess positive or negative charges present in the blood. As a result, the protein cannot function effectively as the shape of a protein is a key to the chemical reactions in which it is part. Thus, fast, accurate and reliable pH measurements are vitally important in many applications, including medicine. pH sensors have found use in several other area, such as industrial hygiene, pollution measurement and control,

hazard monitoring, process control and combustion control. A variety of metal/metal oxide materials show ideal or near-ideal Nernstian responses; these materials have been explored for use as pH sensing layers. Some examples are IrO_x, RuO₂, nanoporous PtO₂, RuO₂, βTiO₂, TiO₂, β-PVC, PaO₂, Sb/Sb₂O₃, WO₃, PbO₂, Co₃O₄ and SnO₂.

Marzouk *et al.* [61] in 2002 measured extracellular pH in ischemic rabbit papillary muscle for the first time. Author have used iridium oxide (IrO_x) film as pH sensing layer, electrodeposited on a planar sputtered platinum electrode fabricated on a flexible Kapton substrate. Later, Ryan *et al.* [62] used atomic layer deposition (ALD) technique for the fabrication of IrO_x as pH sensitive layer with an average sensitivity of ~67 mV/pH at 22 °C and a detection range of pH 4 to pH 10. However, Nguyen *et al.* [63] synthesized IrO_x nanoparticle, and developed IrO_x nanoparticle based sensing platform to detect pH, and found to have no issues on drift interference during the pH measurement. As Lu *et al.* [64] reported there is an optimum thickness for IrO₂ electrodeposited coating. Coating electrochemical performance increase when its CSCc and thickness increase, but when CSCc approach to ~45mC/cm² delamination of IrO₂ coating was detected. Their demonstrated iridium oxide electrode showed a pH sensitivity -75.51 mV/pH in broad pH range of 1-13.

Fulati *et al.* [65] developed ZnO nanotube and nanorod as pH sensors. The sensor display good reproducibility, repeatability and long-term stability and exhibit a pH-dependent electrochemical potential difference vs. Ag/AgCl reference electrode over a large dynamic pH range. It has been found that the ZnO nanotubes provide sensitivity as high as twice that of the ZnO nanorods. It can be ascribed to the fact that small dimensional ZnO nanotubes have a higher level of surface and subsurface oxygen vacancies and provide a larger effective surface area with higher surface-to-volume ratio as compared to ZnO nanorods, thus affording the ZnO nanotube pH sensor a higher sensitivity.

Manjakkal *et al.* [66] fabricated a pH sensor based on RuO₂ thin film sensing materials. It has been found that the sensor can be stored both in water and in air; and found to have sensitivity close to the Nernst behavior. However, it has also been found that RuO₂ based sensor not stored in water, can have drift in potential during initial measurements.

Later in 2015, Sardarinejad *et al.* [67] investigated RuO₂ based pH sensor and the influence of Ar/O₂ gas ratio during radio frequency (RF) sputtering on RuO₂. The

developed pH sensor consists in an RF sputtered ruthenium oxide thin-film sensing electrode, in conjunction with an electroplated Ag/AgCl reference electrode. The performance and characterization of the developed pH sensors in terms of sensitivity, response time, stability, reversibility, and hysteresis are investigated. Experimental results show that the pH sensor exhibits super-Nernstian slopes in the range of 64.33–73.83 mV/pH for Ar/O₂ gas ratio between 10/0–7/3.

Yao *et al.* [68] reported a pH electrode based on lithium carbonate melt-oxidized iridium oxide film with the composition of Li_xIrO_y·nH₂O. The electrode based on this oxide film exhibits promising pH sensing performance and high chemical stability, with an ideal Nernstian response 58.9 mV/pH over the pH range of 1 to 13. The electrode also shows a fast potential response with a 90% response time less than 0.2 s, and a low open-circuit potential drift 0.1 mV/day measured in pH 6.6 solution. The reproducibility in terms of the Nernst slopes and the apparent standard electrode potentials has been improved among electrodes within the same batch. However, the biocompatibility due to inclusion of lithium salt was not assessed. The iridium oxide-based solid-state micro-pH electrodes have been used in many clinical research studies, such as measuring extracellular pH in ischemic hearts, in bio-films and in esophagus tubes.

2.4 Polymers and poly nano-composite based pH sensor

In recent years, considerable interest has focused on development of chemical or biological sensors using functional polymers. Conducting polymers and as well as its nanocomposite could act as good candidates for replacement of popular glass pH electrodes [69]. The examples of pH chemical sensors using polymer-film-coated electrodes include electropolymerization of pyrrole, aniline, thiophene, or benzene derivatives [69]. However, the measurements of pH using the above-mentioned conductive polymers had poor reliability due to defects and pinholes present in the films structure.

Jamal *et al.* 2013 recently developed, a novel electrochemical pH sensor was fabricated through the use of an anthraquinone–ferrocene (AQ–Fc) complex based on a vertically aligned gold nanowire array electrode (AuNAE) (Fig. 2.2). In SWV measurements, the modified electrode was found to be linear over the range of pH 2–11, with a sensitivity of

1.38 $\text{pH}^1\text{cm}^{-2}$ at 25 $^{\circ}\text{C}$. The electrode was found to respond both in the presence and absence of oxygen, further expanding the potential applications to include de-oxygenated environments. Their sensor showed a potential drift of 1.0–3.3% after three hours and 95% of the signal was retained after one week [8].

The pH sensing properties of polyaniline (PANI), which belongs to the group of organic conducting polymers, were explored by Tsai *et al* [70]. The use of PANI receives attention due to its high conductivity, ease of synthesis, and its stability under ambient conditions. The spectral response in the pH range from 2.15 to 12.54 of PANI film deposited onto ITO glass employing constant-potential (0.80 V) electro-polymerization. These pH-dependent spectral variations of PANI films were explained by their transformation from the protonated to the unprotonated form.

Sha. *et al.* [71] report a grapheme-polyaniline (Gr-PANi) composite modified glassy carbon electrode (GCE) as an amperometric pH sensor. Gr-PANi composite was synthesized by electrodeposition of PANi on the surface of Gr modified GCE using the CV technique. XRD and Raman analysis confirmed high crystallinity of Gr-PANi composite. FESEM analysis revealed that Gr flakes are surrounded by PANi film because of the heterogeneous nucleation and growth of PANi during electro-polymerization. In acidic region, current of the composite-based pH sensor increased with decreasing pH values of the solution, whereas in alkaline region, current increased with the increasing pH values of the solution. The as-fabricated pH sensor exhibits shorter response time with an excellent sensitivity of $-50.14 \mu\text{ApH}^1\text{cm}^{-2}$ in the range of pH 1-5 and $139.2 \mu\text{ApH}^1\text{cm}^{-2}$ in the range of pH 7-11. The composite-based sensor showed enhanced sensitivity compared with pure Gr-based pH sensor because unlike pristine Gr-based pH sensor, it utilizes both charge-storage mechanisms in EDLCs and pseudo-capacitors, thereby resulting in excellent synergy between Gr and PANi. Reproducibility of the pH sensor was also examined between three different electrodes in the solution of pH 5. Insignificant variation in the current response suggested excellent reproducibility of pH sensor. Gr-PANi-based pH sensor offers a simple, low-cost, promising, real-time amperometric pH sensor in chemistry, clinical diagnostics, bio-sensing, and environmental monitoring application.

Clarke *et al.* [72] developed a new luminescence lifetime-based pH sensor system. The system is based on $[\text{Ru}(\text{Ph}_2\text{phen})_2\text{DCbpy}]^{2+}$ (DCbpy = 4,4'-dicarboxy-2,2'-bipyridine) immobilized in a mixed domain network copolymer utilizing hydrophobic regions in a hydrophilic, water-swellaable, poly(ethylene oxide) matrix. The metal complex binds irreversibly to the hydrophobic domains leaving the pH-sensing COOHs projecting into an aqueous-rich poly(ethylene oxide) region. The complex shows a strong pH dependence of its lifetime (3-4-fold) and provides a usable pH range of about 3-5. The long (approximately 1 micros) excited-state lifetime and visible absorption of the sensor simplifies measurements. It is a model for the combined pH and oxygen-quenching sensitivity of the complex is provided; this allows use of the pH system over a wide range of oxygen concentrations.

Vieira *et al.* [73] developed PANI nanostructures which were prepared by an interfacial polymerization method that enables the easy manipulation of polymer at molecular level by LbL technique. Self-assembled films of N-PANI doped with HCl alternated with PVS were successfully produced, characterized and applied as pH sensing membrane in SEGFET devices. PVS/N-PANI exhibited a Nernstian behavior in the pH range from 2 to 12, (sensitivity of ca. 58 mV pH^{-1} with small voltage drift), suggesting that nanostructured multilayer films could be a useful platform for pH sensing.

X. H. Yang *et al.* [74] was successfully prepared a pH-sensitive dye-doped CA-film-modified MPOF probe by using a liquid-phase coating method. Author demonstrated a kind of optical pH sensor that based on a pH-sensitive fluorescence dye-doped (eosin) cellulose acetate (CA) thin film modified micro-structured polymer optical fiber (MPOF). It was obtained by directly inhaling an eosin-CA-acetic acid mixed solution into array holes in a MPOF and then removing the solvent (acetic acid). The sensing film showed different fluorescence intensities to different pH solutions in a pH range of 2.5-4.5. Furthermore, the pH response range could be tailored through doping a surfactant, hexadecyl trimethyl ammonium bromide (CTAB), in the sensing film. By tailoring the pH response range with surfactants CTAB, the eosin-CA film-modified MPOF or eosin-CTAB-CA film-modified MPOF as an optical pH sensor probe showed both a short response time and a wide response range from pH 1.5 to 4.5. It also demonstrates new possibilities for applications of MPOF in the fields of optical microanalysis or in vivo biosensing, such as acidity detection in the human body.

Sotomayora *et al.* [75] describes the preparation of a polyaniline (Pani)±porous Vycor glass (PVG) nanocomposite and its use as sensing phase in an optical fibre pH sensor. Nanocomposites of Pani±PVG were prepared by in situ polymerisation of aniline absorbed inside the pores of a PVG (Corning 7930) with an average porous size of 8 nm. The optical sensor was constructed by fixing a PVG slide onto a distal end of bifurcated optical bundle, with a cyano-acrylic resin. The sensor response was found to be reversible in the pH range from 5 to 12 and linear from pH 7.4 to 9.5. Response times of 4, 8 and >16 min were obtained for slide thickness' of 0.5, 1 and 1.5 mm, respectively. Changes of temperature, ranging from 20 to 40.8 °C, showed minor effect on the dynamic range. Similarly, the ionic strength (0.15, 0.30 and 0.50 mol) and the nature of the ions (NaCl, KCl and NaClO₄) showed minor influence on the sensor response. Leaching of Pani was not observed and the sensor lifetime was determined as being at least 5 months. Pani±PVG nanocomposite is suitable for the construction of optical pH sensors, with good analytical performance, since the glass slides can be prepared with good reproducibility and durability. This sensor indicates that Pani±PVG nanocomposite is suitable for the construction of optical pH sensors. As long as the polymer is formed inside the pores of the glass, cross-linking and structural defects are avoided, leading the formation of well-orientated chains. In addition, the polymer is less prone to leach. Therefore, nano-composites can be produced with good reproducibility and long lifetime. As Pani possesses several acid groups with distinct pKa's, the sensor also shows an extended dynamic range and its response is only slightly influenced by ionic strength of the medium, since the emeraldine salt presents a highly charged surface.

2.5 Solid-state pH sensors

The miniaturized pH sensors are of great importance in biomedical and clinical applications. By taking advantage of all-solid-state configurations, the sensor size can be greatly reduced and the sensors can be mass produced with improved reproducibility. An all-solid-state pH sensor uses direct electrical contact between the pH sensitive membrane and the inner metal contact. Among pH sensitive membranes used in the fabrication of all-solid-state pH sensors, metal and metal oxides show clear advantages over other membranes, such as glass membranes [76] and polymer membranes [77], due to their well-defined metal/metal oxide interface and compatibility with micro fabrication techniques. As an all-solid-state pH sensor, ISFET has an insulator/metal interface.

Tong Lau *et al.* [78] developed a low-power, high sensitivity, very low-cost light emitting diode (LED)-based device developed for low-cost sensor networks was modified with bromocresol green membrane to work as a solid-state pH sensor. In this approach, a reverse-biased LED functioning as a photodiode is coupled with a second LED configured in conventional emission mode. A simple timer circuit measures how long (in microsecond) it takes for the photocurrent generated on the detector LED to discharge its capacitance from logic 1 (+5 V) to logic 0 (+1.7 V). The entire instrument provides an inherently digital output of light intensity measurements for a few cents. A light dependent resistor (LDR) modified with similar sensor membrane was also used as a comparison method. Both the LED sensor and the LDR sensor responded to various pH buffer solutions in a similar way to obtain sigmoidal curves expected of the dye. The pKa value obtained for this sensor was found to agree with the literature value.

Oujai *et al.* [79] developed a solid-state (free of internal electrolyte solution) reference electrode based on metallic silver is simply fabricated via a simple electro-deposition from AgNO_3 . Potentiometry is carried out to study the performance of the solid-state reference electrode in comparison with the commercial Ag/AgCl reference electrode. In addition, the proposed solid-state reference electrode has been integrated with the PPy-modified pH electrode to form an all-solid-state pH sensor, showing the capability of pH measurement. Absence of the internal solution leads to the pH sensor that is convenient to use and maintenance. In addition, the proposed pH sensor is possibly applied to biochemical and medical processes as well as flow infection analysis. Solid state reference electrode was fabricated by electrodeposited silver metallic layer on stainless steel rod. The potentiometric measurement showed that the potential of the silver reference electrode did not significantly change over the pH range of 2 to 10. The silver reference electrode, however, can be applied as a single-use reference electrode. The PPy-modified pH electrode was integrated with silver reference electrode to fabricate an all-solid-state pH sensor. The all-solid state-pH sensor based on conducting polymer showed the response slope of -46 mV/pH . The advantage of this approach is that the fabrication of the all-solid-state pH sensor is relatively simple, inexpensive and convenient for mass production and miniaturization.

Yan Wang *et al.* [80] reported a pH-sensitive material to fabricate all solid-state pH electrode was used Titanium nitride. The fabrication and the response performance of the

pH electrode were described in the paper. The TiN film electrode showed a linear response in the pH range 2-12 with a near-Nernstian response (-55 mV/pH). The response time was within 1 min, and the electrode had good reproducibility, stability, and low sensitivities for different species. Compared with the glass pH electrode, the electrode exhibited some advantages, for example, without activation, rapid response and high mechanical strength. In addition, the electrode performed excellently in a corrosion medium containing F^- (1M). Electrochemical behaviors of TiN electrode in Britton-Robinson buffer were studied with Electrochemical Impedance Spectroscopy (EIS).

M. Wajrak *et al.* [81] developed a pH-sensitive RuO_2 electrode that coated in a commercial cyanoacrylate adhesive typically exhibits very low pH sensitivity, and could be paired with a RuO_2 working electrode as a differential type pH sensor. However, such sensors display poor performance in real sample matrices. A pH sensor employing a RuO_2 pH-sensitive working electrode and a SiO_2 -PVB junction-modified RuO_2 reference electrode is developed as an alternative high-performance solution. This sensor exhibits a performance similar to that of a commercial glass pH sensor in some common sample matrices, particularly, an excellent pH sensitivity of 55.7 mV/pH, a hysteresis as low as 2.7 mV, and a drift below 2.2 mV/h. The developed sensor structure opens the way towards the development of a simple, cost effective, and robust pH sensor for pH analysis in various sample matrices. The attractive features of the developed pH sensing structure open the way towards the development of cost-effective, high-performance, and robust pH sensors for various applications.

T. M. El-Agez *et al.* [82] fabricated a solid-state pH sensor using a transparent conductive tin oxide film on a glass substrate. The coating of the glass substrate was achieved by a novel simple chemical vapor deposition (CVD) procedure. The response time of the pH sensor was substantially reduced when a thin graphite film was deposited onto the tin oxide conductive film. The sensor slope was found to increase as the temperature of the solution was increased. The performance of the sensor was investigated in the pH range from 0.3 to 11.0. A straight-line calibration graph was achieved throughout the whole range tested, especially when the solution temperature was 80 °C. The working pH range was found to decrease on the expense of the lower range as the temperature was decreased. Results obtained by the suggested sensor compares very well with conventional pH electrodes where the square of the correlation coefficient was 0.999.

Here author present a novel and simple method for the preparation of transparent conductive tin oxide films on a glass substrate. Diluted headspace tin tetrachloride vapors were focused on preheated glass substrates. Thus the formed solid-state conductive material is used as a pH sensor.

Yoon *et al.* [83] also reported an all-solid-state sensor for blood analysis. The sensor consists of a set of ion-selective membranes for the measurement of H^+ , K^+ , Na^+ , Ca^{2+} and Cl^- . The metal electrodes were patterned on a ceramic substrate and covered with a layer of solvent processible polyurethane (PU) membrane. However, the pH measurement was reported to suffer severe unstable drift due to the permeation of water vapor and carbon dioxide through the membrane to the membrane–electrode interface. For conducting polymer-modified electrodes, the adhesion of conducting polymer to the membrane has been improved by introducing an adhesion layer. For example, polypyrrole (PPy) to membrane adhesion is improved by using an adhesion layer, such as Nafion or a composite of PPy and Nafion.

Another problem that is common for all membrane-based solid-state sensors is the ill-defined membrane–metal interface. A large exchange current density is required to produce a reversible interface for a stable potentiometric sensor response. One approach to improving this interface is to use conducting polymers. Conducting polymers are electroactive π -conjugated polymers with mixed ionic and electronic conductivity. They are able to transduce an ionic signal into an electrical signal. Such polymers provide an interface between pH selective membranes and metallic transducers, which replaces the internal electrolyte of a conventional pH sensor. Research efforts have been made to utilize conducting polymers in a number of designs of all-solid-state miniaturized sensors. Electroactive π -conjugated polymers, like PANI and polypyrrole (PPy), are most commonly used in sensor fabrications.

2.6 Potentiometric pH sensors

Potentiometric pH sensors have two electrodes: one of them is fabricated from an inert metal and is used as a reference electrode (usually made from Ag/AgCl), while the other electrode has a pH-sensitive layer deposited onto it. When the sensor comes into contact

with a test solution, metal oxides adsorb hydrogen ions at the surface sites and thus change the valency of the oxygen atom. As a result, a potential difference is generated between the two electrodes (open circuit potential), and its magnitude is proportional to the pH of the solution. However, potentiometric metal oxide pH sensors exhibit drift, resulting in poor accuracy and frequent calibration, which makes them less favorable for medical applications. Various materials have been considered suitable for potentiometric pH sensors.

Shiu *et al.* [84] evaluated a electrochemically activated glassy carbon electrodes adsorbed with anthraquinonesulfonate species that showed potentiometric responses toward pH changes for pH range between 1 and 11, with a near Nernstian slope of about 56.4 mV/pH and a lifetime of more than one month. The effects of electrode pretreatment and preparation conditions, as well as the effects of interfering ions on the electrode response were studied. Such AQS-adsorbed electrodes could be prepared easily and showed near Nernstian response with changes in solution pH. Common ions did not show pronounced interference on the potentiometric responses. The electrodes usually offered a lifetime of at least two months for potentiometric measurements. There was no significant difference in the potentiometric behavior towards pH changes for the AQS-electrodes obtained by the three different preparation procedures described in this study.

Walaiporn *et al.* [85] developed a potentiometric pH sensor that responses of the HQS-doped PPy modified electrodes. The sensor showed a slope response of 50.54 ± 1.67 mV/pH (28°C), a linear working range of pH 2 to 12 and an average response time less than 100 seconds. Adhesion between the PPy film and the supported electrode was improved by adding oxalic acid (Ox) as a co-dopant, leading to better potentiometric responses. It was found that the HQS/Ox-doped PPy electrodes exhibited the greater slope response of 54.67 ± 0.70 mV/pH (28°C) and more stable than those of the HQS-doped PPy electrodes. A combination of X-ray photoelectron spectroscopy and time-of-flight secondary ion mass spectrometry was performed to investigate the surface composition and characteristics of the electrodes, including the chemical basis of electrode performance. Easy fabrication and excellent potentiometric responses to pH changes of the functionalized polypyrrole offer potential for a novel integrated pH sensor.

Li-Te Yin *et al.* [86] reported an electrochemical potential measurement instrument using a potentiometric method is designed. A novel signal processing circuit which can be used for the measurement of H^+ ion and urea concentration is presented. In this paper, a potentiometric method is used to detect the concentrations of H^+ ions and urea by using H^+ ion-selective electrodes and urea electrodes, respectively. The experimental data shows that this measuring structure has a linear pH response for the concentration range within pH 2 and 12, and the dynamic range for urea concentration measurement is in the range of 0.25 to 64 mg/dL. The designed instrumentation circuit possesses a calibration function and it can be applied to different sensing electrodes for electrochemical analysis. It possesses the advantageous properties of being multi-purpose, easy calibration and low cost. It is applied to the concentration measurements of pH value and urea by connecting hydrogen ion-selective electrodes and urea electrodes. The urea concentration is obtained by virtue of the measurement of hydrogen ion concentration of solution after the reaction of urea sensing electrode and urea solution. Its feasibility and accuracy are considered by practical measurements. In the same way, with different sensing electrodes, the instrument can be used for the electrochemical measurement of different objects by slight adjustment of internal program. The instrument has the advantageous properties of multi-purpose, easy calibration and low cost.

T. A. Alia *et al.* [87] developed a potentiometric method based on modified screen-printed and modified carbon paste ion-selective electrodes was described for the determination of lidocaine hydrochloride in different pharmaceutical preparations and biological fluids (urine and serum). It was based on potentiometric titration of lidocaine hydrochloride using modified screen-printed and carbon paste electrodes as end point indicator sensors. The influences of the paste composition, different conditioning parameters and foreign ions on the electrodes performance were investigated and response times of the electrodes were studied. The electrodes showed Nernstian response of 58.9 and 57.5 mV decade⁻¹ in the concentration range of 1×10^{-7} – 1×10^{-2} and 6.2×10^{-7} – 1×10^{-2} mol L⁻¹ for modified screen-printed and carbon paste electrodes, respectively. The electrodes were found to be usable within the pH range of 2.0–8.0 and 2.0–7.5, exhibited a fast response time (about 6 and 4) low detection limit (1×10^{-7} and 6.2×10^{-7} mol L⁻¹), long lifetime (6 and 4 months) and good stability for modified screen-printed electrodes. The electrodes were successfully applied for the determination of lidocaine hydrochloride in

pure solutions, pharmaceutical preparation and biological fluids (urine and serum) samples.

Y. Ma *et al.* [88] fabricated a novel potentiometric pH sensor based on TiN NTA. The electrode was characterized by SEM, TEM, EDS, XRD and Raman spectroscopy. potential application of new pH electrodes based on titanium nitride can be expected. The titanium nitride nanotube array (TiN NTA) electrode was fabricated through anodic oxidation of titanium and reduction and nitridation of TiO₂NTA. The obtained TiN NTA was vertically oriented and highly ordered with inner diameters of about 120 nm and a wall thickness of 15–20 nm. Open-circuit potentials were measured to evaluate the TiN TNA electrode related to pH sensitivity, response time, stability, selectivity, hysteresis and reproducibility in the pH range of 2.0–11.0 at 20 ± 1 °C. The prepared TiN NTA electrode exhibits a near-Nernstian slope of 55.33 mV per pH with the correlation coefficient value of 0.995. It shows good selectivity for H⁺ ions in the presence of cations and anions, especially in fluoride-containing media. It also has good stability and reproducibility with a response time of 4.4 s. These make it a promising candidate as a pH electrode sensor.

Flavia E. Galdino *et al.* 2015 recently developed a reagent less pH sensor based upon disposable and economical graphite screen-printed electrodes (GSPEs). The potentiometric pH sensor utilizes GSPEs which are chemically pretreated to form surface immobilized oxygenated species that, when their redox behavior is monitored, give a Nernstian response over a large pH range (1-13). An excellent experimental correlation is observed between the voltammetric potential and pH over the entire pH range of 1-13 providing a simple approach with which to monitor solution pH [89].

Recently published research [90] demonstrated a strategy for covalent grafting of fluorophores into a self-plasticized polymer matrix, and a plasticizer-free bulk optode microsphere sensor for sodium using the polymer–fluorophore composite. Two types of Nile Blue derivatives were synthesized by covalently grafting the Nile Blue structure into self-plasticized poly (n-butyl acrylate) via urea (NBurea) or amide (NB-amide) linkers. Modification of n-butyl acrylate with a suitable functional group into the polymer backbone for polymerization was followed by the reaction with Nile blue. The grafted NB-urea and NB-amide polymers prepared using this method can be used as fluoroionophore in ion selective optodes in the same way as commercial

chromoionophores, but with improved lifetimes [91]. Plasticizer-free fluorescent ion-sensing microspheres were prepared using the two polymer-fluorophore composite for sodium, and showed good selectivity toward potassium, calcium and magnesium. The measuring ranges of sodium ions were found as 10^{-1} – 10^{-4} M and 1 – 10^{-3} M, for NB-urea and NB-amide-PnBA, respectively, at physiological pH.

2.7 Calibration curve

Calibration is performed to compensate the potential change between the measuring and reference electrodes. To compensate for the pH electrode performance degradation over time, it must be recalibrated from time to time. This time period depends on the application and its unique conditions [92]. The principle of pH electrode sensing mechanisms which are based on glass or polymer membranes is well investigated and understood. Common to all potentiometric ion selective sensors, a pH sensitive membrane is the key component for a sensing mechanism. When the pH sensitive membrane separates the internal standard solution with a constant pH from the test solution, the potential difference E_a across the membrane is determined by the Nernst equation:

$$E = \text{constant} + (RT/F) \ln [H^+]$$

where R is the gas constant, T is the absolute temperature (K), F is the Faraday constant, and $[H^+]$ is the hydrogen ion concentration in mol/L. Replaced with $\text{pH} = -\log[H^+]$, the equation has a form as follows:

$$E = \text{constant} - (2.303RT/F) \text{pH} = \text{constant} - (\text{slope}) \text{pH}$$

Where $2.303RT/F$ is the slope of the line plot of E vs pH (also known as the slope factor), which is the basis of the pH electrode calibration curve. Strictly speaking, the activity of hydrogen ions should be used in the Nernst equation. However, in dilute solutions, activity of H^+ almost equals its molar concentration. In *in-vivo* and clinical applications, the molar concentration is used rather than the activity of H^+ . Using a series of calibration solutions, the response curve or calibration curve of a pH electrode can be experimentally determined by plotting the cell voltage vs. the pH of the calibration solution. The linear range of the calibration curve is applied to determine the pH in any unknown solution. The slope of the calibration curve within the linear range is used to determine the

response slope or electrode sensitivity in mV/pH. This response slope is an important diagnostic characteristic of the electrode; generally, the slope gets lower as the electrode gets old or contaminated [93]. For a pH sensor with a Nernstian response, the slope, calculated from $2.303RT/F$, is 59.16 mV/pH at 298 K. A useful slope range can be regarded as 50–70 mV/pH.

2.8 Analytical performance of the pH sensor

Sensitivity of the pH sensor: Sensitivity refers to the ratio of output change for a given input change. Another way to define sensitivity is to find the slope of calibration line relating the input to the output. A high sensitivity implies that a small change in input causes a large change in output. Here the sensitivity of a pH electrode is determined by the linear response slope of the pH electrode as defined by the Nernst equation. Typically, the electrode calibration curve exhibits a linear response range between a pH of 2 and 9. At very high and very low pH, there are deviations from linearity. The high detection end (high $[H^+]$, low pH) of most pH sensors is limited by the so-called acid error. The electrode reads higher than the actual pH in very acidic solutions. The mechanism of such an error is not well understood. The lower detection limit (low $[H^+]$, high pH) is often governed by the selectivity of the sensor [94].

Reproducibility/accuracy of the pH sensor: Accuracy is a measure of how close the result is to the true value; while reproducibility or precision is a measure of how close a series of measurements on the same sample are to each other. The accuracy and reproducibility of pH measurements can be highly variable and are dependent on several factors: electrode stability (drift and hysteresis), response slope/calibration curve, and accuracy of the pH meters. While some of these factors are determined by the properties of electrodes, some measures can be taken to improve measurement accuracy and reproducibility. The concentration is proportional to the measured voltage and so any error in voltage measurement will cause an error in the solution concentration. The measured voltage is the cell voltage including different potentials generated at all solid–solid, solid–liquid and liquid–liquid interfaces of both sensing and reference electrodes. The potential of the electrochemical cell, E_{cell} , is mainly given.

$$E_{\text{cell}} = E_{\text{pH}} - E_{\text{ref}} + E_j + E_{xy}$$

Where E_{pH} is the half-cell potential of the pH electrode, E_{ref} is the half-cell potential of the reference electrode, E_j is the liquid-junction potential, and E_{xy} is the interfering ions induced potential which affects the electrode's selectivity. Any variations in these potentials will cause changes in the overall cell voltages. Frequent recalibration can minimize potential drift, while using protection membranes can reduce the effect from interfering ions. Liquid-junction potentials develop at the interface between two electrolytes because of the differences in the migration rates of charged species across the interface. By using reference filling solutions with nearly equitransferent electrolytes such as KCl, in which both ions have similar mobility when diffusing through the liquid junction, E_j can be minimized. E_{pH} is more strongly dependent on temperature in most cases than E_{ref} and E_j are. Calibrations and measurements should therefore be carried out under temperature controlled conditions [95].

Stability and reliability: Poor operational stability due to drift has largely limited the long-term or implantable application of pH sensors. Some oxide-based electrodes present very high initial potential drift but their stability is improved after soaking for a certain amount of time ranging from hours to days [96]. Shelf-life also affects the storage stability of some sensors, such as glass electrodes. When all or most of the above properties are optimized, a reliable pH sensor system can be achieved for *in-vivo* measurements.

Biocompatibility: Biomaterials are inert substances that are used in contact with living tissue, resulting in an interface between living and non-living substances [97]. Biocompatibility of this interface is achieved by using such biomaterials for encapsulation in the construction of sensor devices. The interaction in an interface of device/tissue is limited by two factors. There is the corrosive environment, such as biological fluid, which contains salts and proteins among other cellular structures in which the sensor device must survive [98]. Second, there is the encapsulation material which may induce a toxic reaction due to poor biocompatibility and hemocompatibility [99]. It is crucial to use a biomaterial that can overcome both limiting factors to maintain the lifetime of the sensor device and protect the body [100].

The review has highlighted some novel approaches to the fabrication of electrochemical pH sensors. Several methods for the detection and measurement of pH have been described and compared. These sensors are scientifically relevant because they can be used for monitoring pH in biological and environmental fields. Some method enables multiple measurements and great sensitivity, but has very poor lateral and temporal resolution. Therefore the measurement itself generates its own measure and, which is very unfavorable.

Table 2.1: List of various pH sensing materials that has been used as pH sensors

Material	Detection Method	Advantages	Disadvantages	Ref.
AQ-FC/AQ-Sulfonate	Conducting polymer based pH sensor	Good stability over a wide pH range and first response	No information	8
Anthraquinonesulfonate	Potentiometric pH sensor	lifetime of more than one month.	No information	84
Polyaniline particles and polypyrrole	Conductimetric composite thick film pH sensor	No information	Adding polypyrrole need to higher voltages	101
Polyaniline	Conducting polymer pH sensor	Hydrofluoric acid don't influence the response of electrode	No information	102
polymeric film, poly(diallyldimethylammonium chloride) (PDDA) and poly(acrylic acid) (PAA)	optical fiber-based pH sensors	miniature sensor can easily be interrogated remotely	limited linear operating range of pH (from 4.66 to 6.02) due to the high RI of the coating	103
W/W ₂ O ₃ /WO ₃ /CuO	Metal oxide pH sensor	1) Good stability over a wide pH range even at high temperature, high pressure and aggressive environment 2) fast response	No information	54
IrO ₂	Metal oxide pH sensor	1) Good stability over a wide pH range even at high temperature, high pressure and aggressive	No information	104

		environment 2) fast response		
pAA-IOA, PEGD cross linker, AIBN initiator	Magnetoelastic pH sensor	Cheap fabrication	No information	105
an indium tin oxide, a silicon dioxide and a niobium pentoxide (ITO/SiO ₂ /Nb ₂ O ₅) layers	ISFET based pH sensors	Sensor has presented its potentials for rapid and low-cost hydrogen ion detection.	No information	106
Boron-doped silicon nano-wires (SiNWs)	ISFET based pH sensors	Small size and capability of nanowires for sensitive, label free and real time detection of a wide range of bio-chemical species		107
4-aminobutyltriethoxysilane, and 11- mercaptoundecanoic acid	silicon (SiO ₂) and silicon nitride (Si ₃ N ₄) microcantilevers , metal-modied (Au/Al) surfaces	This sensor can also be used under solution for detect biochemical reactions	No information	108

In this study, we fabricated a CuO nanoparticle based pH sensor. We choose CuO for sensing material because, CuO is a very promising material regarding it has low production cost and availability, improved stability, good morphological and structural control of the synthesized nanostructures, exceptional electrochemical activity, sensitivity, selectivity, biocompatibility and has the possibility of promoting electron transfer at a low potential. Furthermore, CuO is a well-studied wide band gap semiconductor (~1.2 eV) used for several applications as chromogenic material, sensing material, and catalyst. In conclusion, the development of novel pH sensors is still essential for their use in biological and environmental field.

Chapter-III

Experimental

Among metal oxides nanoparticle, cupric oxide (CuO) has been exhibited the excellent electrochemical behavior on glassy carbon electrode. The sensitivity of CuO nanoparticle modified glassy carbon electrode has been observed using cyclic voltammetry (CV), square wave voltammetry (SWV) and zero current potentiometry (OCP). Copper oxide nanoparticle was prepared by hydrothermal method and the nanoparticles appear as a brownish-black powder. Its surface morphology has been characterized by Energy Dispersive X-ray spectroscopy (EDX) and Scanning Electron Microscope (SEM). The brief information of this section are given below.

3.1 Reagent and material

Copper nitrate $\text{Cu}(\text{NO}_3)_2 \cdot 3\text{H}_2\text{O}$, hexamethylenetetramine (HMT), Ammonia $\text{NH}_3 \cdot \text{H}_2\text{O}$, were purchased from E. Merck, Germany. Disodium hydrogen phosphate (Na_2HPO_4), sodium dihydrogen phosphate ($\text{NaH}_2\text{PO}_4 \cdot 2\text{H}_2\text{O}$), sodium bicarbonate (NaHCO_3), sodium carbonates (Na_2CO_3), NaOH pellets, Nafion and chitosan were purchased from Sigma-Aldrich, India. All chemicals were of analytical grade with high purity. Different pH solutions were prepared using phosphate buffer, sodium hydrogen carbonate, sodium hydroxide, sodium acetate and acetic acid.

3.2 Equipments

SWV and zero current potentiometric (OCP) measurements were performed using a potentiostat / galvanostat (model: μStat 8400, DropSens (Spain)). Here three electrode cells has been used, where CuO/GCE were in use as a working electrode with Ag/AgCl and Pt wire acts as reference and counter electrodes, respectively. SWV measurements were conducted using a frequency of 50 Hz, pulse width of 20 mV and step height of 10 mV. The pH of the buffer solutions were perfectly determined using an Orion 2 Star

commercial pH meter. Morphology of the nanoparticle was examined using SEM and EDX. For the synthesis of nanoparticle crystal, steel autoclaves has been used.

3.3 Preparation of iridium oxide nanoparticles electrodeposition solution

Alkaline hydrolysis of iridium (IV) salt was used to synthesize iridium oxide nanoparticle dispersion. 2.0 mM aqueous K_2IrCl_6 solution was adjusted to pH 13 with 10 wt% of aqueous NaOH to obtain a yellow solution, which was then heated at 90°C for 20 minutes. The resulting solution was cooled to room temperature, and then kept in an ice bath to obtain a blue solution. The cold solution was then adjusted to pH 1 by rapidly adding 3 M HNO_3 and stirred continuously for 80 minutes until the solution became deep blue. The solution, which could be adjusted to pH 1–13 by addition of 10 wt% of aqueous NaOH solution, was then stored in a refrigerator at 2 °C [109].

3.4 Preparation of PANI electrodeposition solution

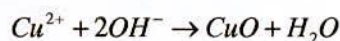
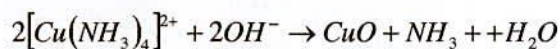
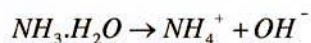
To electrochemical polymerization of aniline the solution consisted of 0.20M aniline and 0.60 M H_2SO_4 . An oxidation peak occurs on first cycle, which is caused by aniline oxidation that results in the polymerization of aniline. However, the peak shifts towards the third cycle because of the autocatalytic polymerization of aniline by polyaniline itself [110].

3.5. Preparation of CuO Nanoparticle

Hydrothermal method

The chemicals used will be of analytical grade without further purification. For the hydrothermal Synthesis of CuO Nanoparticle, 0.7345 g $Cu(NO_3)_2 \cdot 3H_2O$ and 0.8230g hexamethylenetetramine (HMT) were dissolved into 25 ml distilled water under magnetic stirring. After that 5.0 ml $NH_3 \cdot H_2O$ (5%) was introduced into the mixture under stirring, the clear solution was transferred into a Teflon-lined steel-stainless autoclave of 40 ml. The autoclave was allowed to cool down to room temperature naturally after the system had been hydrothermally treated at 160°C for 6 h. Black precipitates were collected,

washed with distilled water and ethanol several times to remove impurities. Finally, the precipitates were dried in air at 50°C for 6 h [111].



3.6 Modification the Working Electrode

It's essential to modify the working electrode for electrochemical analysis. Glassy carbon electrode is used in this purpose. For modification the glassy carbon electrode, CuO nanoparticle has been used. CuO nanoparticle has been synthesis by hydrothermal methods. A simple casting method has been used for the fabrication of CuO/GCE.

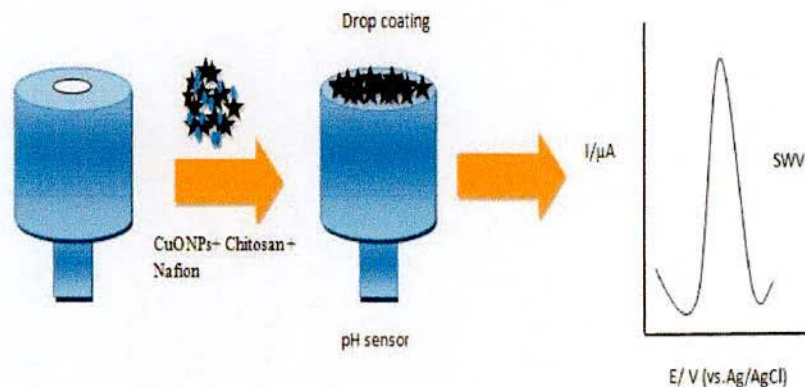


Figure 3.1: Schematic diagram of stepwise fabrication of Working Electrode

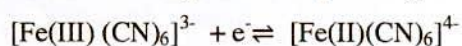
At first, GCE was polished with 1.0 and 0.3 μm alumina powder, followed by washing with water and sonication in ethanol and water respectively. A mixture of 0.2g CuO nanoparticle, 0.1g chitosan and 0.1 ml Nafion was dropped on to the clean surface of GCE, and dried at room temperature for overnight.

3.7 Preparation of different pH Solutions

pH 3-9 solutions were prepared using Phosphate buffer. 1.41 g Disodium Hydrogen Phosphate (0.01M), 1.56 g Sodiumdihydrogen phosphate (0.1M), 0.84 g Sodium hydrogen carbonate (0.1M), 0.4 g Sodium hydroxide (0.1M) ,13.6 g Sodium acetate (0.5 M), 2.9 mL of acetic acid (0.5 M) and made to 100 mL with DI water, the solution was adjusted to the appropriate pH with Orion 2 Star pH meter.

3.8 Standardization of the System

The whole electrochemical set-up was tested using a standard experiment. In the standard experiment we have studied the following redox couple at a glassy carbon (GC) electrode.



The reaction above was studied electrochemically by pumping electrons into the system from a GC electrode and by measuring the change in the flow of current during the reaction. This is done most conveniently by scanning the potential of the electrode at a constant rate.

In general, the peak current of diffusion controlled reversible or quasi-reversible electrochemical reaction follows Randles–Sevcik equation

$$I_p = 0.4463nF \frac{nFD}{RT} AC\sqrt{v}$$

Where, i_p : the peak current, n : the number of electrons, F : Faraday constant, T : the temperature in Kelvin, R : the gas constant, A : the surface area of the working electrode, D : the diffusion coefficient of the electroactive species, C : the bulk concentration of the electroactive species and v : the scan rate of voltammograms.

3.9 Electrochemical measurements

For CV experiments, the definite potential range vs. Ag/AgCl in a cell containing 20.0 mL of 0.1 M buffer solution were performed over the potentiostat. The surface of the electrodes is completely immersed. The cell is deaerated for 5 minutes with high purity

nitrogen gas. The solution has been kept quite for 10 seconds. To determine the potential window, electrochemical scanning is carried out with the supporting electrolyte to obtain the background voltammogram. And for SWV experiments, the voltage was switched directly from open circuit to the appropriate applied potential (vs. Ag/AgCl). Solutions were agitated for both buffer solution and cell media studies.

At first, studies were carried out with the modified electrode in 0.1 M buffer solutions containing pH in order to determine whether the performance is suitable for the subsequent monitoring of the pH response. SWV was performed by applying a potential to the electrode immersed in a 20 ml of 0.1M buffer solution. The resulting real potential time responses were recorded over a period of time.

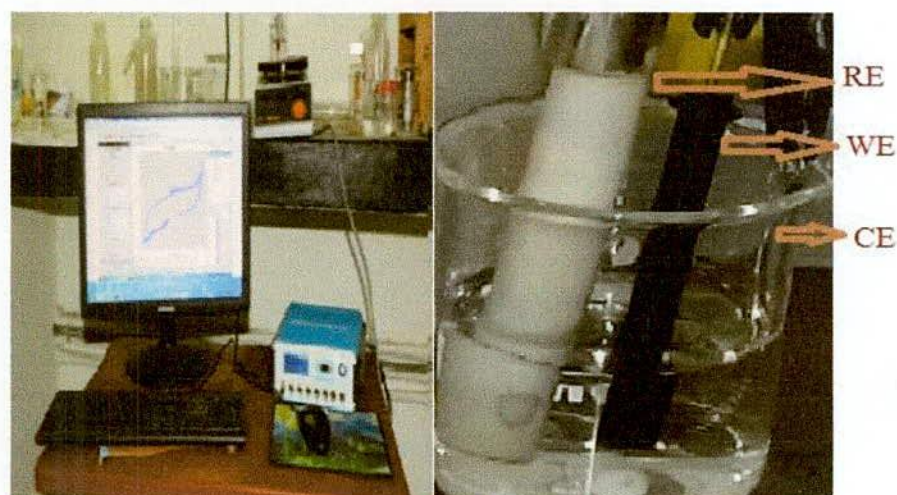


Figure 3.2: Electrochemical experimental setup

3.10 Reproducibility and Repeatability of the pH sensor

For the checking of CuO nanoparticle modified working electrode's output response for stability, reproducibility and repeatability, the sample was tested three to four times in an PBS buffer saline with pH ranging from 3 to 9. It was observed that the CuO NPs showed stable potentiometric response, excellent reproducibility, and good sensor stability.

3.11 Drift and Stability of the pH sensor

SWV was recorded every 30 min for three hours in three buffer solutions with a pH of 5, 7 and 9 to determine the signal drift. The three states of chosen solutions were presented as: acidic, basic and neutral. Which shows that the signal may take between 0 and 30 minutes to stabilize, depending on the pH. To measure the stability, the signal was recorded up to 7 days.

3.12 Effect of Oxygen on the pH sensor

It is required to remove oxygen because Dissolved oxygen can interfere with observed current response. Experimental solution was indolent by purging for at least 5-10 minutes with 99.99% pure and dry nitrogen gas (BOC, Bangladesh). In this way, dissolved oxygen were removed from the solution.

3.13 Real sample test

In different researchers evident from the previous work that new electrode which are proposed to for the sensing of pH usually avoid applying them for the sensing pH in real unbuffered samples. However, in this work, we have validated our sensor against the laboratory standard glass pH electrode in the real sample: malt vinegar and antacid. The next chapter we will describe more about result and discussion on the development of CuO pH sensor.

Chapter IV

Results and discussion

4.1 Electrochemical setup standardization

CVs of ferricyanide at glassy carbon electrode were performed at a concentration of 2mM of ferricyanide 0.1 M KCl as supporting electrolyte, and each solution was scanned at different scan rate equal to 20, 40, 60, 80, 100, 120, 140, 160 mV/s. The resultant CV curves and the electrochemical parameters are shown respectively in Figure 4.1 and Table 4.1.

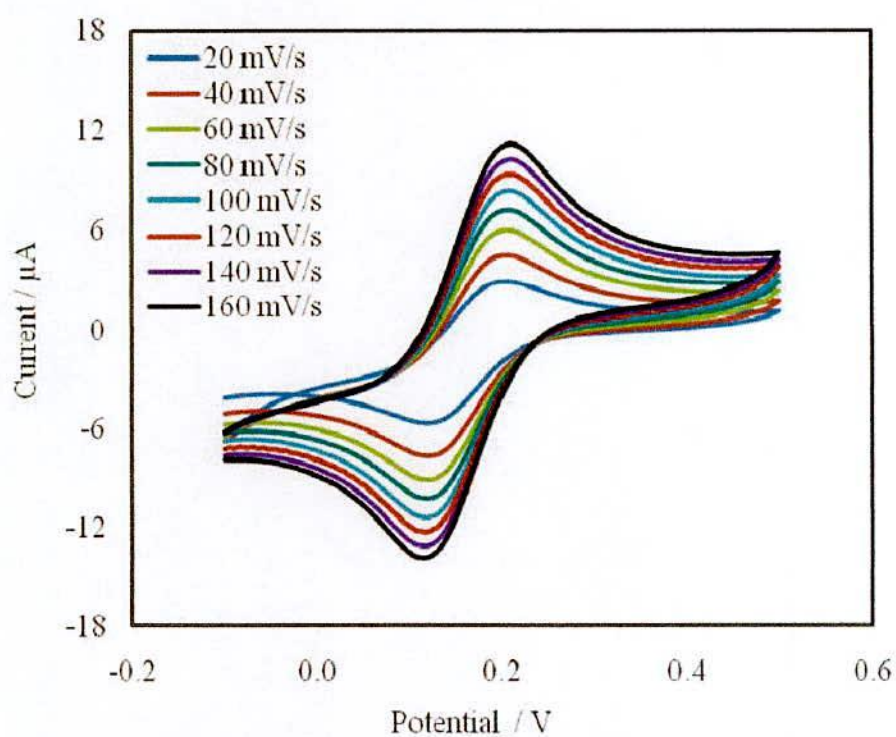


Figure 4.1: CV of Ferricyanide based on GCE at concentration of 2mM of Ferricyanide in 0.1 M KNO₃ as supporting electrolyte, scan rate of 20, 40, 60, 80, 100, 120, 140, 160 mV/s

Table 4.1: Electrochemical parameters obtained from voltammograms using Ferricyanide (from Figure 4.1)

scan rate Vs ⁻¹	SQRT of scan rate v ^{1/2}	anodic peak potential (E _{pa})	cathodic peak potential (E _{pc})	anodic peak current (i _{pa})	cathodic peak current (i _{pc})	i _{pa} /i _{pc}
0.02	0.141421	0.19	0.11	3.814	-3.654	1.0437
0.04	0.20	0.19	0.11	4.683	-4.632	1.0110
0.06	0.244949	0.19	0.10	5.839	-5.432	1.0749
0.08	0.282843	0.19	0.11	7.011	-6.432	1.0900
0.10	0.316228	0.19	0.11	7.961	-7.765	1.0258
0.12	0.34641	0.19	0.10	8.891	-8.632	1.0301
0.14	0.374166	0.19	0.11	9.659	-9.562	1.0101
0.16	0.4	0.19	0.11	9.821	-9.486	1.0353

v = scan rate; v^{1/2}= SQRT of scan rate; E_{pa}= anodic peak potential; E_{pc}= cathodic peak potential; i_{pa}= anodic peak current; i_{pc}= cathodic peak current.

In general, the peak current of diffusion controlled reversible or quasi-reversible electro-chemical reaction follows Randles-Sevcik equation

$$I_p = 0.4463nF \sqrt{\frac{nFD}{RT}} AC \sqrt{v}$$

Where i_p: the peak current, n: the number of electrons, F: Faraday constant, T: the temperature in Kelvin, R: the gas constant, A: the surface area of the working electrode, D: the diffusion coefficient of the electro active species, C: the bulk concentration of the electro active species and v: the scan rate of voltammograms. Thus, if we know the value of diffusion coefficient of ferricyanide at 298K the surface areas for ferricyanide are calculated from the slope of the plot of i_p versus \sqrt{v} (Figure 4.2).

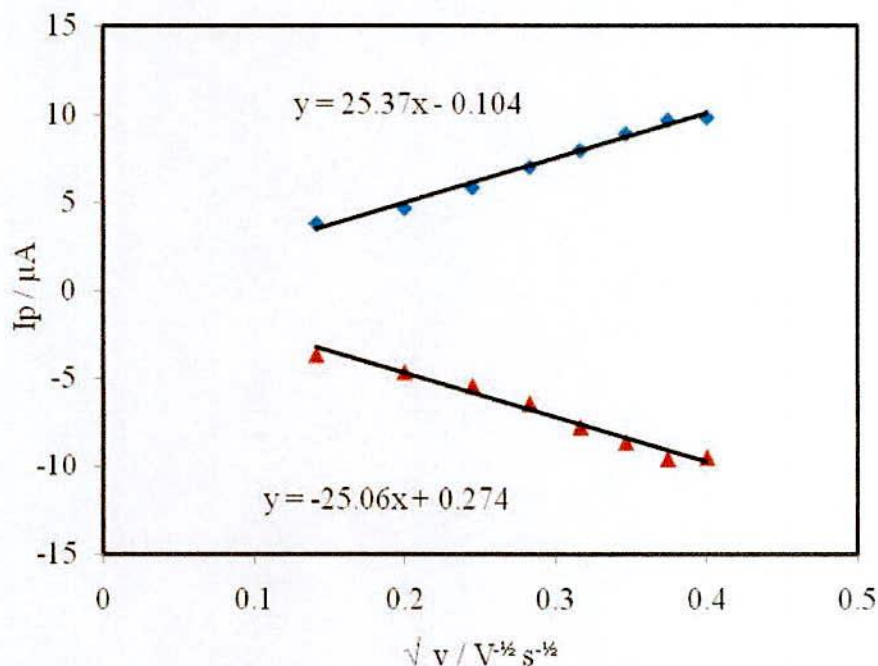


Figure 4.2: The anodic and the cathodic peak heights as function of the square root of the scanning rate for glassy carbon electrode

From Equation (1) we get,

$$\text{Slope} = 0.4463nF \sqrt{\frac{nFD}{RT}} AC$$

$$A = \frac{\text{Slope}}{0.4463nF \sqrt{\frac{nFD}{RT}} C}$$

From the curve (Figure 4.2) the value of slope is 25.37×10^{-6} and the standard value of diffusion coefficient for ferricyanide in GCE is $1.52 \times 10^{-6} \text{ cm}^2/\text{s}$. where concentration $C = 2 \times 10^{-6} \text{ mol/cm}^3$ so we get,

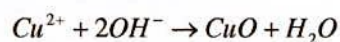
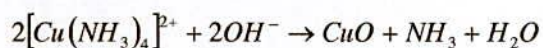
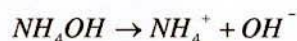
$$A = \frac{25.37 \times 10^{-6}}{0.4463 \times 1 \times 96500 \sqrt{\frac{1 \times 96500 \times 1.52 \times 10^{-6}}{8.314 \times 298}} \times 2 \times 10^{-6}}$$

$$A = 0.029 \text{ cm}^2$$

From the theoretical value, the surface area of GC electrode, i.e. used for the experiment is 0.03cm^2 . We show that the experimental value of the surface area is very close to theoretical value. This calculated result has been used in further studies. Also it proves that the electrochemical work station uses with minimum interferences.

4.2 Synthesis of nanoparticle and its physical characterizations

The morphology of the hydrothermally synthesized CuO nanoparticles was observed by SEM with a magnification of (5000X to 50,000X) (Fig. 4.3). A flower shape CuO nanostructure can be seen that the particle sizes are less than 100 nm width of each rod. According to the EDX datas (Fig. 4.4), the average content of copper (Cu) and oxygen (O) is 8.09% (atomic percentage) and 7.17% (atomic percentage) respectively, which confirm the copper oxide (Cu: O=1:1) component. However, C peak appeared, possibly from sample holder. Due to the higher in density of nanostructure, flower like CuO has a huge potential, as high surface area would improve the sensitivity of the current response. Therefore, from all the characterization results, it can be concluded that the hydrothermally synthesized CuO nano particle is formed with a flower like shape with particle size was estimated to be approximately 100 nm. The reduced nano particle size has higher surface area that exposed to the test environment and better response to pH changes [111].



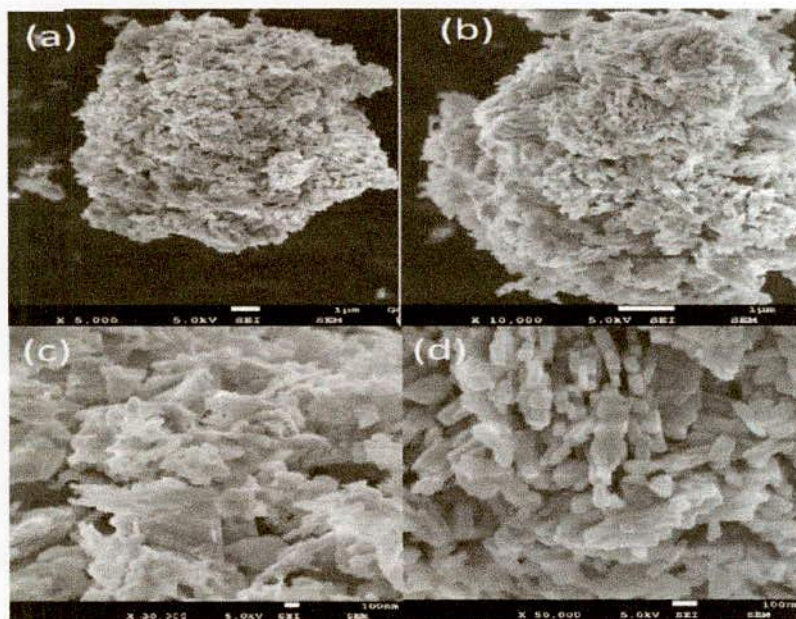


Figure 4.3: (a-d) Scanning electron microscopy (SEM) images of CuO nanoparticles at different magnifications (5000 to 50000X)

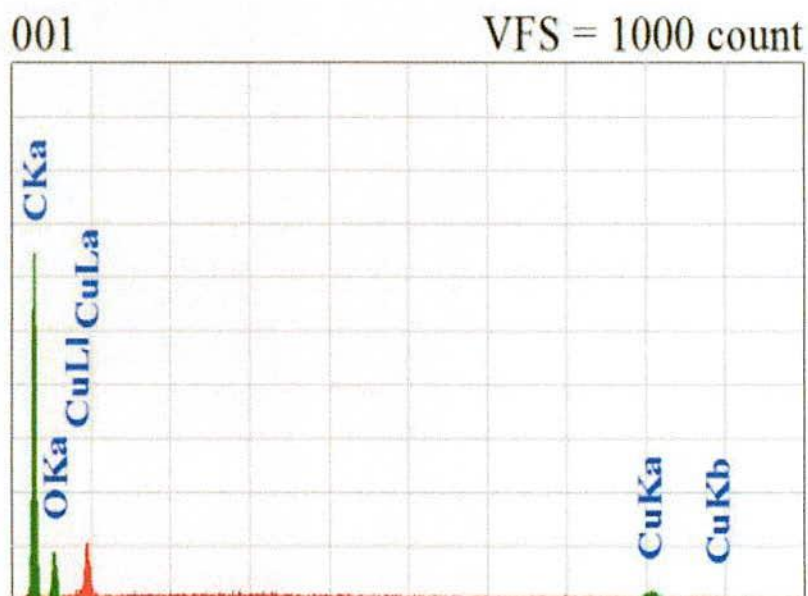


Figure 4.4: Energy Dispersive X-ray spectroscopy (EDX) images of CuO nanoparticles

4.3. Sensor fabrication

A simple casting method has been used for the fabrication of CuO/GCE [112]. At first, GCE was polished with 1.0 and 0.3 μm alumina powder, followed by washing with water and sonication in ethanol and water respectively. A mixture of 0.2g CuO nanoparticle, 0.1g chitosan and 0.1 ml Nafion was dropped on to the clean surface of GCE, and dried at room temperature for overnight (Figure 4.5).

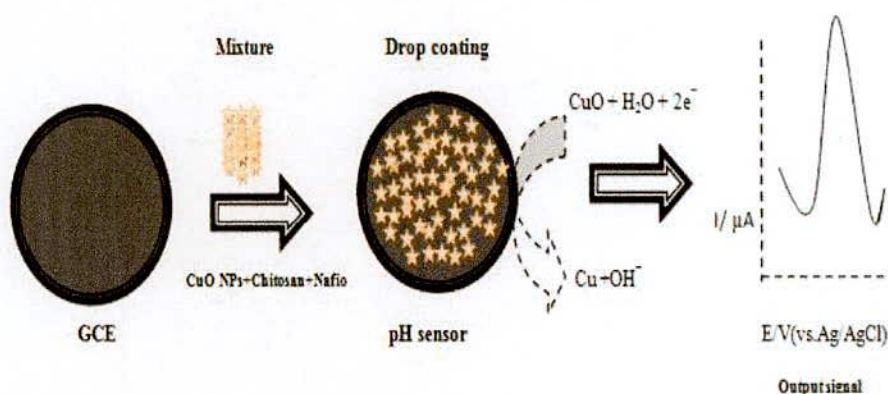


Figure 4.5: Schematic diagram of stepwise fabrication of the pH sensor

4.4 Electrochemical characterization of CuO nanoparticle modified GCE

To demonstrate the sensing application of CuO/GCE, it was constructed by deposition of the aqueous dispersion of nanoparticle on GCE surface in the presence of chitosan and Nafion (Figure 4.6). Nafion is an anionic ion exchange resin, which facilitates holding CuO on the surface of the electrode, as well as block anionic interferences. To investigate the properties of modified electrode, cyclic voltammograms (CVs) with different scan rates have been conducted with scan rates of 60-160 mVs^{-1} . On the increase of both anodic and cathodic current linearly with the scan rates, indicating that the electrochemical reaction is surface controlled (Figure 4.6). The current increases with scan rate for the sensor shows no significant resistance on the electrode surface [113].

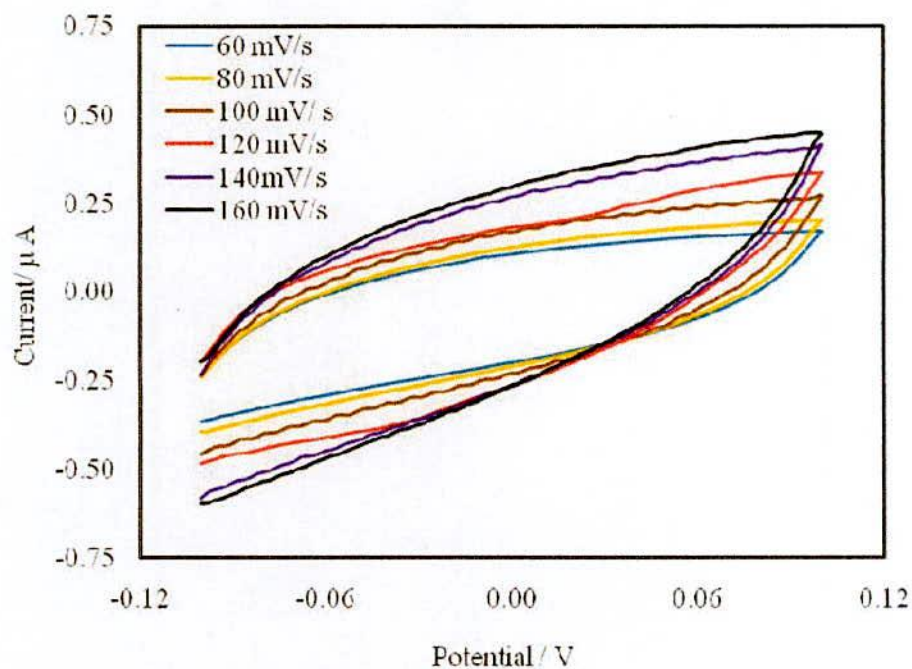


Figure 4.6: CVs detailing the effect of scan rate (60 - 160) mV / s using CuO/GCE at 0.1M PBS

4.5 Electrochemical characterization of bare GCE

We investigated the electrochemical behavior of bare GCE using CV (Figure 4.7) and SWV (Figure 4.8) in 0.1 M buffer solution with pH ranging 3 to 9 at a scan rate of 0.05 Vs^{-1} . It is seen that bare GCE exhibits two peaks at potential around 0.02 and -0.15 V with different pH value, and no linear relation has been obtained with pH changes (Figure 4.9). From this, it can be concluded that the bare GCE cannot sense pH change.

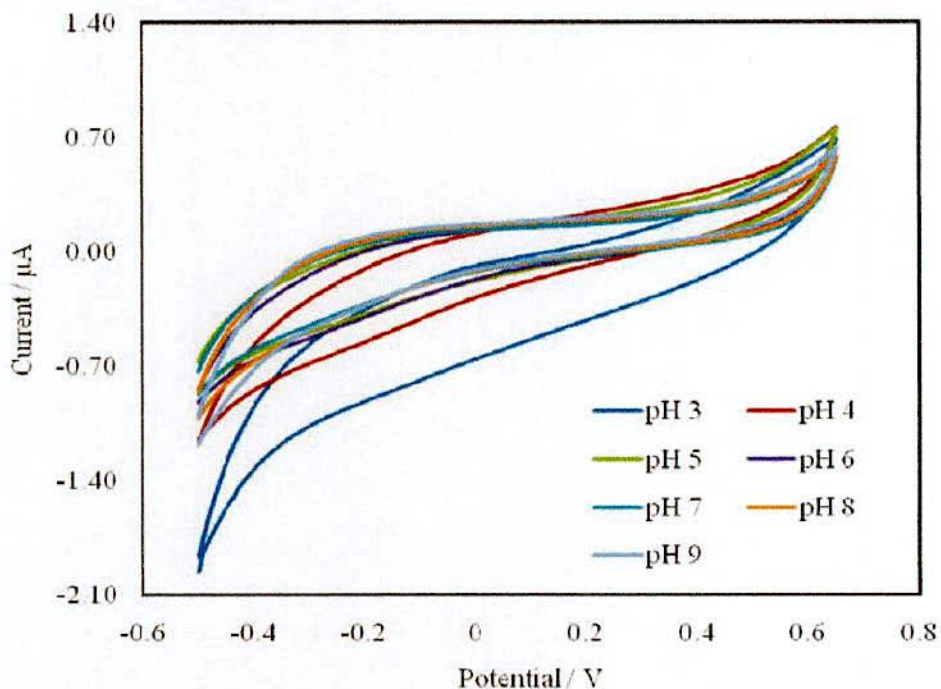


Figure 4.7: CVs of 0.1 M buffer at different pH values (3-9) on bare GCE

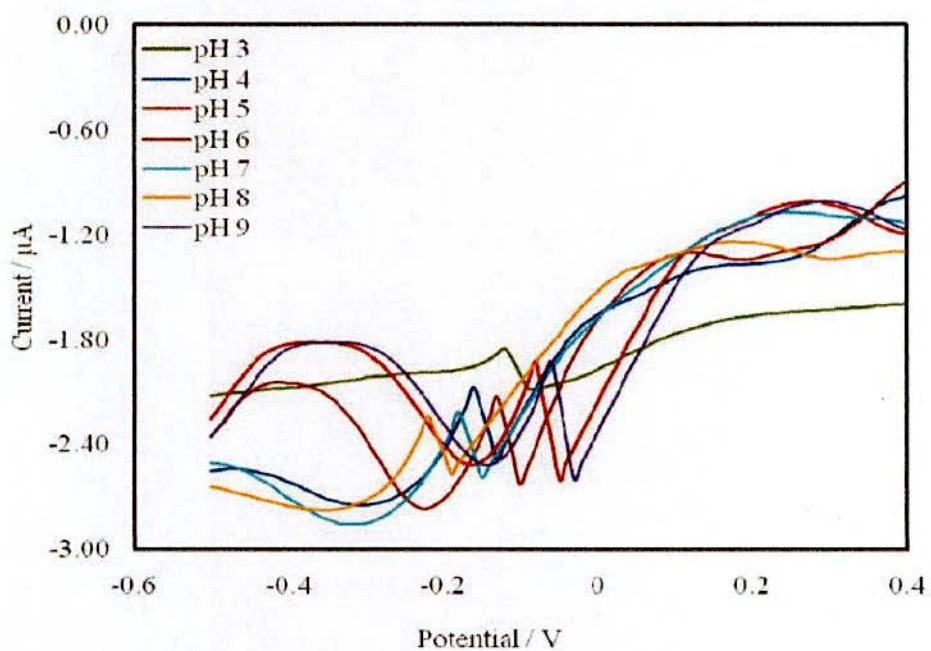


Figure 4.8: SWV of bare GCE at different pH values (3-9) on bare GCE in 0.1M PBS buffer

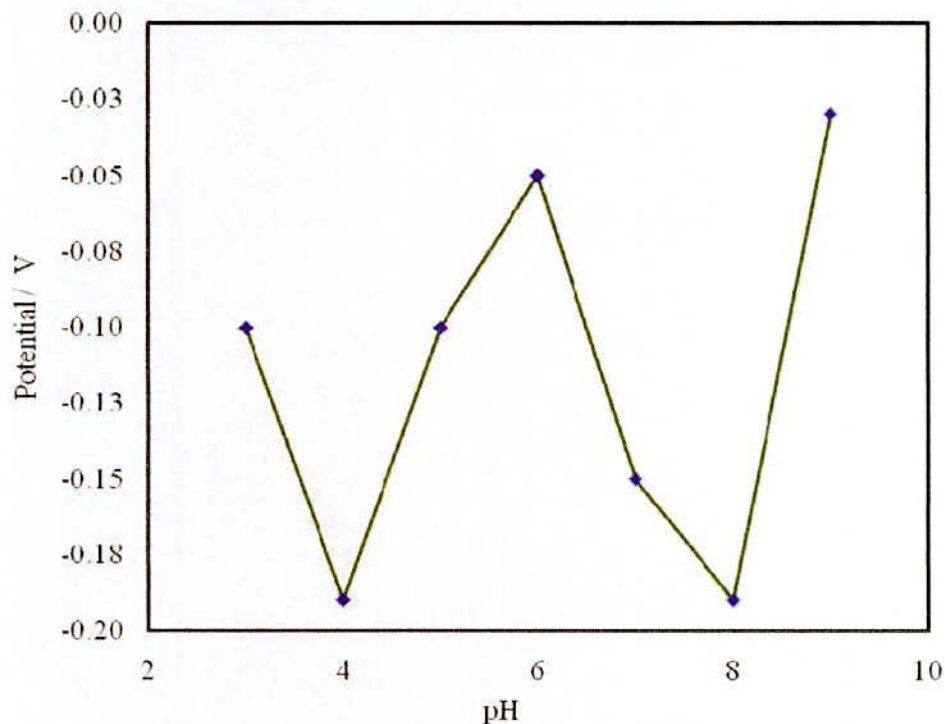


Figure 4.9: pH sensitivity measured from pH 3 to 9 at bare GCE

4.6 Electrochemical characterization of polyaniline modified PGE

At first, we discuss the electrochemical behavior of PANI modified PGE (PANI/PGE). The modification system (Figure 4.10) shows the electrochemical polymerization of aniline on a bare pencil graphite electrode. After that, Using SWV (Figure 4.11) by the modified electrode, it is seen that PANI modified PGE exhibits peak potential with different pH values, but their potential shift changes is randomly. That's why the total potential change is irregular and no potential change is linearly (Figure 4.12) obtained for PGE. It can be concluded that the PANI/PGE cannot sense pH.

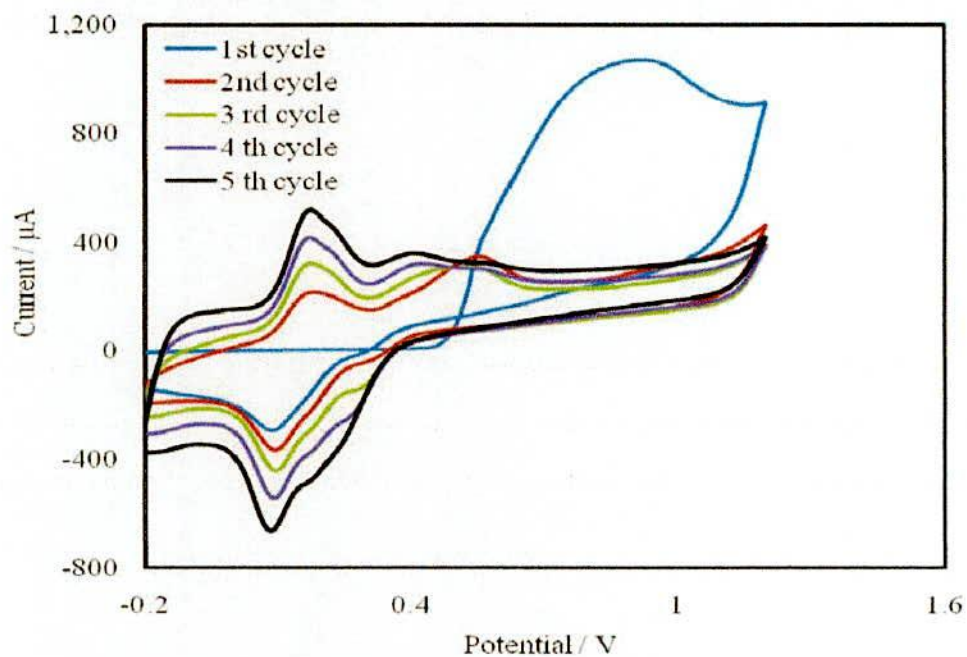


Figure 4.10: CVs of electrochemical polymerization of aniline on bare PGE

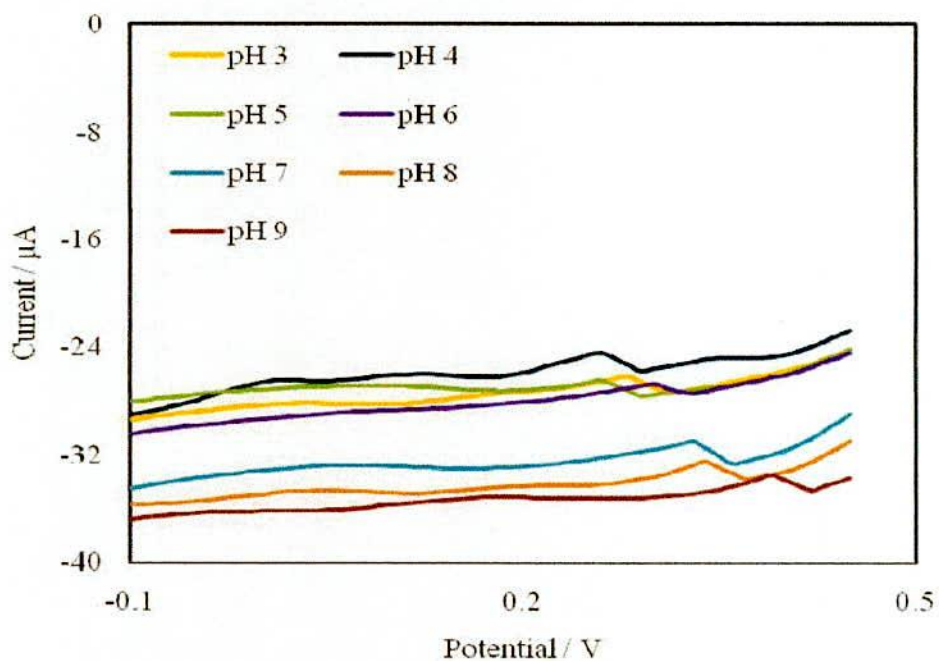


Figure 4.11: SWV of 0.1M PBS buffer at different pH values (3-9) on PANI/PGE

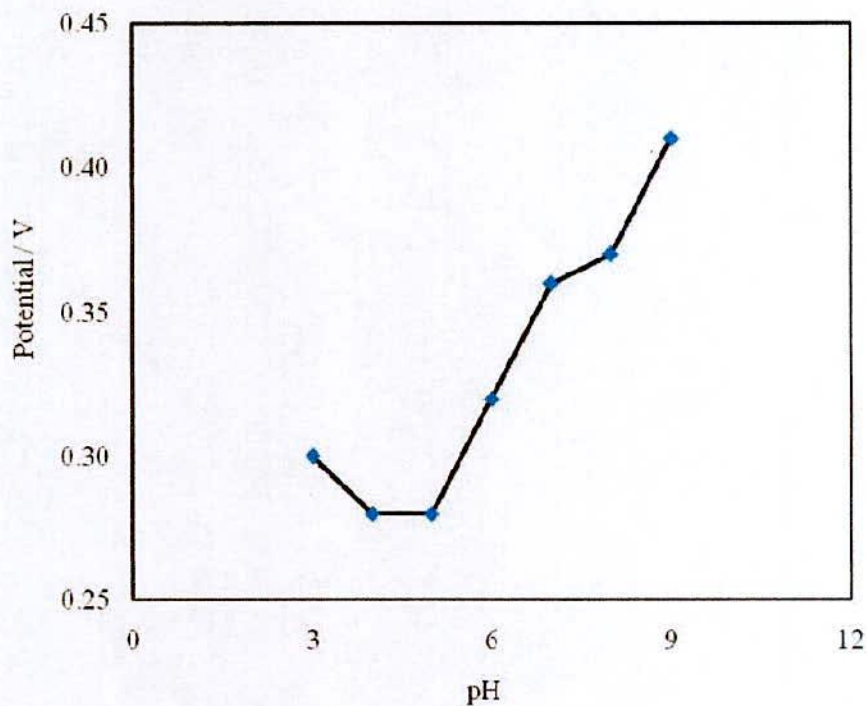
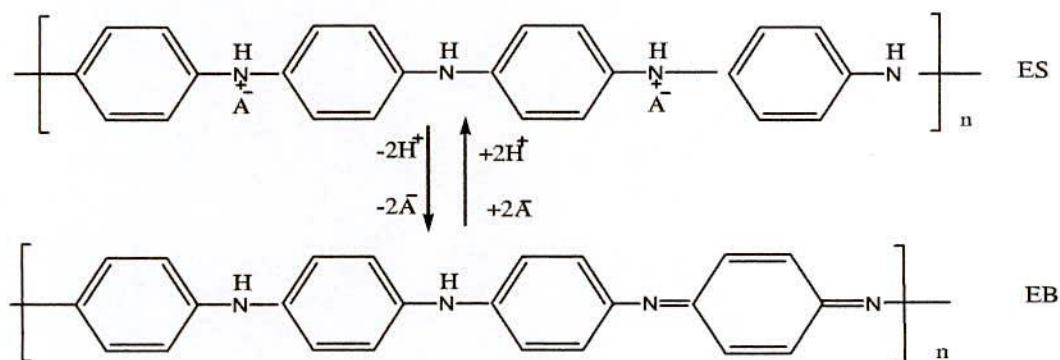


Figure 4.12: pH sensitivity measured from pH 3 to 9 using PANI/PGE

4.7 Electrochemical characterization of polyaniline modified GCE

Then, we investigated the electrochemical behavior of PANI modified GCE (PANI/GCE). Here, pH dependent interface potential variation corresponding to the ES-EB transition of PANI film that is normally used in PANI film based potentiometric pH sensors (following equation).



The modification CVs (Figure 4.13) shows the electrochemical polymerization of aniline on a bare GC electrode. After using SWV (Figure 4.14) it is seen that PANI modified GCE exhibits peak potential shift with different pH values, but linear from pH range 3-6 (Figure 4.15). It can be concluded that PANI/GCE may not be acts as a good pH sensor.

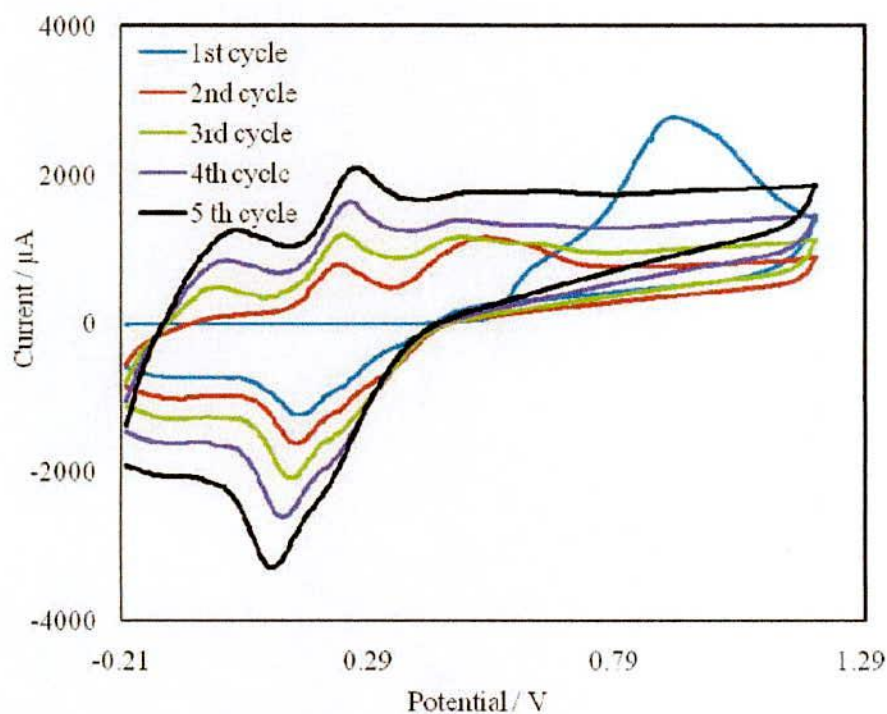


Figure 4.13: CVs of electrochemical polymerization of aniline on bare GCE

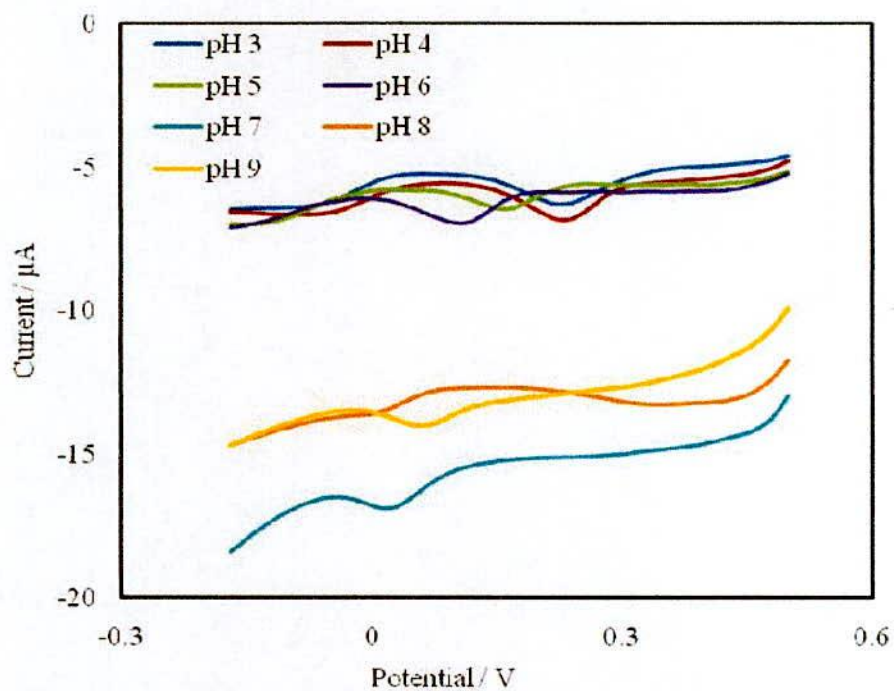


Figure 4.14: SWV of 0.1 M PBS buffer at different pH values (3-9) on PANI/GCE

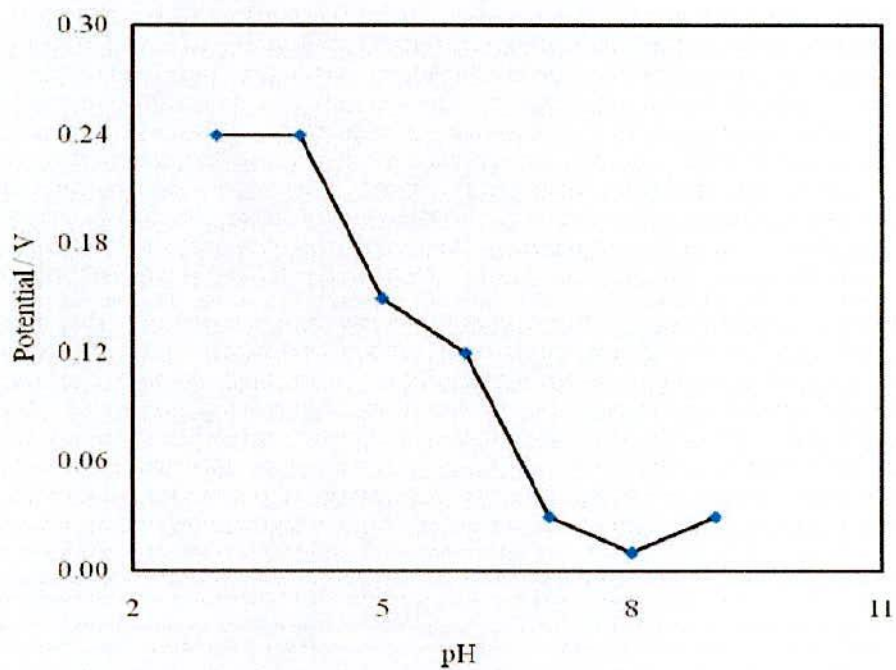
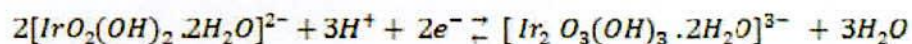


Figure 4.15: pH sensitivity measured from pH 3 to 9 using PANI/GCE

4.8 Electrochemical characterization of iridium oxide nanoparticle modified GCE

After investigated the electrochemical behavior of PANI modified PGE and GCE electrode, now we discuss the electrochemical behavior of iridium oxide nanoparticle modified GCE. At first nanoparticle was electrodeposited on GCE using CV between -0.5 to 0.65V (Figure 4.16) and pH response has been investigated using SWV (Figure 4.17) and found to be linear from pH range 3 to 6. The sensing

However, weak response has been obtained from pH range 3 – 9 and not exactly linear (Figure 4.18). It can be concluded that may be the reason of electrochemical deposition of Iridium Oxide nanoparticle on narrow electrode surface area the Iridium oxide nanoparticle is weak sensing system to sense pH. In a general way, the oxidation-reduction of the hydrated iridium oxide taking place on the surface of the electrode can be written as follows:



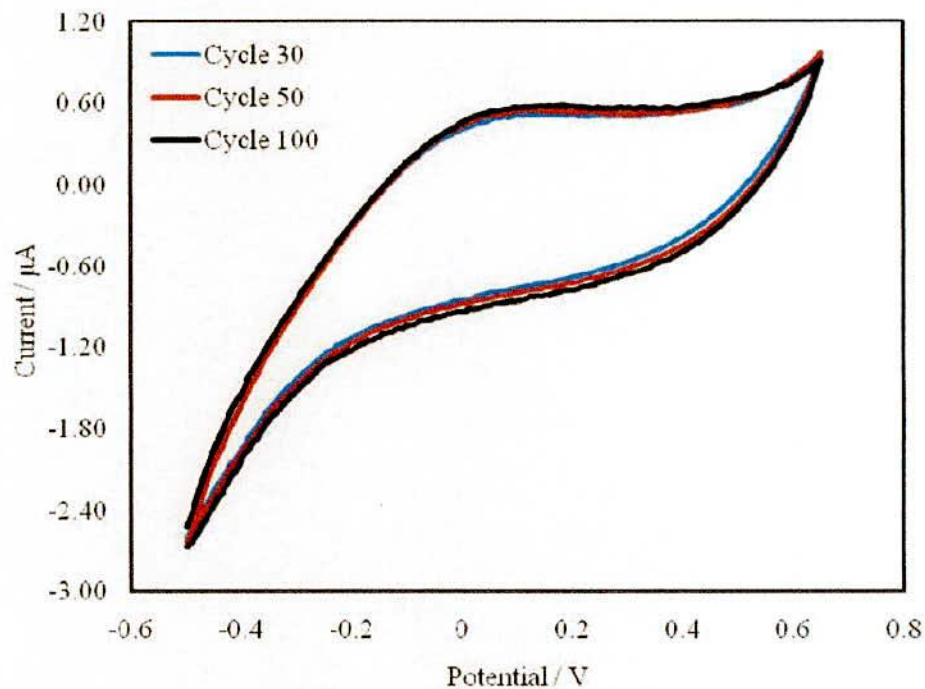


Figure 4.16: CVs of electrodeposition of Iridium Oxide nanoparticle using bare GCE

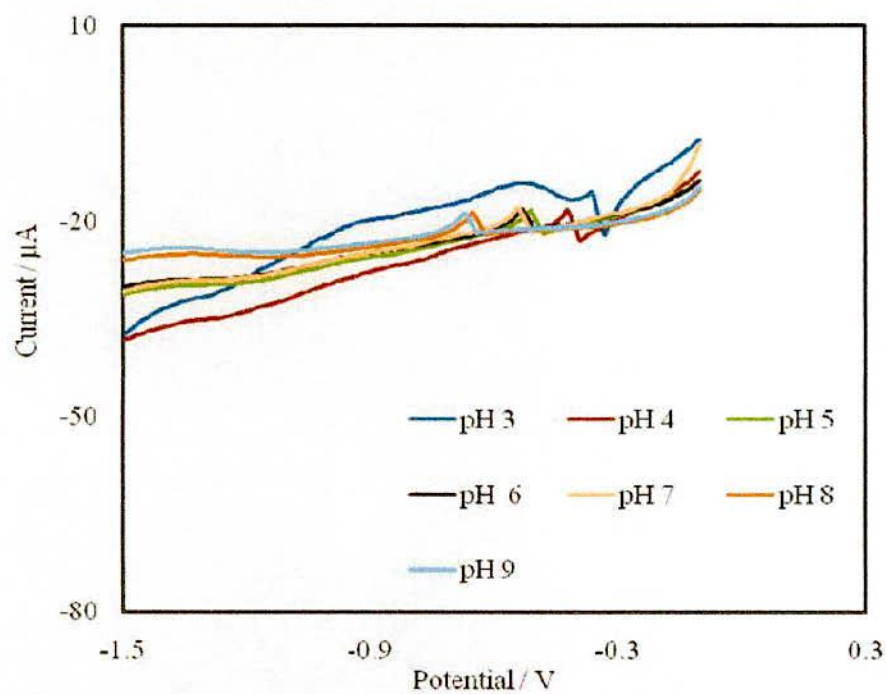


Figure 4.17: SWV of Iridium Oxide nanoparticle/GCE in 0.1 M buffer at different pH values 3 to 9

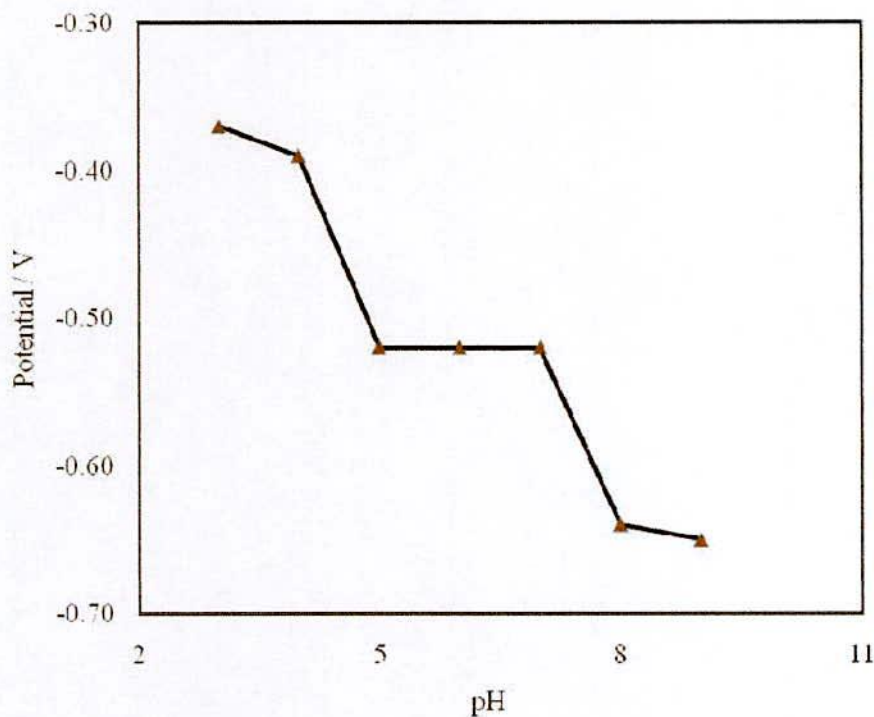
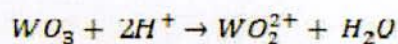
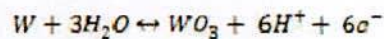


Figure 4.18: pH sensitivity measured from pH 3 to 9 using Iridium Oxide nanoparticle/GCE

4.9 Electrochemical characterization of WO_3 /PGE using SWV

Now, we discuss the electrochemical behavior of WO_3 nanoparticle modified PGE. At first, WO_3 nanoparticle was modified on PGE, that's collected from my group and then their electrochemical behavior was investigated using CVs (Figure 4.19) and SWV (Figure 4.20) of WO_3 modified PGE in 0.1M different pH value at scan rate of 0.05 VS^{-1} . It is seen that WO_3 / PGE exhibits peak potential with different pH values, and their potential change is randomly. For this reason the total potential change is irregular and no potential change is linearly (Figure 4.21) obtained for WO_3 / PGE. From this it can be concluded that the WO_3 /PGE can not sensing pH. The following equations are:



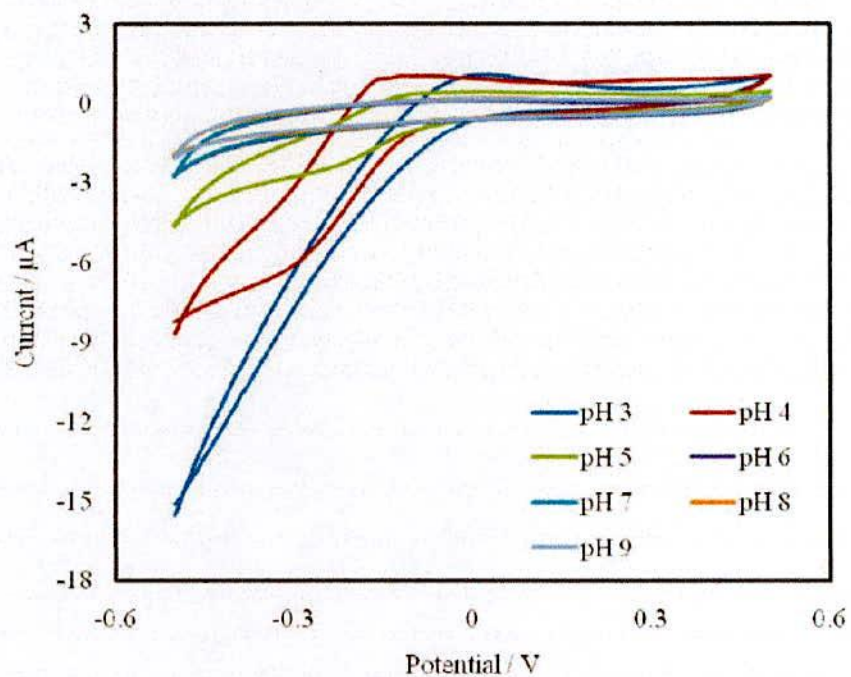


Figure 4.19: CVs of 0.1 M buffer at different pH values in the presence of WO_3/PGE (scanrate 0.05 V / s)

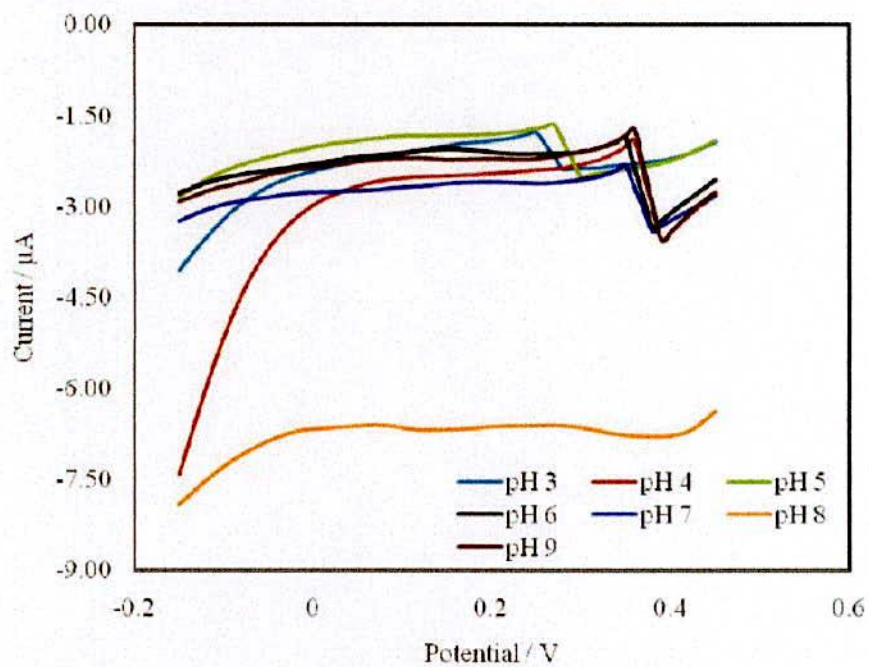


Figure 4.20: SWV of WO_3/PGE at different pH values (3 to 9) in 0.1 M PBS buffer

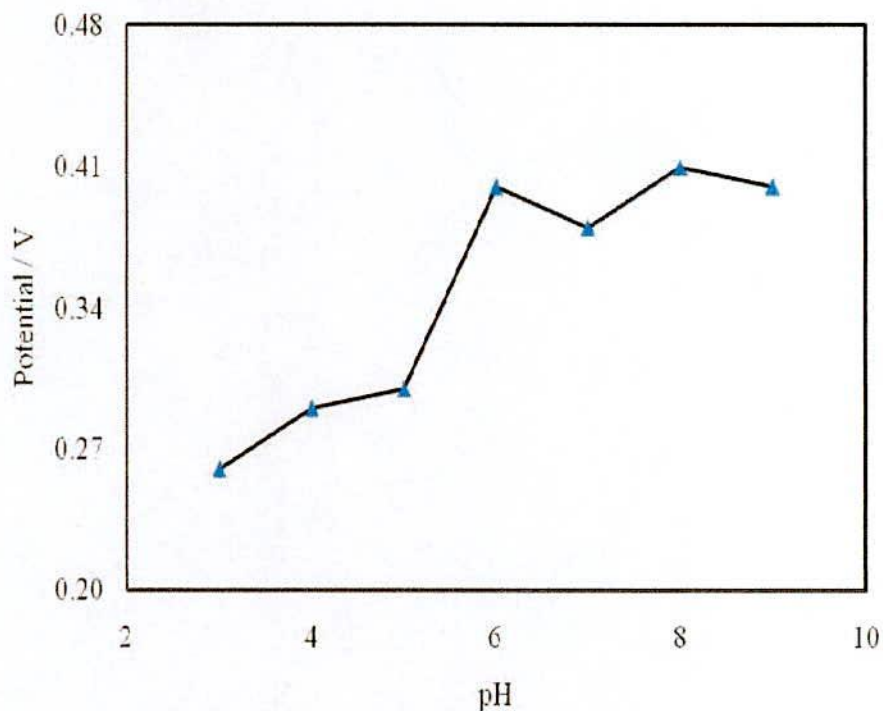


Figure 4.21: pH sensitivity measured from pH 3 to 9 using WO_3/PGE

4.10 Electrochemical characterization of CuO /PGE using SWV

We investigated the electrochemical behavior of CuO nanoparticle modified PGE. At first, CuO nanoparticle was modified on PGE and then their electrochemical behavior was investigated using CVs (Figure 4.22) and SWV (Figure 4.23) in 0.1M different pH value at scan rate of 0.05 V s^{-1} .

It is seen that CuO /PGE exhibits peak potential with different pH values (3 – 9) but their potential positively changed. For this reason the total potential change is irregular and no potential change is linearly (Figure 4.24) obtained negatively for CuO/PGE . From this it can be concluded that the CuO/PGE can not sensing pH.

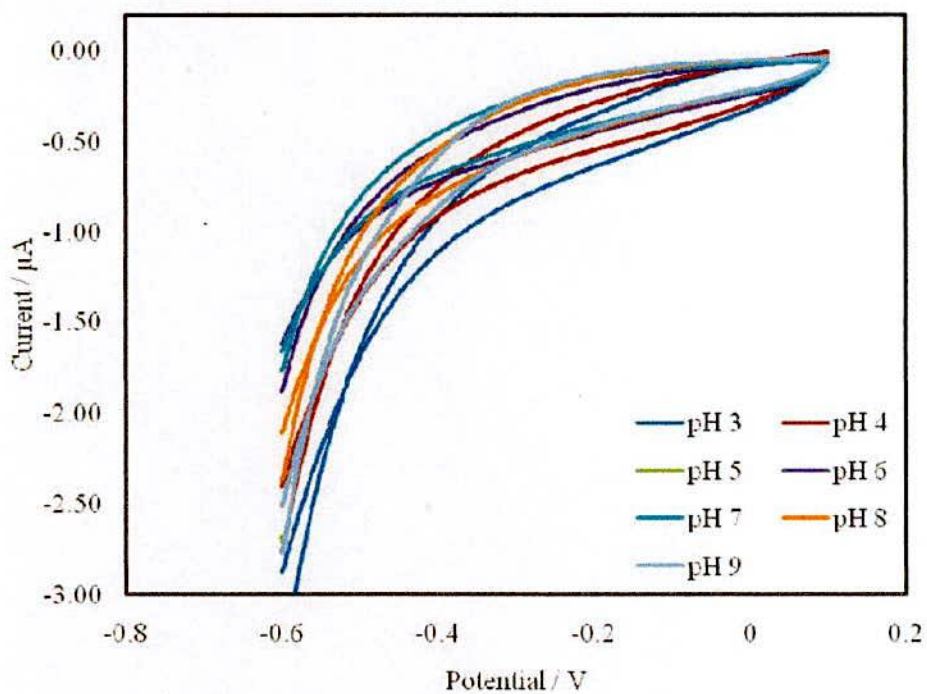


Figure 4.22: CVs of 0.1 M buffer at different pH values in the presence of CuO/PGE

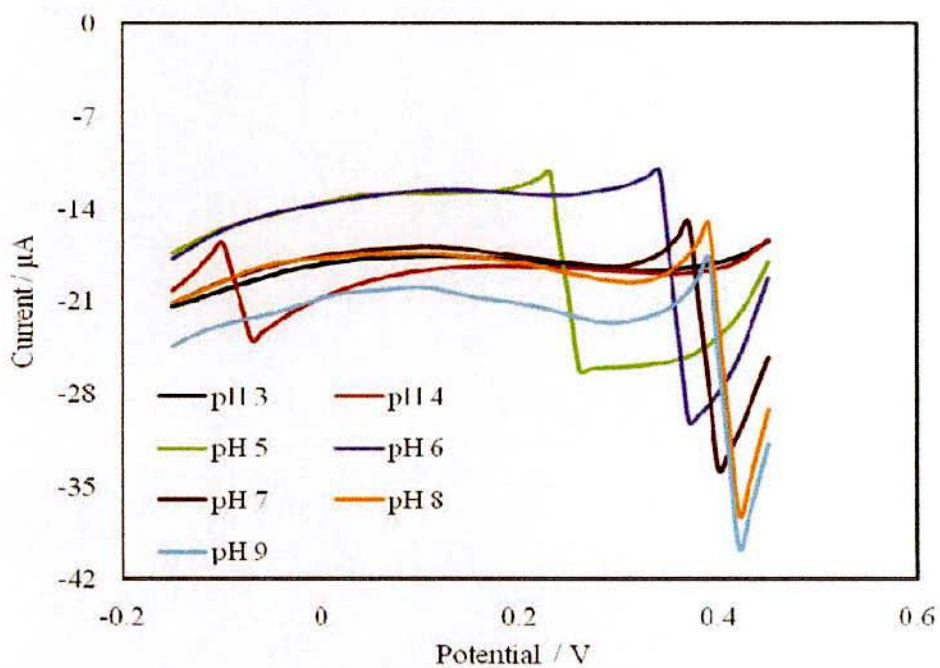


Figure 4.23: SWV of CuO/PGE at different pH values (3-9) in 0.1M PBS buffer

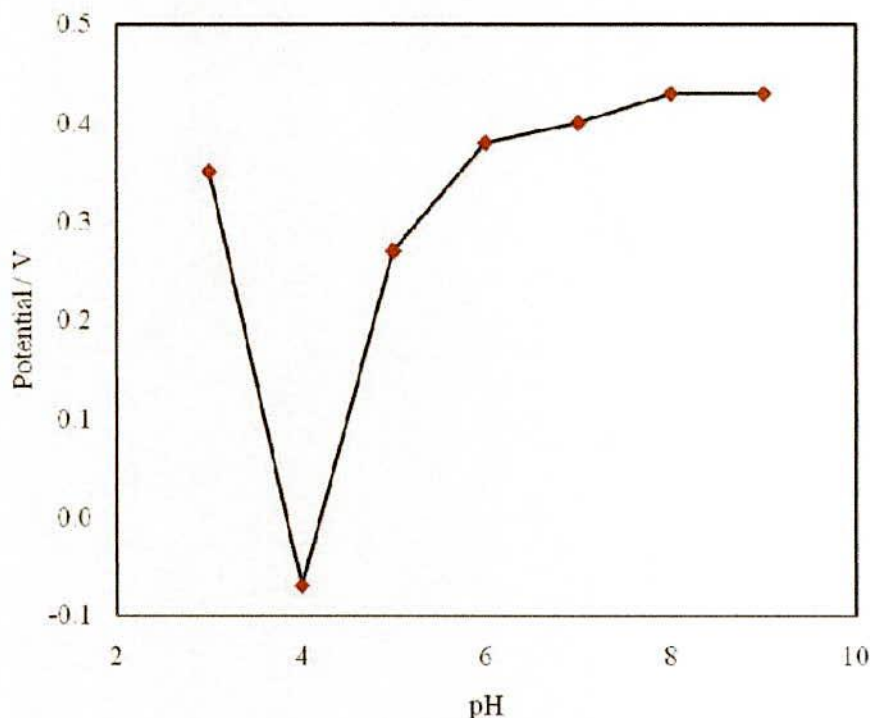


Figure 4.24: pH sensitivity measured from pH 3 to 9 using CuO/PGE

4.11 Electrochemical characterization of CuO/GCE using SWV

Since the primary focus of this paper is to fabricate and characterize the CuO/GCE as pH sensor, the SWV response in a series of aqueous buffer solutions ranging from pH 3 to 9 has been conducted. SWV is the fast, accurate and sensitive in compare to other relevant voltammograms [114].

A defined peak has been obtained in every buffer solution using CuO/GCE as electrode. Several different accurately measured 0.01M buffer (HCl, PBS) [115] ranging from pH 3-9 were electrochemically tested with SWV using GCE and A defined peak has been obtained in every buffer solution using CuO/GCE as electrode. This sharp peak at around 0.04V at pH 7 belongs to the reduction of Cu^{2+} to Cu. However, as the pH changes from 3 to 9, the peak potential shifts from higher potential to lower potential (Figure: 4.25, 4.26) up to pH 9. Afterward, the electrode shows non linear response. Therefore, in Figure 4.26 an only pH change has been shown from pH 3 to 9. This linear response with different pH solution may attributes to fewer protons available while pH increases, that speeds up the

reduction of Cu^{2+} to Cu; resulted lowering the peak potential. However, we also can see the reduction of peak current, which could be due to the limiting of species that can be reduced.

The sensing mechanism for this material is possibly due to the following the below redox reaction where forming copper with higher conductivity than copper oxide. Possible sensing mechanism has shown in equation [116].



The measured potential is thus dependent on the pH and a linear relation from pH 3 – 9 has been obtained. Also due to each pH changes, potential shift around 60 mV that attributes to Nernstian behavior (Figure: 4.27). According to the equation 2, the sensitivity of the sensor can in that case be obtained by the slope of the linear regression.

$$E = E^0 - (2.303RT/F) \text{pH} = E^0 - 0.05916\text{pH} \quad (2)$$

Where E^0 considered as the standard electrode potential, R is considered as the gas constant, T is considered as the temperature, and F is considered as the faradays constant. In this situation, owing to the redox reaction, all space charges are formed, that indicating a good performance of the sensor. In this work (Figure: 4.27) the pH sensor formed that demonstrated a mean sensitivity value of 60 ± 0.01 mV/pH which is close to the theoretical value. The correlation coefficient of R^2 values of about 0.97. This confirms the good sensitivity of the CuO/GCE to the variation of proton concentration in solution due to the redox reaction involved in the process.

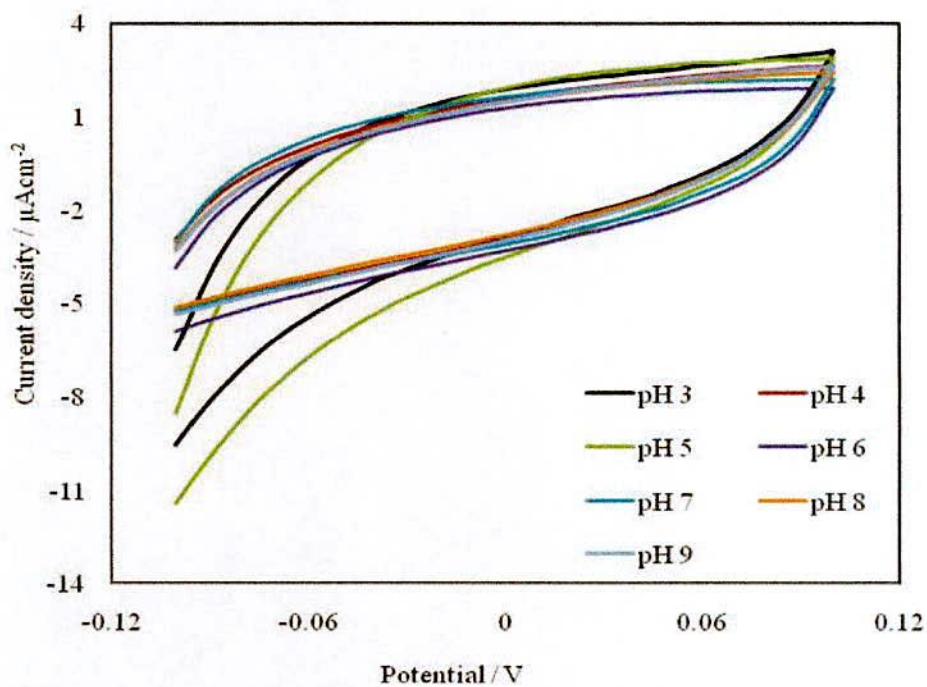


Figure 4.25: CVs of 0.1 M buffer at different pH values (3-9) on CuO/GCE

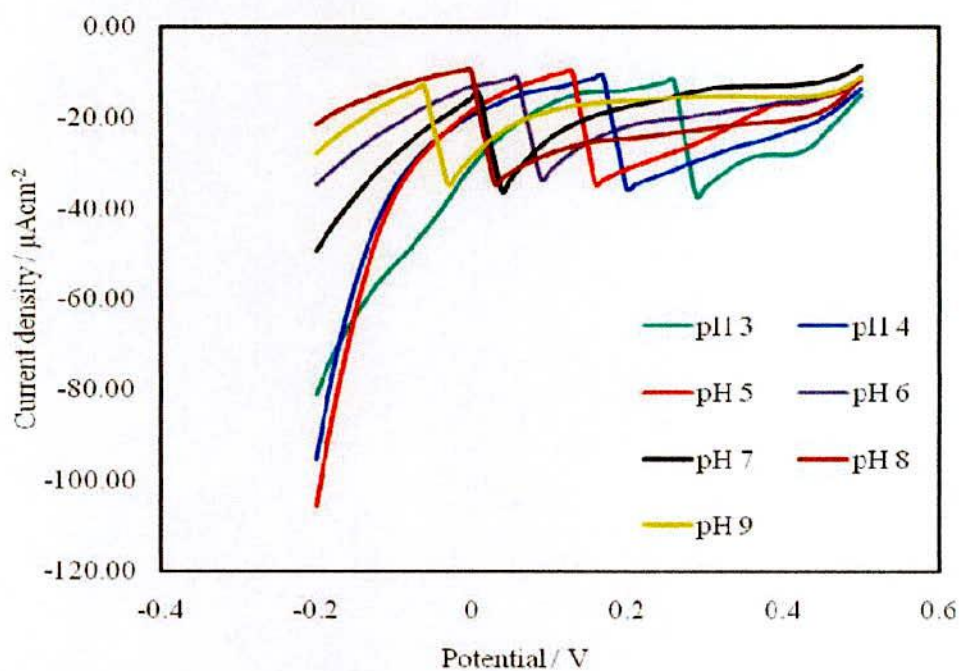


Figure 4.26: SWV of CuO/GCE at different pH values (3-9) in 0.1M PBS buffer

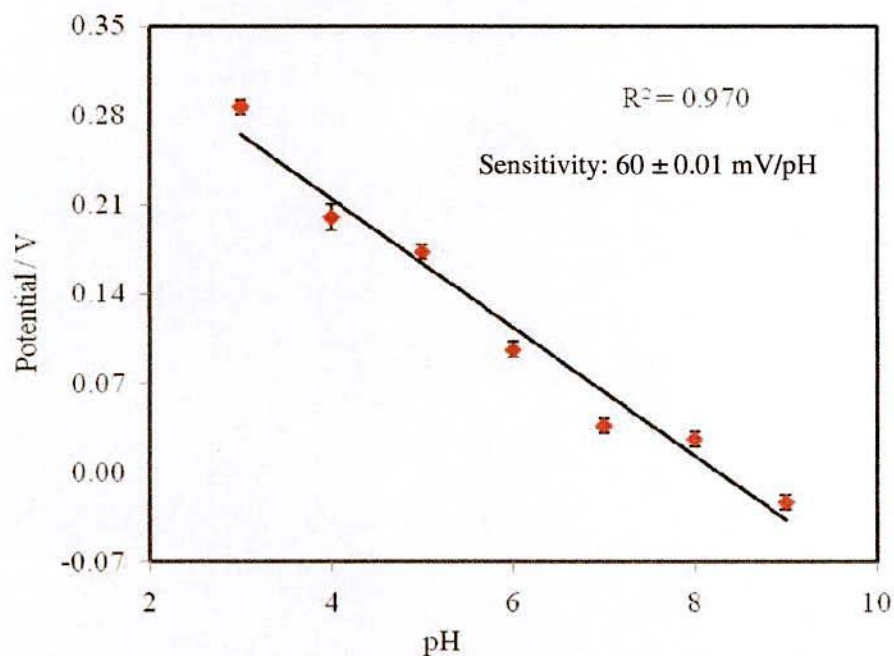


Figure 4.27: pH sensitivity measured from pH 3 to 11 using CuO/GCE

4.11.1 Zero current potentiometric (OCP) sensing and analytical performance of pH sensor

The pH sensitivity was also confirmed by measuring the OCP when dipping the electrode in buffer solution for 120 s. Figure 4.28- 4.29 shows electrodes OCP as a function of time to step pH changes of buffer solution between pH 3-9. The pH changes were realized by changing pH buffer solutions. The calibration of the electrode was carried out in both directions, from pH 3-9 and vice versa. It is apparent that the electrodes provide excellent reversibility and the potential response was independent against pH value or direction of pH changes. The potential response of the prepared electrode demonstrates pH sensitivity of 60 mV/pH. By measuring both SWV and OCP, it has been found that CuO/GCE can successfully sense the pH ranging from 3 – 9.

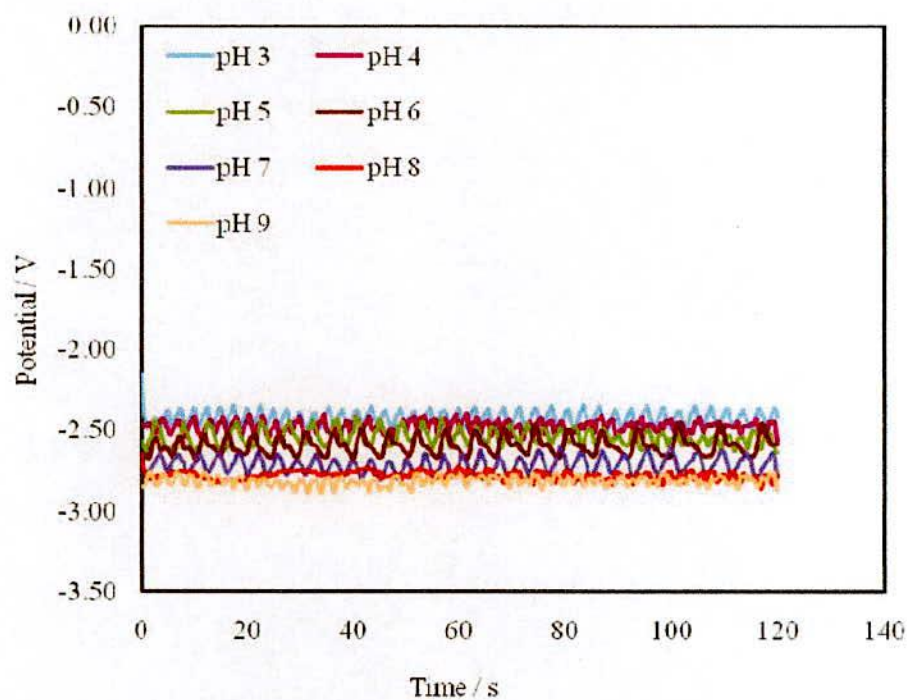


Figure 4.28: Zero current potentiometry (OCP) of 0.1 M buffer at different pH values (3-9) in the presence of CuO/GCE

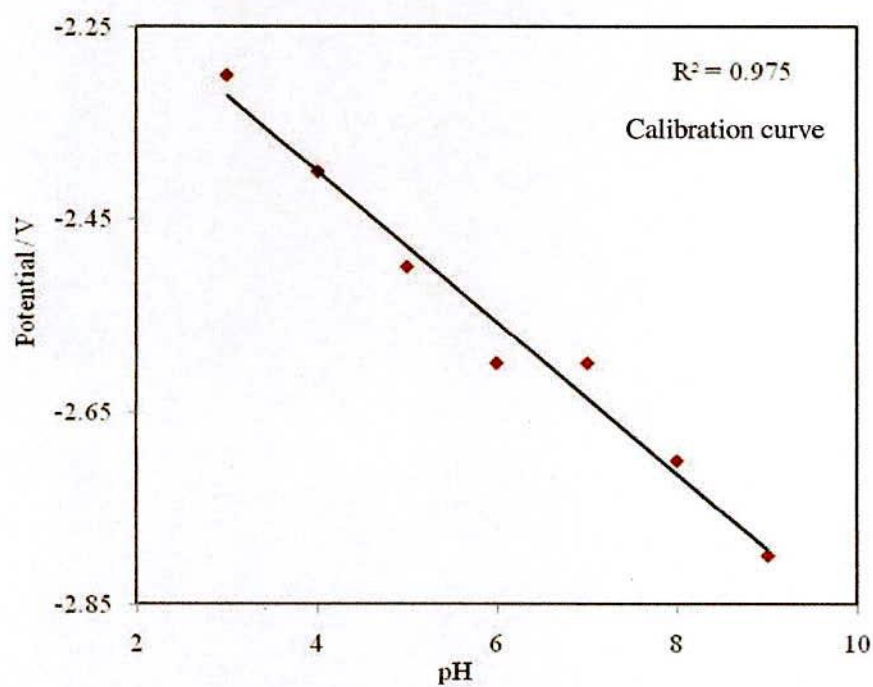


Figure 4.29: pH sensitivity measured from pH 3 to 9 using CuO/GCE

4.12 Electrochemical characterization of CuO /GCE in the presence and absence of oxygen

In this work, we have evaluated the possibility of the CuO/GCE to be used in both an oxygenated and de-oxygenated atmosphere. Figure 4.30 shows the voltammetric response of CuO/GCE that placed in buffer solution both in the absence and presence of oxygen. As oxygen is always present in the atmosphere, therefore, it is crucial that pH electrode should be performed equally in both environments. From the comparative results, it clearly can be seen that the reductive current differences slightly increases in the presence of oxygen. However, peak potential is unaltered; that concluded that this sensor can be used to measure the pH of solutions, irrespective of the O₂ concentration. Similar tests have been obtained by Jamal et al. [8] work where author have modified anthraquinone-ferrocene (AQ-Fc) complex based on a vertically aligned gold nanowire array electrode (AuNAE).

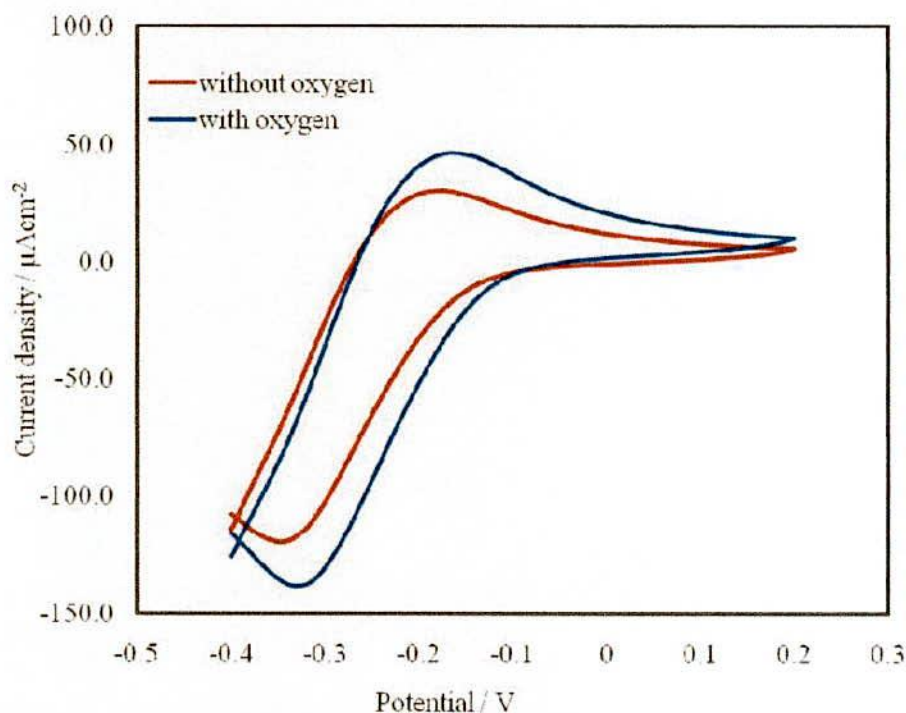


Figure 4.30: CVs showing the response of the CuO immobilized layer to the presence and absence of oxygen at pH 6

4.13 Real sample test

It is evident from different research works that new electrode which are proposed as pH sensor usually avoid applying them for the sensing pH in real unbuffered samples. However, in this work, we have validated our sensor against the laboratory standard glass pH electrode in the real sample: malt vinegar and antacid. Electro-analytical SWV and OCP signals gained are visible in Figure: 4.31 to Figure: 4.34 and comparable values of pH were obtained in antacid at the pH value of 9.00 and malt vinegar at the pH value 4.00 using CuO/GCE as pH sensor. These results demonstrated that CuO/GCE showed same potential value for antacid as measured by the commercial pH sensor. Thereby, it can be concluded that our proposed pH sensor has a huge potential to be developed a solid state, cost effective, portable and reliable pH sensor.

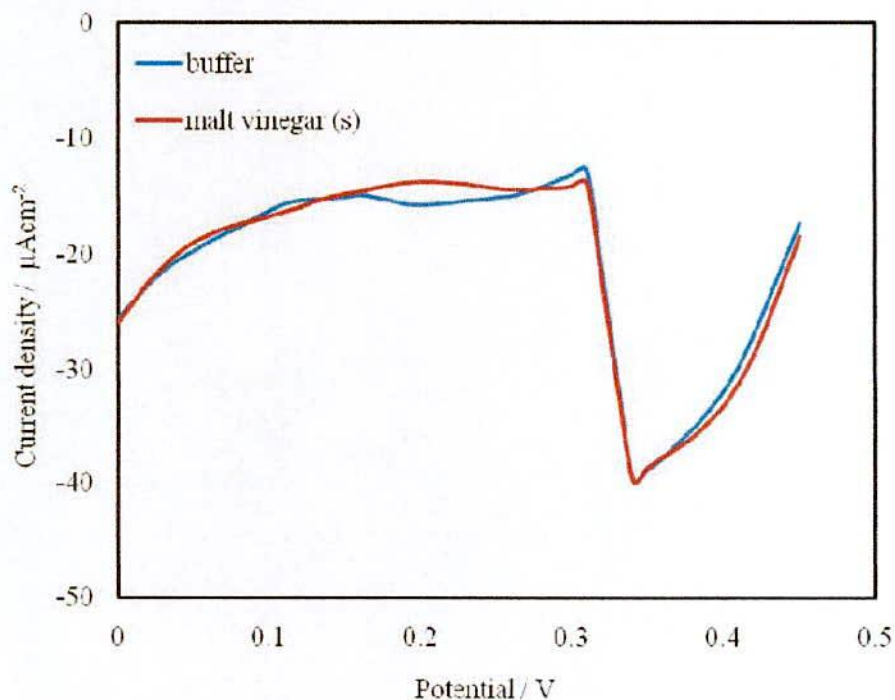


Figure 4.31: Electrochemical signal (SWV) obtained in “real” unbuffered samples for maltvinegar using CuO / GCE

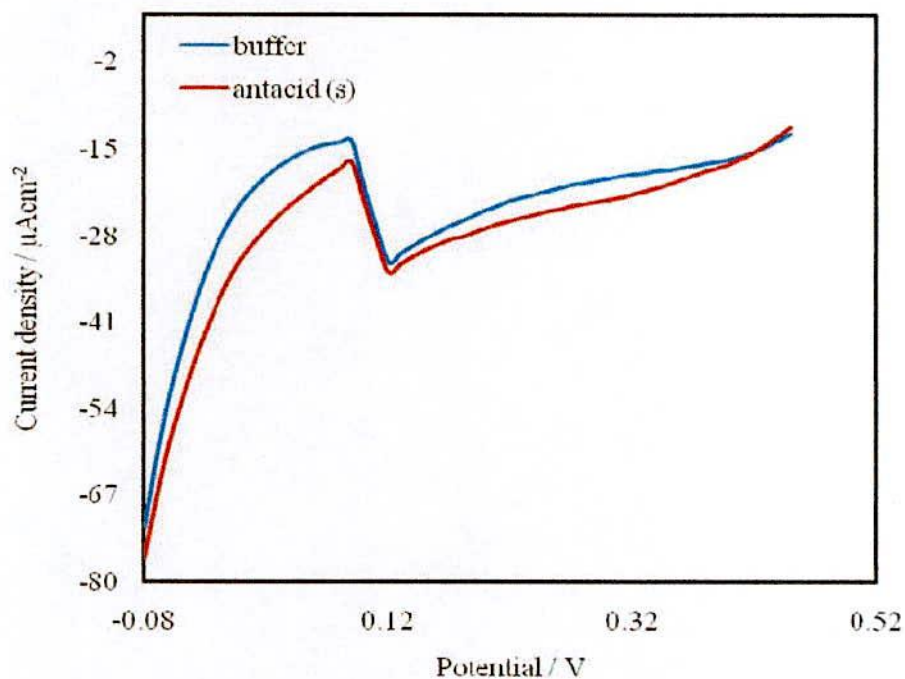


Figure 4.32: Electrochemical signal (SWV) obtained in “real” unbuffered samples for antacid using CuO/GCE

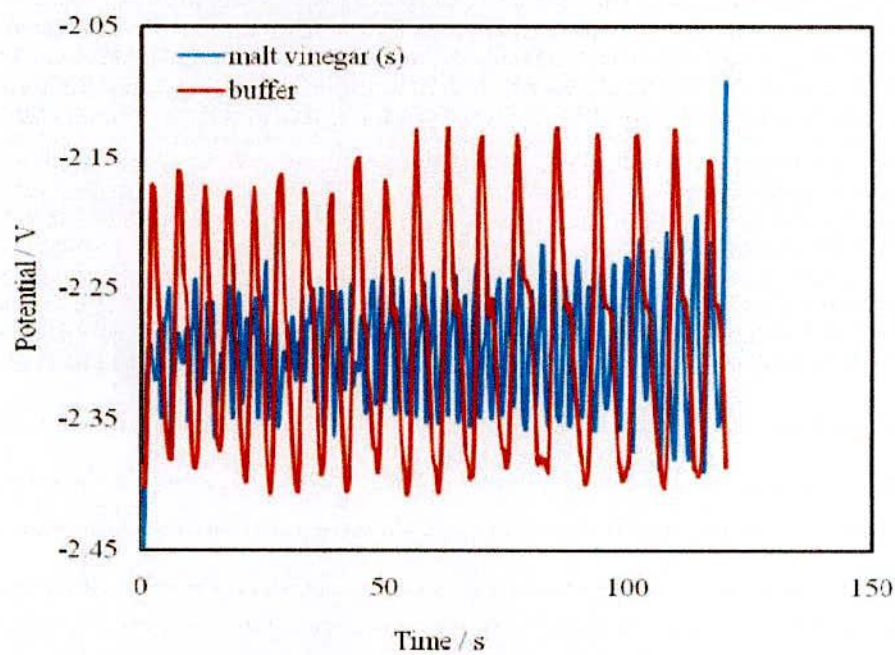


Figure 4.33: Electrochemical signal (OCP) obtained in “real” unbuffered samples for malt vinegar using CuO/GCE.

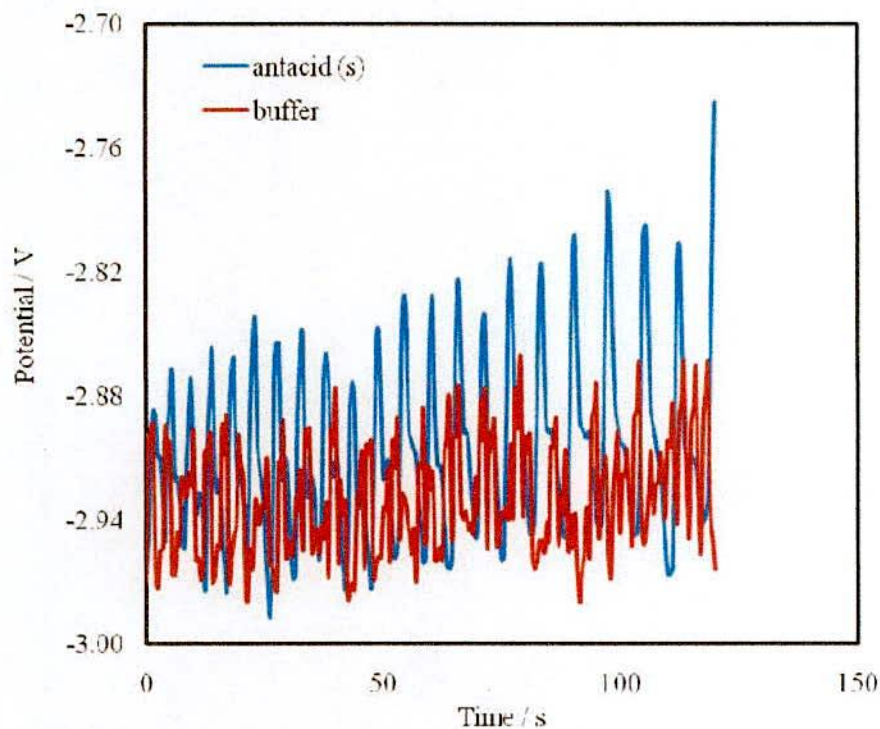


Figure 4.34: Electrochemical signal (OCP) obtained in “real” unbuffered samples for antacid using CuO/GCE

4.14 Repeatability and reproducibility measurement

To check the output response, stability, and repeatability of the electrode, the sample was tested three to four times in a PBS buffer solution with pH ranging from 3 to 9; the result is shown in (Figure 4.35). It was observed that the CuO NPs showed stable potentiometric response, excellent reproducibility, and good sensor stability. Similar tests have been obtained by Zaman *et al.* [7] work where author have modified CuO NFs on gold electrode.

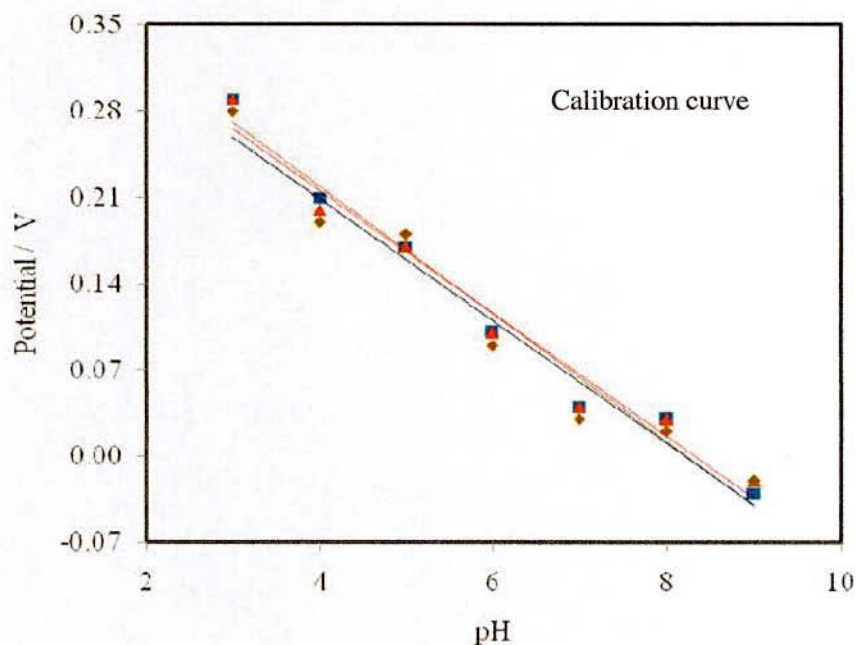


Figure 4.35: Repeatability and reproducibility test of three CuO NPs pH sensor electrodes at various pH buffer solutions

4.15 Drift and stability measurement of pH sensor

Fabricated electrode has been examined for the drift study and three buffer solutions with pH 5, 7 and 9 were chosen to determine the contribution the signal drift played. (Figure:4.36) showed that pH signal needed 0 – 90 minutes to stabilize, depending on the pH values. However, a good accuracy has been obtained thereafter. The drift of the potential reading in a neutral pH buffer was 0.83 mV within 3 hours. In the same way a potential drift of 1.97 mV was recorded in an acidic solution and 3.33 mV for a basic media. Largest drift has been obtained for pH 9 buffer, however, less than 4%. Stability of the electrode has been investigated, and found 95% of its initial activity after 7 days of continuous uses. The method described herein demonstrates how the CuO/GCE could be utilized as a pH sensor over a large pH range, with good stability and excellent sensitivity

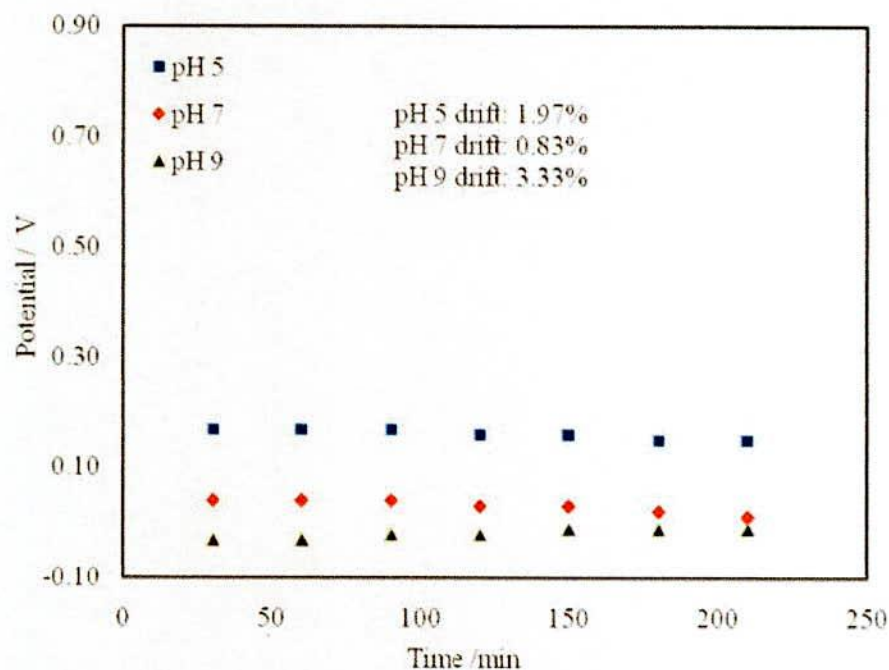


Figure 4.36: Electrode drift of CuO nanoparticle immobilized on the GCE; potential readings of pH 5, 7 and 9, signals have been taken every 30 min over period over 3 hours

Sensitivity in this work compare favorably with recent reports tabulated in Table 1. To the best of our knowledge, no articles have demonstrated the use of CuO based GCE as sensing platform for detecting pH. We also have demonstrated stability, drift study on this system for pH detection. The method described herein demonstrates how the CuO/GCE could be utilized as a pH sensor with good stability and excellent sensitivity over a large pH range. The arrangement we described a low cost pH sensor than the cost of the nearest anthraquinone modified electrode. Although the use of AQ-FC on AuNAE exhibited more sensitivity but, there cost is very high.

Table 4.2: A comparison of different pH sensors

Electrode	Sensitivity mV/pH	Drift %	pH range	Reference
GCE/CuO	60 ± 0.01	1.9 – 3.33	3 - 9	This work
Gold /CuO NF	28	-	2-11	[7]
Gold /WO ₃ NPs	-56.7 ± 1.3	-	5 - 9	[54]
GCE/WO ₃ NPs	60 ± 0.01	2.4 – 5.0	3-11	[116]
AQ-Fc/AuNAE	70	1-3	2-11	[8]
AQ-Fc/GCE	52	< 5	3 - 8	[117]
AQ-CNT/GCE	51	1.4	3 - 10	[118]
AQ Sulfonate/GCE	38	2 – 3	2 - 10	[119]
Thick Film/RuO ₂	30	-	4-10	[120]

The table shows the comparison of different pH sensors as well as the sensors sensitivity, drift also has been shown here. In this study, we have developed a sensitive, selective and cost effective pH sensor using CuO nanoparticle through a ion exchanging surfaces. The results of electrochemical detection of pH indicate CuO nanocrystal exhibit high selectivity and sensitivity toward the redox reaction with pH solution. Our present study is important because it provides us a novel method for detection of pH by using metal oxides nanocrystal sensing materials along with Nafion as a ion exchanging surfaces. The fabrication method and sensing material is very cheap and easy compare to the previously reported some sensing platform.

Chapter V

Conclusions

- ❖ A pH sensor has been successfully fabricated using CuO nanoparticle as sensing materials in presence of chitosan and Nafion, where Nafion acts as ions exchanging surfaces.
- ❖ The morphology of the hydrothermally synthesized CuO nanoparticles was observed by SEM and EDX and a flower like nanostructure with 100 nm particle size has been observed.
- ❖ In this study, H⁺ ion has been detected using CuO/GCE and sensitivity found to be $60 \pm 0.01 \text{ mVpH}^{-1}$ and a potential drift of 1.97-3.33% after three hours of continuous use. The sensor showed linearity range of pH 3-9 and could retain 95% of its initial sensitivity after 1 week of use.
- ❖ The electrode was found to respond both in the presence and absence of oxygen, further expanding the potential applications to include de-oxygenated environments.
- ❖ This prototype has been validated against commercial pH meter and found promising to develop a low cost solid state pH sensor for environmental as well as clinical applications.

Recommendations

Further work is needed to improve the pH sensor. Recommendations are as follows

- Direct growth of nanoparticle on flexible substrate would enhance the applicability of the sensor
- Open circuit potential need to apply more precisely to replace square wave voltammetry (SWV), as SWV is electrolyte dependent
- More characterizations of nanoparticle such as XPS, XRD, Raman, FT-IR is needed

- ion sensitive field-effect transistor (ISFET).*" Proc. Micro and IEEE Regional Symposium on Nanoelectronics (RSM), Vol.5, pp. 204-207.
- [11] Dutta, J., 2010, "*Modeling ion sensitive field effect transistors for biosensor applications.*" Inter. J. of Adv. Res. in Eng. and Tech. (IJARET), Vol. 1, pp. 38-57.
- [12] Hu Y., and Georgiou, P., 2014, "*A robust ISFET pH-measuring front-end for chemical reaction monitoring.*" IEEE Transactions on Biomedical Circuits and Systems, Vol. 8, pp. 1-11.
- [13] Hizawa, T., Sawada, K., Takao, H., Ishida, M., 2006, "*Fabrication of two dimensional pH image sensor using a charge transfer technique.*" Sensns. Act. B, Vol 117, pp. 509-515.
- [14] Tian, Y., Bradley, R., S., Youngbull, A., C., Yongzhong, L., Alex, K. Y. J., Roger, H. J. and Deirdre, R. M., 2010, "*Dually fluorescent sensing of pH and dissolved oxygen using a membrane made from polymerizable sensing monomers.*" Sens. Act. B., Vol. 147(2), pp. 714–722.
- [15] Cai, Q.Y., Grimes, C.A., 2000, "*A remote query magnetoelastic pH sensor.*" Sens. Act. B., Vol. 71, pp. 112-117.
- [16] <http://www.springerlink.com/content/vt5q5873550n5472/fulltext.pdf>.
- [17] Galster, H., 1991, "*pH measurements fundamentals, methods, applications, instruments.*" VCH Publishers: New York, NY, USA.
- [18] Koryta, J., Stulik, K., 1983, "*Ion selective electrodes.*" Cambridge Univ. Press., Cambridge, UK.
- [19] Covington, A. K., 1978 "*Ion Selective Electrode Methodology.*" CRC Press., Vol. 1-2, pp..147-197.
- [20] Gadzekpo, V.P., Hungerford, J.M., Kadry, A.M., Ibrahim, Y.A., Christian, G. D., 1985, Anal. Chem., Vol. 57, pp.493-496.
- [21] Miao, Y. and Chen, J. and Feng, K., 2005, "*New technology for the detection of pH.*" J. Appl. Phys., vol. 44, pp. 4838-4842.
- [22] Wilson, G. S. and Gifford, R., 2005, "*Biosensors for real-time in vivo measurements.*" Biosens. Bioelectron., Vol. 20, pp. 2388-2403.
- [23] Eggins, B. R., 2008, "*Chemical Sensors and Biosensors (Google eBook).*" John Wiley & Sons.

- [24] Adibi, M., Pirali-Hamedani, M. and Norouzi, P., 2011, "*Copper nano composite potentiometric sensor.*" Int. J. of Electro. Sci., Vol. 6, pp. 717-726.
- [25] Silvester, D. S., 2011, "*Recent advances in the use of ionic liquids for electrochemical sensing.*" Analyst., Vol. 136, pp. 4871-4882.
- [26] Ni, Y. N. and Kokot, S., 2008, "*Does chemo metrics enhance the performance of electroanalysis.*" Analytica. Chimica. Acta., Vol.626, pp. 130-146.
- [27] Walcarius, A., Minteer, S. D., Wang, J., Lin, Y., Merkoci, A., 2013, "*Nanomaterials for bio-functionalized electrodes: recent trends.*" J. Mater. Chem. B, Vol. 1, pp. 4878-4908.
- [28] Murray, R. W., 1984, "*Chemically modified electrodes.*" Electro. Anal. Chem., Vol. 13, pp. 611-635.
- [29] Scott, S. N. S., Oyama, N. and Anson, F. C., 1980, J. Electro anal. Chem. Vol. 110, pp. 303-307.
- [30] Wang, J. and Taha, Z., 1990, "*Catalytic oxidation and flow detection of carbohydrates at ruthenium dioxide modified electrodes.*" Anal. Chem., Vol. 62, pp. 1413-1416.
- [31] Ugo, P. and Moretto, L. M., 1995, "*Environmental technology and green economy.*" Electro anal. Chem., vol. 7, pp. 1105-1113.
- [32] Oliveira, M. F., Mortimer, R. J. and Stradiotto, N. R., 1991, "*Electro oxidation and determination of dopamine using a nafion-cobalt hexacyanoferrate film modified electrode.*" J. Microchem., Vol. 64, pp.155-159.
- [33] Alkire, R., Kolb, D. and Lipkowsky, J., 2009, "*Chemically modified electrodes.*" Germany: Wiley-VCH, Weinheim.
- [34] Murray, R. W. and Albery, W. J., 1981, "*Modified electrodes: chemically modified electrodes for electro catalysis.*" Phil. Tran. Roy. Soc. A., Vol. 302, pp. 253-265.
- [35] Orazio, D., 2003, "*Biosensors in clinical chemistry.*" Clin. Chim. Acta, Vol. 334, pp. 41-69.
- [36] Durst, R., Baumner, A., Murray, R., Buck, R. and Andrieux, C., 1997, "*Chemically modified electrodes: Recommended terminology and definitions.*" IUPAC, pp. 1317-1323.

- [37] Colorado State University Fort Collins Department of Chemistry, 1994, "*Chemically modified electrodes.*" Vol. 98, pp. 5714-5720.
- [38] Sanghav, B. and Srivastava, A., 2010. "*Simultaneous voltammetric determination of acetaminophen, aspirin and caffeine using an in situ surfactant-modified multiwalled carbon nanotube paste electrode*" Electrochim. Act. Vol. 55, pp. 8638-8648.
- [39] Chandu, T., Sharma, C.P., 1990, "*Chitosan-as a biomaterial.*" Biomater. Artif. Cells Artif. Organs, Vol. 18, pp. 1-24.
- [40] Kumar, M.N., Muzzarelli, R.A., Muzzarelli, C., Sashiwa, H., Domb, A.J., 2004, "*Chitosan chemistry and pharmaceutical perspectives.*" Chem. Rev., Vol. 104, pp. 6017-6084.
- [41] Krajewska, B., 2004, "*Application of chitin- and chitosan-based materials for enzyme immobilizations: a review.*" Enzyme Microbe. Technol., Vol. 35, pp. 126-139.
- [42] Heitner, W. C., 1996, "*Recent advances in perfluorinated ionomer membranes: structure, properties and applications.*" J. Membr. Sci., Vol. 120, pp. 1-33.
- [43] Zhao, Xi., X.U., Shuo, L.I.U. Jing, 2017, "*Surface tension of liquid metal: role, mechanism and application.*" Front. Energy, Vol. 11(4), pp. 535-567.
- [44] Grahame, D. C. 1947, "*The electrical double layer and the theory of electrocapillarity.*" Chem. Reviews, Vol. 41, pp. 441-501.
- [45] Wang, J., 2000, Anal. Electrochem. 2nd ed., Wiley-VCH, New York.
- [46] Cooper, J., Cass, T., 2004, Biosensors 2nd eds (Oxford University Press Inc., New York Eds).
- [47] <https://www.edaq.com/potentiostats-for-electrochemistry>.
- [48] Kissinger, P. T. and Heineman, W. R., 1983, "*Cyclic voltammetry,*" J. Chem. Educ., Vol. 60, pp. 701-702.
- [49] Lovric, M., 2002, "*Square-wave voltammetry.*" Electroanalytical Methods (Ed: F. Scholz) Springer, Berlin.
- [50] Valentin M., Rubin G., Milivoj, L., Ivan, B., Reinhard K., Markus H., 2013 "*Square-wave voltammetry: a review on the recent progress.*" Electro. Anal., Vol. 25, pp. 1-11.

- [51] Mirceski, V., Komorsky-Lovric, S., Lovric, M., 2007, "*Square-wave voltammetry: theory and application.*" (Ed: F.Scholz), Springer, Heidelberg.
- [52] <http://www.microtechsciences.com/how-the-sem-works.php>
- [53] Padigi, S.K.; Reddy, R.K.K.; Prasad, S., 2007, "*Carbon nanotube based aliphatic hydrocarbon sensor.*" *Biosens. Bioelectron.*, Vol. 22, pp. 829-837.
- [54] Lidia, S., Joana, C., Ana, Daniela, N., Nuno, C., Isabel, M. F., Pedro, B., Luis, P., Jorge, S., Rodrigo, M. and Elvira, F., 2014, "*WO₃ Nanoparticle-based conformable pH sensor.*" *ACS Appl. Mater. Interfaces*, Vol. 6, pp. 12226-12234.
- [55] Nadzirah, Sh., Hashim, U., Ruslinda, A. R., 2014, "*Titanium dioxide nanoparticles for pH sensor.*" *IEEE International Conference on Biomedical Engineering and Sciences Kuala Lumpur, Malaysia*, Vol. 7, pp. 960-963.
- [56] Yi. C., Seong, C. M., Jaehwan, K., 2013, "*A wide range conductometric pH sensor made with titanium dioxide/multiwall carbon nanotube/cellulose hybrid nanocomposite.*" *IEEE Sens. J.*, Vol. 13, pp. 4157-4162.
- [57] Chen, X., Cheng, X. and J. Justin, 2012, "*Multifunctional modified silver nanoparticles as ion and pH sensors in aqueous solution.*" *Analyst*, Vol.137, pp. 2338-2343..
- [58] Feng, G., Lun, W., Lijuan, T. and Changqing, Z. 2005, Springer-Verlag.
- [59] Millica, J., Jonnatha, C.H.A., and Hubert, H., 2013, Giraulta,envirobot RTD.
- [60] Zhenhua, B., Rui, C., Peng, S., Youju, H., Handong, S. and Dong, K. H., 2013, *ACS Appl. Mater. Interf.*, Vol. 5, pp. 5856-5860.
- [61] Marzouk, S. A. M., Buck, R. P., Dunlap, L. A., Johnson, T. A., and Cascio, W. E., 2002, "*Measurement of extracellular pH, K⁺, and lactate in ischemic heart.*" *Anal. Bio.chem.*, Vol.308(1), pp. 52-60.
- [62] Ryan, T., Nurminen, K., Hamalainen, J., Leskelä, M. and Lekkala, J., 2010, "*pH electrode based on ALD deposited iridium oxide procedia engineering.*" Vol. 5, pp. 548-552.
- [63] Nguyen, C. M., Huang, W. D., and Chiao, J.C., 2011, "*An electro-deposited IrOx thin film pH sensor.*" *BMES Biomedical Engineering Society Annual Meeting, Hartford.*

- [64] Lu, Y., Wang, T., Cai, Z., Cao, Y., Yang, H. and Duan, Y.Y., 2009, "Anodically electrodeposited iridium oxide films microelectrodes for neural micro stimulation and recording." *Sens. Act.*, Vol. 137, pp. 334-338.
- [65] Fulati, A. S. M., Ali, U., Riaz, M., Amin, G. Nur O. and Willande, M. 2009, "Miniaturized pH sensors based on zinc oxide nanotubes/nanorods sensors." Vol. 9, pp. 8911-8923.
- [66] Manjakkal., 2013, "A low-cost pH sensor based on RuO₂ resistor material." *Nano Hybrids*, Vol. 5, pp. 1-15.
- [67] Sardarinejad, A., Maurya D. K. and Alameh, K., 2015, "The pH sensing properties of rf sputtered RuO₂ thin-film prepared using different Ar/O₂ flow ratio." *J. materials.*, Vol. 8, pp.3352-3363.
- [68] Yao, S., Wang, M. and Madou, M., 2001, "A pH electrode based on melt-oxidized iridium oxide." *J. Electrochem. Soc.*, Vol. 148, pp. 29-36.
- [69] Herlem, G., Lakard, B., Herlem, M. and Fahys, B., 2001, "pH sensing at Pt electrode surfaces coated with linear poly ethylenimine from anodic polymerization of ethylenediamine." *J. Electrochem. Soc.*, Vol. 148, pp.435-439.
- [70] Tsai Y. T., Wen, T. C., Gopalan, 2003, "A. Tuning the optical sensing of pH by poly(diphenylamine)". *Sens. and Act. B. Chemi.*, Vol. 96, pp. 646-657.
- [71] Rinky, S., kikuo, K., Sushmee, B., 2017, "Amperometric pH sensor based on graphene-polyaniline composite" *IEEE Sens. J.*, Vol. 17, PP. 5038 – 5043.
- [72] Clarke. Y., Xu. W., Demas, J. N., Graff, B. A., 2000, "Lifetime-based pH sensor system based on a polymer-supported ruthenium(II) complex." *Anal. Chem.*, Vol. 72(15), pp. 3468-3475.
- [73] Vieira, C.S., Edson G. R., Fernandes, Angelo, D. Faceto, Valtencir, Z., Francisco, E. G., Guimaraes, 2011, "Nanostructured polyaniline thin films as pH sensing membranes in FET-based devices Nirton." *Sens. and Act. B.*, Vol. 160, pp. 312-317.
- [74] H. Yang and Wang, L. L., 2007, "Fluorescence pH probe based on microstructured polymer optical fiber." *Optical Society of America.*, Vol. 15, pp. 16478-16483
- [75] Sotomayora, T., Ivo, M. Raimundo Jr. A., Aldo, J. G., Zarbinb , Jarbas, J .R., Rohweddera , Graciliano, O. N., Oswaldo L. A., 2001, "Construction and

- evaluation of an optical pH sensor based on polyaniline-porous Vycor glass nanocomposite Pilar.*” Sens. and Act. B., Vol. 74, pp. 157-162.
- [76] Vonau, W., Gabel, J. and Jahn, H., 2005, “*Potentiometric all solid-state pH glass sensors.*” Electrochim. Acta., Vol. 50, pp. 4981-4987.
- [77] Yoon, H.J., Shin, J.H., Lee, S.D., Nam, H., Cha, G.S., Strong, T. D. and Brown, R.B., 2000, “*Solid-state ion sensors with a liquid junction-free polymer membrane-based reference electrode for blood analysis.*” Sens. Act. B., Vol. 64, pp. 8-14.
- [78] King, T., L., Shepherd, R., Danny, D., and Dermot, D., 2006, “*Solid State pH sensor based on light emitting diodes (LED) as detector platform.*” Sensors, Vol. 6, pp. 848-859.
- [79] Natedungta, W., and Prissanaroon, O., W., 2010, “*All-solid-state pH sensor based on conducting polymer.*” Advan. Mater. Res., Vol. 93, pp 591-594.
- [80] Yan, W., Hongyan, Y, Xulin, L, Zaide, Z., Dan, X., 2006, “*All solid-state pH electrode based on titanium nitride sensitive film.*” Electroanal., Vol. 18, pp. 1493–1498.
- [81] Lonsdale, W., Magdalena, W., and Kamal, A., 2017, “*RuO₂ pH sensor with super-glue-inspired reference electrode.*” Sensors, Vol. 17, pp. 2036-2043.
- [82] Taher, M., El-Ageza, Manal, R., Al-Sarajb, and Monzir, S., Abdel, L., Naturforsch, Z., 2004, “*Development of a novel solid-state pH sensor based on tin oxide thin film.*” Vol. 59(b), pp. 877 – 880
- [83] Yoon, H. J., Shin, J. H., Lee, S. D., Nam, H., Cha, G. S., Strong, T. D. and Brown, R. B., 2000, “*Solid-state ion sensors with a liquid junction-free polymer membrane-based reference electrode for blood analysis.*” Sens. Act. B., Vol. 64, pp. 8-14.
- [84] Kwok-Keung, S., Fayi, S., and Hong-Ping, B., 1996, “*Potentiometric pH sensor with anthraquinonesulfonate adsorbed on glassy carbon electrodes.*” Elrectro. anal., Vol. 8, pp. 12-16.
- [85] Walaiporn, P. O., Paul, J., Pigram and Anuvat, S., 2008, “*Potentiometric responses of functionalized polypyrrole based pH sensors.*” J. of Metals, Materials and Minerals, Vol.18, pp. 23-26.
- [86] Li-Te, Y., Hung-Yu, W., Yang-Chiuan, L. and Wen-Chung, H., 2012, “*A novel*

- instrumentation circuit for electrochemical measurements.*” Sensors, Vol. 12, pp. 9687-9696.
- [87] Tamer, A. A., Gehad, G. M. and Ghada A. Y., 2017, “*Development of novel potentiometric sensors for determination of lidocaine hydrochloride in pharmaceutical preparations, serum and urine samples.*” Iranian J. of Pharma. Res., Vol. 16 (2), pp. 498-512.
- [88] Mengyang, L., Yanling, M., Lei, S., Kuo-Chih, C., and Xinmei, H., 2016, “*A titanium nitride nanotube array for potentiometric sensing of pH.*” The Roy. Soc. of Chem., Vol. 5, pp 1-7.
- [89] Flavia, E. G., Jamie, P. S., Sophie, I. K., Dimitrios, K. K., Iniesta, I., Graham, C. S., Juliano, A. B. and Craig, E. B., 2015, “*Graphite screen-printed electrodes applied for the accurate and reagent less sensing of pH.*” Anal. Chem, Vol. 87, pp. 11666-11672.
- [90] Ngeontae, W., Xu, C., Ye, N., Wygladacz, K., Aeungmaitrepirom, W. and Tuntulani, T., 2007, “*Polymerized Nile blue derivatives for plasticizer-free fluorescent ion optode microsphere sensors.*” Anal. Chimica. Acta., Vol. 599, pp. 124.
- [91] Mathison, S. and Bakker, E., 1999, “*Renewable pH cross-sensitive potentiometric heparin sensors within incorporated electrically charged H⁺ ionophores.*” Anal. Chem., Vol. 71, pp. 4614-4621.
- [92] Mettler-Toledo, A. G., 2013, “*A guide to pH measurement—the theory and practice of pH applications.*” CH-8902 Urdorf/Switzerland.
- [93] Rundle, C., 2005, “*A beginner’s guide to ion-selective electrode measurements.*” <http://www.nico2000.net/Book/Guide1.html>.
- [94] Ges, I. A., Ivanov, B. L., Schaffer, D. K., Lima, F. A., Werdich, A. A. and Baudenbacher, F. J., 2005, “*Thin-film IrOx pH microelectrode for microfluidic-based microsystems.*” Biosens. Bioelectron., Vol. 21, pp. 248-256.
- [95] Buck, R.P., Rondinini, S., Covington, A. K., Baucke, F. G., Brett, C. M., Camoes, M. F., Milton, M. J., Mussini, T., Naumann, R., Pratt, K. W., Spitzer, P. and Wilson, G. S., 2002, “*The measurement of pH definition, standards and procedures (IUPAC Recommendations 2002).*” Pure Appl. Chem., Vol. 74, pp. 2169-2200.
- [96] Park, S., Boo, H., Kim, Y., Han, J., Kim, H. C. and Chung, T. D., 2005, “*pH-*

- sensitive solid-state electrode based on electrodeposited nonporous platinum.*" Anal. Chem. Vol. 77, pp. 7695-7701.
- [97] Yuen, T., Agnew, W., Bullara, L. and McCreery, D., 1990, "*Biocompatibility of electrodes and materials in the central nervous system in Neural Prostheses: Fundamental Studies.*" pp. 171-321.
- [98] Guth, U., Oelbner, W. and Vonau, W., 2001, "*Investigation of corrosion phenomena on chemical micro sensors.*" Electrochim. Acta., Vol. 47, pp. 201-210.
- [99] Frost, M. C., Batchelor, M. M., Lee, Y., Zhang, H., Kang, Y., Oha, B., Wilson, G. S., Gifford, R., Rudich, S. M. and Meyerhoff, M. E., 2003, "*Preparation and characterization of implantable sensors with nitric oxide release coatings.*" J. Microchem. Vol. 74, pp. 277-288.
- [100] Oelbner, W., Zosel, J., Guth, U., Pechstein, T. Babel, W. Connery, J. G., Demuth, C. Gansey, M. G., and Verburg, J. B., 2005, "Encapsulation of ISFET sensor chips." Sens. Act. 105, 104-117.
- [101] Edric, I. G., Arousian, A., Khalil, A. and Olga K., 2008, "*Conductimetric pH Sensor Based on Novel Conducting Polymer Composite Thick Films.*" IEEE, Vol. 978, pp. 478 – 483.
- [102] Ayad, M. M., Salahuddin, N. A., Alghaysh., M. O. and Issa, R. M., 2010, "*Phosphoric acid and pH sensors based on polyanniline films.*" Current App. Phy., Vol. 10, pp. 235-240.
- [103] Li-Yang, S., Ming-Jie, Y., Hwa-Yaw, T. and Jacques, A., 2013, "*Fiber optic pH sensor with self-assembled polymer multilayer nanocoatings.*" Sensors, Vol. 13, pp. 1425-1434.
- [104] Wen, D. H., Hung, C., Sanchali, D., Mu, C. and Chiao, J. C., 2011, "*A flexible pH sensor based on the iridium oxide sensing film.*" Sens. Act., Vol. 169, pp. 1-11.
- [105] Qingyun, C., Kefeng, Z., Chuanmin, R., Tejal, A. D. and Craig, A. G., 2004, "*A Wireless, Remote Query Glucose Biosensor Based on a pH-Sensitive Polymer.*" Anal. Chem., Vol. 76, pp. 4038-4043.
- [106] Shang-Jing, W., Yong-Cheng, W., and Che-Hsin, L., 2014, "*High performance isfet-based ph sensor utilizing low cost industrial-grade touch panel film as the gate structure.*" 18th International Conference on Miniaturized Systems for

- Chemistry and Life Sciences, San Antonio, Texas, USA, pp. 2131-2133.
- [107] Andrej, D. J., Hayssam, E. H. and Kohn, E., 2007, "*pH sensor on O-terminated diamond using boron-doped channel.*" *Diamond and Related Materials.*, Vol. 16, pp. 905-910.
- [108] Hai-Feng J., Hansen, K. M. Hu, Z., Thundat, T., 2001, "*Detection of pH variation using modified microcantilever sensors.*" *Sens. and Act. B.*, Vol. 72, pp. 233-238.
- [109] Zhao, Y., Hernandez-Pagan, E. A., Vargas-Barbosa, N. M., Dysart, J. L. and Mallouk T. E., 2011, "*A high yield synthesis of ligand-free iridium oxide nanoparticles with high electrocatalytic activity.*" *J. Phy. Chem. Lett.*, Vol. 2, pp. 402-408.
- [110] Wellin, C., Sholin, M., 2011, "*The electrocatalytic oxidative polymerizations of aniline and aniline derivatives by graphene.*" *Electrochim. Acta.*, Vol. 56, pp. 2284-2289.
- [111] Zhang, Li., Yuan, F., Zhang, X. Yong, L., 2011, "*Facial synthesis of flower like copper oxide and their application to hydrogen peroxide and nitrite sensing.*" *Chem. Cent. J.*, Vol.5, pp. 75-82.
- [112] Liu, S., Yu, B. and Zhang, T., 2013, "*Corresponding pore volume distribution.*" *Electrochim. Acta.*, Vol. 102, pp. 104-107.
- [113] Xingyou, L., Akihiko H., Takeshi F. and Mingwei, C., 2011, WPI Advanced Institute for Materials Research, Tohoku University, Sendai., Vol. 309, pp. 980-8577.
- [114] Harris, D. C., 2010, "*Quantitative chemical analysis.*" WH Freeman and Company, New York, 8th ed.
- [115] Flavia, E. G., Jamie, P. S., Sophie, I. K., Dimitrios, K. K., Iniesta, I., Graham, C. S., Juliano, A. B. and Craig, E. B., 2015, "*Graphite screen-printed electrodes applied for the accurate and reagent less sensing of pH.*" *Anal. Chem.*, vol. 87, pp. 11666-11672.
- [116] Kurzweil, P., 2009, "*Metal Oxides and Ion-Exchanging Surfaces as pH Sensors in Liquids: State-of-the-Art and Outlook.*" *Sensor*, Vol. 9, pp. 4955-4985.
- [117] Akter, I. and Jamal, M., MSc thesis, KUET, Khulna, Bangladesh 2016.

- [118] Lafitte, G. H., Wang, W., Yashina, A. S. and Lawrence, N. S., 2008, *Electrochem. Commun.*, Vol. 10, pp. 1831-1834.
- [119] Kumar, A. S. and Swetha, P., 2011, *Colloids and surfaces a physicochemical and engineering aspects.*, *Colloids. Surf., A*, Vol. 384, pp. 597-604.
- [120] Glance-Gostkiewicz, M., Sophocleous, M., Atkinson, J.K., Garcia-Breijo, E., 2012, "*Performance of miniaturized thick-film solid state pH sensors.*" *Sens. Act. A*, Vol. 202, pp. 2-7.

Publications

Journal

1. **Sanzida M. Toma**, Jayanta Mistri, Mohammad A. Yousuf and Mamun Jamal, Fabrication of a pH Sensor Based on Metal Oxide Nano-Particle and Ion Exchanging Surfaces, *Journal of Engineering Science*, Accepted March 2018.

Conference Proceedings

1. **Sanzida M. Toma**, Jayanta Mistri, Mohammad A. Yousuf and Mamun Jamal, Development of copper oxide based solid state pH sensor, *Proceedings of the 4th International Conference on Civil Engineering for Sustainable Development*, (ICESD 2018), 9~11 February 2018, KUET, Khulna, Bangladesh (oral presentation) (<http://www.iccesd.com/images/Program.pdf>).
2. **Sanzida M. Toma** and Mamun Jamal, Synthesis of metal oxide nanostructures and its electrochemical characterization, *International Conference on Chemical Science & Technology* (ICCST-Chem 2018), 24-25 February 2018, KUET, Khulna, Bangladesh. (poster presentation) (www.iccstk.com)